

Supplementary Information

Copper-promoted synthesis of epoxy-bridged [60]fullerene-fused lactones and further derivatization

Wen-Qiang Lu,[†] Dian-Bing Zhou,[†] Zheng-Chun Yin,[†] Qing-Song Liu[†] and Guan-Wu Wang^{*,†,‡}

[†]Hefei National Laboratory for Physical Sciences at Microscale, and Department of Chemistry, University of Science and Technology of China, Hefei, Anhui 230026, P. R. China

E-mail: gwang@ustc.edu.cn; Fax: +86 551 3607864; Tel: +86 551 3607864

[‡]State Key Laboratory of Applied Organic Chemistry, Lanzhou University, Lanzhou, Gansu 730000, P. R. China

Table of Contents

1. General information	S2
2. Optimization of the reaction conditions	S2–3
3. General procedure for the reaction of C ₆₀ with substrates 1a–n	S3
4. Synthesis and spectral data of compounds 2a–n , 3a , 4a and 4a'	S4–14
5. Control experiments	S14–15
6. Device fabrication	S15
7. NMR spectra of compounds 2a–n , 3a , 4a , 4a' , TEMPO-A, 5a and 6a	S16–51
8. UV-vis spectra of compounds 2a–n , 3a , 4a and 4a'	S52–54
9. CV of compounds 2a–n , 3a , 4a and 4a'	S55–61
10. X-Ray data of compounds 2b and 4a'	S61–63
11. References	S63

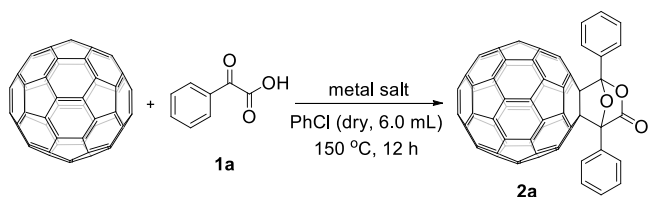
1. General information

NMR spectra were recorded on a 400 MHz NMR spectrometer. ^1H NMR chemical shifts were determined relative to TMS or residual DMSO (δ 2.50 ppm). $^{13}\text{C}\{\text{H}\}$ NMR chemical shifts were determined relative to residual CDCl_3 (δ 77.16 ppm) or residual $\text{C}_2\text{D}_2\text{Cl}_4$ (δ 74.18 ppm) or residual DMSO (δ 39.50 ppm). Data for ^1H NMR and $^{13}\text{C}\{\text{H}\}$ NMR are reported as follows: chemical shift (δ , ppm), multiplicity (s = singlet, d = doublet, t = triplet, m = multiplet). High-resolution mass spectra (HRMS) were measured with MALDI-TOF in a negative mode. In UV-vis spectra, the red lines were the enlargements (10 times) in the same wavelength range of the black lines and the concentration of a compound in CHCl_3 was 0.02 mM. Experimental conditions of CVs: 1 mM of a compound and 0.1 M of *n*-Bu₄NClO₄ in anhydrous *o*-dichlorobenzene (2 mL); reference electrode: SCE; working electrode: Pt; auxiliary electrode: Pt wire; scanning rate: 100 mV s⁻¹ or 50 mV s⁻¹. The presented figures were not corrected, but that ferrocene was added as internal reference, and that all given CV data were given versus ferrocene/ferrocenium.

2. Optimization of the Reaction Conditions

In our initial study, we used commercially available 2-oxo-2-phenylacetic acid (**1a**) as the representative substrate to react with C_{60} to optimize the reaction conditions. Typically, C_{60} (0.05 mmol), **1a** (0.15 mmol), $\text{Pd}(\text{OAc})_2$ (10 mol %) and $\text{CuCl}_2 \cdot 2\text{H}_2\text{O}$ (0.10 mmol) in anhydrous chlorobenzene (6 mL) were performed in a sealed tube and heated with stirring in an oil bath at 150 °C for 12 h. To our surprise, a novel epoxy-bridged C_{60} -fused lactone **2a** was produced in 39% yield (Table S1, entry 1). However, the absence of $\text{CuCl}_2 \cdot 2\text{H}_2\text{O}$ gave only a trace amount of **2a** (Table S1, entry 2), indicating its crucial role in this reaction. It turned out that the use of $\text{CuCl}_2 \cdot 2\text{H}_2\text{O}$ without the Pd catalyst afforded **2a** in a slightly higher yield of 41% (Table S1, entry 3 vs. entry 1). When anhydrous CuCl_2 was used to replace $\text{CuCl}_2 \cdot 2\text{H}_2\text{O}$, a slightly lower yield of 38% was obtained (Table S1, entry 4 vs. entry 3). Next, we investigated the effect of different copper salts in this reaction. Replacement of $\text{CuCl}_2 \cdot 2\text{H}_2\text{O}$ with $\text{Cu}(\text{OAc})_2 \cdot \text{H}_2\text{O}$ decreased the yield of **2a** to 22% (Table S1, entry 5). We further examined $\text{CuSO}_4 \cdot 5\text{H}_2\text{O}$, $\text{Cu}(\text{OTf})_2$ and CuBr_2 , which dramatically suppressed the formation of **2a** (Table S1, entries 6–8). When CuF_2 was chosen, the yield of **2a** was only 19% (Table S1, entry 9). While cuprous salts such as Cu_2O , CuCl and CuI were used, only a trace amount of **2a** was obtained (Table S1, entries 10–12). The silver salts including AgOAc and Ag_2CO_3 could not promote the reaction effectively (Table S1, entries 13 and 14). Shortening the reaction time to 8 h afforded **2a** in 33% yield, while prolonging the reaction time to 16 h could not enhance the product yield further (Table S1, entries 15 and 16 vs. entry 3). Unfortunately, decreasing or increasing the amount of **1a** or $\text{CuCl}_2 \cdot 2\text{H}_2\text{O}$ could not give better yields (Table S1, entries 17–20), and reducing the temperature of the oil bath from 150 °C to 140 °C lowered the yield of **2a** to 33% (Table S1, entry 21).

Table S1 Optimizing the reaction conditions^a



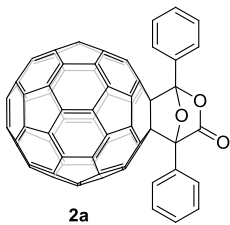
Entry	Metal salt	Molar ratio	Yield (%) ^b
1 ^c	Pd(OAc) ₂	1:3:0.1	39 (60)
2	Pd(OAc) ₂	1:3:0.1	trace
3	CuCl₂·2H₂O	1:3:2	41 (70)
4	CuCl ₂	1:3:2	38 (70)
5	Cu(OAc) ₂ ·H ₂ O	1:3:2	22 (49)
6	CuSO ₄ ·5H ₂ O	1:3:2	trace
7	Cu(OTf) ₂	1:3:2	trace
8	CuBr ₂	1:3:2	trace
9	CuF ₂	1:3:2	19 (34)
10	Cu ₂ O	1:3:2	trace
11	CuCl	1:3:2	trace
12	CuI	1:3:2	trace
13	AgOAc	1:3:2	8 (40)
14	Ag ₂ CO ₃	1:3:2	trace
15 ^d	CuCl ₂ ·2H ₂ O	1:3:2	33 (62)
16 ^e	CuCl ₂ ·2H ₂ O	1:3:2	42 (69)
17	CuCl ₂ ·2H ₂ O	1:2:2	25 (89)
18	CuCl ₂ ·2H ₂ O	1:4:2	43 (69)
19	CuCl ₂ ·2H ₂ O	1:3:1	32 (91)
20	CuCl ₂ ·2H ₂ O	1:3:3	28 (62)
21 ^f	CuCl ₂ ·2H ₂ O	1:3:2	33 (97)

^aUnless otherwise noted, the reactions were performed in sealed tube with the indicated molar ratio of C₆₀ (0.05 mmol):**1a**:metal salt in anhydrous chlorobenzene (6 mL) heated in an oil bath at 150 °C for 12 h. ^bIsolated yield. Values in parentheses were based on consumed C₆₀. ^cCuCl₂·2H₂O (2 equiv) was added to the reaction. ^dThe reaction time was 8 h. ^eThe reaction time was 16 h. ^fThe temperature was 140 °C.

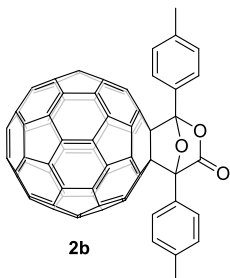
3. General procedure for the reaction of C₆₀ with substrates 1a–n

A mixture of C₆₀ (0.05 mmol), **1** (0.15 mmol) and CuCl₂·2H₂O (0.10 mmol) were completely dissolved in anhydrous chlorobenzene (6 mL), and the reaction was performed in a sealed tube. After being stirred in an oil bath at 150 °C or 140 °C for desired time, the reaction mixture was filtered through a silica gel plug to remove any insoluble material. After evaporation in vacuo, the residue was separated on a silica gel column with carbon disulfide as the eluent to give unreacted C₆₀ and product **2**.

4. Synthesis and spectral data of compounds 2a–n, 3a, 4a and 4a'

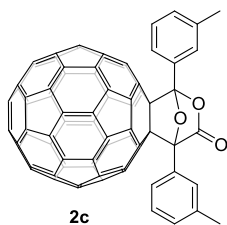


Preparation of **2a**: by following the general procedure, the reaction of C₆₀ (36.2 mg, 0.05 mmol) with **1a** (22.5 mg, 0.15 mmol) and CuCl₂·2H₂O (17.1 mg, 0.10 mmol) at 150 °C for 12 h afforded **2a** (19.9 mg, 41%) as brown amorphous solid along with unreacted C₆₀ (14.9 mg, 41%). ¹H NMR (400 MHz, CS₂/DMSO-*d*₆) δ ppm 7.96–7.92 (m, 2H), 7.86–7.81 (m, 2H), 7.36–7.21(m, 6H); ¹³C{¹H} NMR (100 MHz, CS₂/DMSO-*d*₆, all 1C unless indicated) δ ppm 167.32 (C=O), 149.62, 148.54, 147.18, 147.05, 146.88, 146.82, 146.26, 146.23, 146.17, 146.12, 146.10, 146.03, 145.85, 145.79, 145.71, 145.65, 145.52 (2C), 145.35, 145.23, 145.20, 145.17, 145.11, 145.09, 145.05, 145.02, 144.95, 144.84, 144.14, 144.00, 143.92, 143.87, 142.68, 142.65, 142.53 (2C), 142.49, 142.40, 142.03 (3C), 141.87, 141.83, 141.77, 141.75, 141.69, 141.60, 141.56, 141.43, 141.23, 139.80, 139.74, 139.65, 139.56, 138.52, 138.43, 137.00, 136.80, 130.41 (aryl C), 130.34 (aryl C), 129.39 (aryl C), 129.01 (aryl C), 128.58 (4C, aryl C), 126.43 (2C, aryl C), 126.29 (2C, aryl C), 112.53, 92.07, 82.20 (sp³-C of C₆₀), 76.61 (sp³-C of C₆₀); FT-IR ν/cm⁻¹ (KBr) 2922, 2854, 1811, 1496, 1446, 1426, 1355, 1297, 1180, 1047, 1018, 979, 900, 842, 740, 694, 645, 552, 523; UV-vis (CHCl₃) λ_{max} nm (log ε) 258 (5.23), 315 (4.55), 429 (3.41); MALDI-TOF MS *m/z* calcd for C₇₅H₁₀O₃ [M]⁺ 958.0635, found 958.0633.

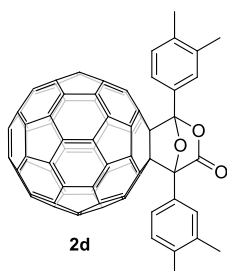


Preparation of **2b**: by following the general procedure, the reaction of C₆₀ (36.0 mg, 0.05 mmol) with **1b** (24.9 mg, 0.15 mmol) and CuCl₂·2H₂O (17.1 mg, 0.10 mmol) at 150 °C for 12 h afforded **2b** (21.4 mg, 43%) as brown amorphous solid along with unreacted C₆₀ (15.2 mg, 42%). ¹H NMR (400 MHz, 1:1 CS₂/CDCl₃) δ ppm 8.05 (d, *J* = 8.2 Hz, 2H), 7.93 (d, *J* = 8.2 Hz, 2H), 7.34 (d, *J* = 8.7 Hz, 2H), 7.31 (d, *J* = 8.7 Hz, 2H), 2.44 (s, 3H), 2.41 (s, 3H); ¹³C{¹H} NMR (100 MHz, 1:1 CS₂/CDCl₃, all 1C unless indicated) δ ppm 168.45 (C=O), 149.75, 148.67, 147.26, 147.10, 146.81, 146.76, 146.25, 146.13 (2C), 146.08, 146.02, 145.95, 145.78, 145.71, 145.63, 145.57, 145.39 (2C), 145.26, 145.23, 145.14, 145.12, 145.10, 145.03, 144.98, 144.95, 144.88, 144.74, 144.06, 143.93, 143.85, 143.80, 142.61, 142.57, 142.43 (2C), 142.40, 142.31, 141.97 (3C), 141.86, 141.75, 141.68 (2C), 141.62, 141.51, 141.47, 141.37, 141.17, 140.27 (aryl C), 139.68, 139.65, 139.55, 139.47, 139.09 (aryl C), 138.36, 138.26, 136.90,

136.69, 129.20 (2C, aryl C), 129.14 (2C, aryl C), 127.40 (aryl C), 126.22 (2C, aryl C), 126.13 (2C, aryl C), 125.97 (aryl C), 112.90, 92.31, 82.16 (sp^3 -C of C_{60}), 76.65 (sp^3 -C of C_{60}), 21.42, 21.34; FT-IR ν/cm^{-1} (KBr) 2918, 1811, 1692, 1515, 1430, 1355, 1301, 1262, 1180, 1075, 1044, 1017, 983, 902, 804, 748, 553, 525; UV-vis (CHCl_3) λ_{\max} nm (log ε) 257 (4.93), 315 (4.49), 429 (3.54); MALDI-TOF MS m/z calcd for $\text{C}_{77}\text{H}_{14}\text{O}_3$ [M]⁺ 986.0948, found 986.0947.

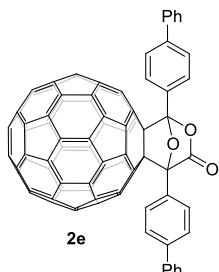


Preparation of 2c: by following the general procedure, the reaction of C_{60} (35.7 mg, 0.05 mmol) with **1c** (25.0 mg, 0.15 mmol) and $\text{CuCl}_2 \cdot 2\text{H}_2\text{O}$ (16.7 mg, 0.10 mmol) at 150 °C for 10 h afforded **2c** (17.1 mg, 35%) as brown amorphous solid along with unreacted C_{60} (14.2 mg, 40%). ¹H NMR (400 MHz, $\text{CS}_2/\text{DMSO}-d_6$) δ ppm 7.95 (s, 1H), 7.92 (d, $J = 8.0$ Hz, 1H), 7.85 (s, 1H), 7.82 (d, $J = 8.0$ Hz, 1H), 7.44–7.35 (m, 2H), 7.31 (d, $J = 7.6$ Hz, 1H), 7.24 (d, $J = 7.6$ Hz, 1H), 2.50 (s, 3H), 2.48 (s, 3H); ¹³C{¹H} NMR (100 MHz, $\text{CS}_2/\text{DMSO}-d_6$, all 1C unless indicated) δ ppm 167.61 (C=O), 149.97, 148.89, 147.56, 147.44, 147.05, 147.00, 146.50, 146.40, 146.34 (2C), 146.28, 146.21, 146.03, 145.97, 145.89, 145.83, 145.70 (2C), 145.52, 145.47, 145.39, 145.37 (2C), 145.28 (2C), 145.21, 145.14, 145.05, 144.33, 144.20, 144.12, 144.07, 143.00, 142.87, 142.84, 142.71 (2C), 142.60, 142.24 (3C), 142.08, 142.03, 141.95 (2C), 141.89, 141.79, 141.75, 141.64, 141.44, 139.97, 139.93, 139.83, 139.74, 138.67, 138.57, 138.28 (aryl C), 138.16 (aryl C), 137.19, 136.95, 131.30 (aryl C), 130.62 (aryl C), 130.36 (aryl C), 129.16 (aryl C), 128.79 (2C, aryl C), 127.08 (aryl C), 126.99 (aryl C), 123.96 (aryl C), 123.78 (aryl C), 112.72, 92.26, 82.41 (sp^3 -C of C_{60}), 76.84 (sp^3 -C of C_{60}), 22.00, 21.95; FT-IR ν/cm^{-1} (KBr) 2924, 2850, 1813, 1513, 1422, 1178, 1039, 1017, 897, 879, 777, 758, 698, 527; UV-vis (CHCl_3) λ_{\max} nm (log ε) 257 (5.04), 316 (4.56), 428 (3.39); MALDI-TOF MS m/z calcd for $\text{C}_{77}\text{H}_{14}\text{O}_3$ [M]⁺ 986.0948, found 986.0931.

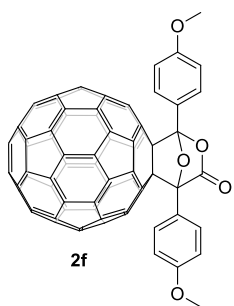


Preparation of 2d: by following the general procedure, the reaction of C_{60} (36.0 mg, 0.05 mmol) with **1d** (27.0 mg, 0.15 mmol) and $\text{CuCl}_2 \cdot 2\text{H}_2\text{O}$ (16.9 mg, 0.10 mmol) at 150 °C for 12 h afforded **2d** (26.4 mg, 52%) as brown amorphous solid along with unreacted C_{60} (15.3 mg, 43%). ¹H NMR (400 MHz, $\text{CS}_2/\text{DMSO}-d_6$) δ ppm 7.86 (s, 1H), 7.81 (d, $J = 7.9$ Hz, 1H), 7.76 (s, 1H), 7.71 (d, $J = 7.9$ Hz, 1H), 7.26 (d, $J = 7.9$ Hz, 1H),

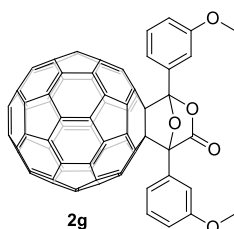
7.22 (d, $J = 7.9$ Hz, 1H), 2.37 (s, 3H), 2.35 (s, 3H), 2.33 (s, 3H), 2.30 (s, 3H); $^{13}\text{C}\{\text{H}\}$ NMR (100 MHz, $\text{CS}_2/\text{DMSO}-d_6$, all 1C unless indicated) δ ppm 168.01 (C=O), 150.06, 148.96, 147.60, 147.49, 146.91, 146.85, 146.47, 146.30, 146.25, 146.19, 146.14, 146.07, 145.89, 145.82, 145.74, 145.68, 145.54 (2C), 145.48, 145.36 (2C), 145.23, 145.19, 145.16, 145.13, 145.07, 145.00, 144.90, 144.20, 144.07, 144.00, 143.92, 142.73, 142.69, 142.55 (3C), 142.45, 142.10 (3C), 141.93, 141.89, 141.82 (2C), 141.77, 141.62, 141.60, 141.53, 141.33, 139.82, 139.79, 139.67, 139.58, 139.05 (aryl C), 138.42, 138.35, 137.86 (aryl C), 137.07, 136.83 (2C, aryl C), 136.72, 130.02 (aryl C), 129.99 (aryl C), 127.98 (aryl C), 127.40 (aryl C), 127.30 (aryl C), 126.54 (aryl C), 124.25 (aryl C), 124.05 (aryl C), 112.79, 92.16, 82.34 ($\text{sp}^3\text{-C}$ of C_{60}), 76.78 ($\text{sp}^3\text{-C}$ of C_{60}), 20.13, 20.10, 19.96, 19.87; FT-IR ν/cm^{-1} (KBr) 2915, 1814, 1618, 1506, 1446, 1353, 1314, 1276, 1224, 1190, 1129, 1089, 1053, 1019, 984, 905, 881, 810, 772, 709, 556, 526; UV-vis (CHCl_3) λ_{max} nm (log ε) 258 (5.04), 315 (4.56), 429 (3.45); MALDI-TOF MS m/z calcd for $\text{C}_{79}\text{H}_{18}\text{O}_3$ [M]⁻ 1014.1261, found 1014.1263.



Preparation of **2e:** by following the general procedure, the reaction of C_{60} (35.8 mg, 0.05 mmol) with **1e** (34.2 mg, 0.15 mmol) and $\text{CuCl}_2 \cdot 2\text{H}_2\text{O}$ (16.7 mg, 0.10 mmol) at 140 °C for 17 h afforded **2e** (16.7 mg, 30%) as brown amorphous solid along with unreacted C_{60} (18.2 mg, 51%). ^1H NMR (400 MHz, $\text{CS}_2/\text{DMSO}-d_6$) δ ppm 8.00 (d, $J = 8.4$ Hz, 2H), 7.90 (d, $J = 8.4$ Hz, 2H), 7.51 (d, $J = 8.5$ Hz, 2H), 7.48 (d, $J = 8.5$ Hz, 2H), 7.35–7.29 (m, 4H), 7.19–7.12 (m, 4H), 7.08 (t, $J = 7.9$ Hz, 2H); $^{13}\text{C}\{\text{H}\}$ NMR (100 MHz, 1:1 $\text{CS}_2/\text{C}_2\text{D}_2\text{Cl}_4$, all 1C unless indicated) δ ppm 169.42 (C=O), 149.68, 148.65, 147.39, 147.28, 147.24, 147.21, 146.58, 146.57, 146.54, 146.48, 146.45, 146.41, 146.25, 146.18, 146.08, 146.02, 145.90, 145.88, 145.76, 145.64, 145.54, 145.51, 145.47, 145.41, 145.38 (2C), 145.34, 145.10, 144.47, 144.36, 144.27, 144.21, 143.52 (aryl C), 143.05, 143.03, 142.88 (2C), 142.84, 142.76, 142.46 (aryl C), 142.37 (2C), 142.36, 142.25, 142.19 (2C), 142.11 (2C), 141.93, 141.91, 141.80, 141.61, 140.19 (2C, aryl C), 140.14, 140.04, 140.01, 139.82, 138.76, 138.69, 137.50, 137.27, 129.29 (aryl C), 129.19 (2C, aryl C), 129.15 (2C, aryl C), 128.29 (aryl C), 128.09 (2C, aryl C), 127.63 (2C, aryl C), 127.59 (2C, aryl C), 127.39 (2C, aryl C), 127.34 (2C, aryl C), 127.16 (2C, aryl C), 127.10 (2C, aryl C), 113.60, 92.93, 82.52 ($\text{sp}^3\text{-C}$ of C_{60}), 77.01 ($\text{sp}^3\text{-C}$ of C_{60}); FT-IR ν/cm^{-1} (KBr) 2918, 1812, 1613, 1484, 1427, 1402, 1355, 1300, 1180, 1074, 1047, 1011, 981, 900, 826, 754, 723, 693, 556, 524; UV-vis (CHCl_3) λ_{max} nm (log ε) 258 (4.99), 314 (4.455), 429 (3.30); MALDI-TOF MS m/z calcd for $\text{C}_{87}\text{H}_{18}\text{O}_3$ [M]⁻ 1110.1261, found 1110.1255.

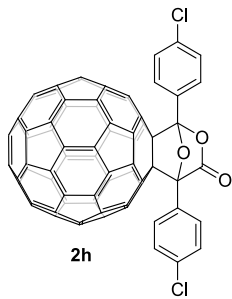


Preparation of 2f: by following the general procedure, the reaction of C₆₀ (35.7 mg, 0.05 mmol) with **1f** (27.4 mg, 0.15 mmol) and CuCl₂·2H₂O (16.8 mg, 0.10 mmol) at 150 °C for 12 h afforded **2f** (14.5 mg, 29%) as brown amorphous solid along with unreacted C₆₀ (17.5 mg, 49%). ¹H NMR (400 MHz, CS₂/DMSO-d₆) δ ppm 7.81 (d, *J*= 8.7 Hz, 2H), 7.70 (d, *J*= 8.7 Hz, 2H), 6.76 (d, *J*= 8.9 Hz, 2H), 6.74 (d, *J*= 8.9 Hz, 2H), 3.61 (s, 3H), 3.59 (s, 3H); ¹³C{¹H} NMR (100 MHz, CS₂/DMSO-d₆, all 1C unless indicated) δ ppm 167.33 (C=O), 160.41 (aryl C), 159.70 (aryl C), 149.73, 148.57, 147.05, 146.92, 146.48, 146.43, 145.98, 145.82, 145.79, 145.75, 145.71, 145.64, 145.46, 145.39, 145.31, 145.24, 145.10, 145.08, 145.01, 144.95, 144.85 (2C), 144.78, 144.72, 144.70, 144.62, 144.55, 144.46, 143.78, 143.62, 143.56, 143.50, 142.30, 142.25, 142.14, 142.13, 142.09, 142.00, 141.68, 141.66, 141.64, 141.52, 141.45, 141.40, 141.36, 141.34, 141.22, 141.17, 141.09, 140.88, 139.43, 139.37, 139.26, 139.19, 138.11, 137.99, 136.54, 136.35, 127.36 (2C, aryl C), 127.27 (2C, aryl C), 122.09 (aryl C), 120.57 (aryl C), 113.54 (2C, aryl C), 113.45 (2C, aryl C), 112.24, 91.64, 81.98 (sp³-C of C₆₀), 76.54 (sp³-C of C₆₀), 54.29, 54.20; FT-IR ν/cm⁻¹ (KBr) 2923, 1807, 1610, 1512, 1457, 1424, 1356, 1304, 1252, 1174, 1024, 898, 823, 605, 553, 524; UV-vis (CHCl₃) λ_{max} nm (log ε) 257 (4.86), 315 (4.39), 429 (3.28); MALDI-TOF MS *m/z* calcd for C₇₇H₁₄O₅ [M]⁺ 1018.0847, found 1018.0849.

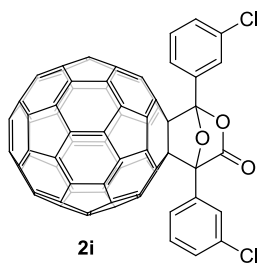


Preparation of 2g: by following the general procedure, the reaction of C₆₀ (35.8 mg, 0.05 mmol) with **1g** (27.3 mg, 0.15 mmol) and CuCl₂·2H₂O (17.3 mg, 0.10 mmol) at 150 °C for 12 h afforded **2g** (19.0 mg, 38%) as brown amorphous solid along with unreacted C₆₀ (14.2 mg, 40%). ¹H NMR (400 MHz, 1:1 CS₂/CDCl₃) δ ppm 7.76 (d, *J*= 7.6 Hz, 1H), 7.71 (s, 1H), 7.65 (d, *J*= 7.6 Hz, 1H), 7.57 (s, 1H), 7.50–7.40 (m, 2H), 7.04 (d, *J*= 8.1 Hz, 1H), 6.98 (d, *J*= 8.1 Hz, 1H), 3.87 (s, 3H), 3.86 (s, 3H); ¹³C{¹H} NMR (100 MHz, CS₂/DMSO-d₆, all 1C unless indicated) δ ppm 166.80 (C=O), 158.92 (2C, aryl C), 149.20, 148.17, 146.78, 146.68, 146.45, 146.40, 145.94, 145.79 (2C), 145.72, 145.67, 145.60, 145.42, 145.35, 145.28, 145.21, 145.09 (2C), 144.94, 144.80, 144.77, 144.72, 144.68, 144.65 (2C), 144.61, 144.54, 144.41, 143.73, 143.57, 143.52, 143.44, 142.26, 142.20, 142.10, 142.07 (2C), 141.99, 141.62 (2C), 141.58, 141.43,

141.42, 141.37, 141.36, 141.30, 141.18, 141.15, 141.02, 140.83, 139.27, 139.26, 139.24, 139.17, 138.03, 137.96, 136.53, 136.23, 131.19 (aryl C), 129.79 (aryl C), 129.22 (aryl C), 129.18 (aryl C), 118.34 (aryl C), 118.14 (aryl C), 115.25 (aryl C), 114.42 (aryl C), 111.92, 111.83 (aryl C), 111.73 (aryl C), 91.65, 81.72 (sp^3 -C of C_{60}), 76.18 (sp^3 -C of C_{60}), 54.35, 54.27; FT-IR ν/cm^{-1} (KBr) 2923, 1808, 1609, 1511, 1454, 1427, 1293, 1230, 1178, 1031, 902, 876, 770, 692, 522; UV-vis (CHCl_3) λ_{max} nm (log ϵ) 258 (4.86), 315 (4.39), 429 (3.29); MALDI-TOF MS m/z calcd for $\text{C}_{77}\text{H}_{14}\text{O}_5$ [M]⁺ 1018.0847, found 1018.0846.

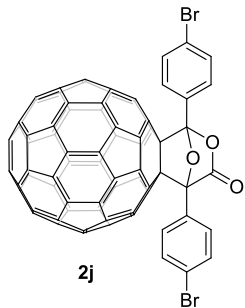


Preparation of 2h: by following the general procedure, the reaction of C_{60} (35.8 mg, 0.05 mmol) with **1h** (27.7 mg, 0.15 mmol) and $\text{CuCl}_2 \cdot 2\text{H}_2\text{O}$ (17.4 mg, 0.10 mmol) at 150 °C for 12 h afforded **2h** (15.4 mg, 30%) as brown amorphous solid along with unreacted C_{60} (16.4 mg, 46%). ¹H NMR (400 MHz, 1:1 $\text{CS}_2/\text{CDCl}_3$) δ ppm 8.17 (d, J = 8.6 Hz, 2H), 8.05 (d, J = 8.6 Hz, 2H), 7.56 (d, J = 8.8 Hz, 2H), 7.54 (d, J = 8.8 Hz, 2H); ¹³C{¹H} NMR (100 MHz, $\text{CS}_2/\text{DMSO}-d_6$, all 1C unless indicated) δ ppm 166.47 (C=O), 148.52, 147.46, 146.52, 146.46, 146.18, 146.07, 145.85, 145.78, 145.74, 145.67, 145.52 (2C), 145.43, 145.36 (2C), 145.29, 145.16 (2C), 145.04, 145.94, 144.80, 144.74, 144.65, 144.58, 144.53 (2C), 144.36, 144.32, 143.72, 143.58, 143.50, 143.44, 142.32, 142.28, 142.18 (2C), 142.12, 142.04, 141.61, 141.60, 141.55, 141.41 (2C), 141.39, 141.34 (2C), 141.23, 141.19, 140.95, 140.76, 139.50, 139.45, 139.39, 139.32, 138.15, 138.06, 136.84 (aryl C), 136.59, 136.41, 135.88 (aryl C), 128.45 (4C, aryl C), 128.26 (aryl C), 127.32 (2C, aryl C), 127.19 (2C, aryl C), 126.89 (aryl C), 111.79, 91.37, 81.55 (sp^3 -C of C_{60}), 75.99 (sp^3 -C of C_{60}); FT-IR ν/cm^{-1} (KBr) 2921, 1811, 1599, 1504, 1427, 1399, 1353, 1297, 1178, 1089, 1042, 1009, 981, 900, 812, 765, 703, 642, 553, 523; UV-vis (CHCl_3) λ_{max} nm (log ϵ) 258 (4.84), 316 (4.38), 429 (3.24); MALDI-TOF MS m/z calcd for $\text{C}_{75}\text{H}_8^{35}\text{Cl}_2\text{O}_3$ [M]⁺ 1025.9856, found 1025.9860.

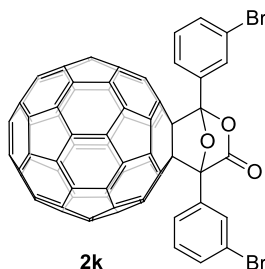


Preparation of 2i: by following the general procedure, the reaction of C_{60} (35.7 mg, 0.05 mmol) with **1i** (27.4 mg, 0.15 mmol) and $\text{CuCl}_2 \cdot 2\text{H}_2\text{O}$ (17.0 mg, 0.10 mmol) at 150 °C

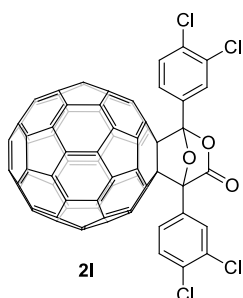
for 12 h afforded **2i** (18.4 mg, 36%) as brown amorphous solid along with unreacted C₆₀ (17.1 mg, 48%). ¹H NMR (400 MHz, CS₂/DMSO-d₆) δ ppm 7.91 (s, 1H), 7.86–7.80 (m, 2H), 7.75–7.69 (m, 1H), 7.32–7.27 (m, 2H), 7.26–7.19 (m, 2H); ¹³C{¹H} NMR (100 MHz, CS₂/DMSO-d₆, all 1C unless indicated) δ ppm 166.78 (C=O), 148.77, 147.73, 147.06, 147.01, 146.59, 146.48, 146.39, 146.33, 146.29, 146.21, 146.03 (2C), 145.97, 145.90, 145.87, 145.83, 145.75 (2C), 145.58, 145.47, 145.35, 145.28, 145.21, 145.14 (2C), 144.99, 144.89, 144.84, 144.26, 144.13, 144.05, 143.99, 142.84, 142.82, 142.72, 142.70, 142.67, 142.58, 142.17 (2C), 142.09, 141.97 (2C), 141.93, 141.90 (2C), 141.79, 141.75, 141.54, 141.35, 140.08, 140.03, 139.96, 139.87, 138.72, 138.63, 137.28, 137.07, 135.39 (aryl C), 135.35 (aryl C), 132.21 (aryl C), 130.86 (aryl C), 130.84 (aryl C), 130.17 (aryl C), 130.10 (aryl C), 129.92 (aryl C), 126.63 (aryl C), 126.58 (aryl C), 124.70 (aryl C), 124.56 (aryl C), 111.99, 91.63, 81.99 (sp³-C of C₆₀), 76.40 (sp³-C of C₆₀); FT-IR ν/cm⁻¹ (KBr) 2921, 1809, 1573, 1518, 1423, 1381, 1273, 1180, 1019, 880, 775, 749, 685, 596, 552, 525, 459; UV-vis (CHCl₃) λ_{max} nm (log ε) 257 (4.81), 316 (4.39), 429 (3.22); MALDI-TOF MS *m/z* calcd for C₇₅H₈³⁵Cl₂O₃ [M]⁺ 1025.9856, found 1025.9851.



Preparation of 2j: by following the general procedure, the reaction of C₆₀ (35.8 mg, 0.05 mmol) with **1j** (34.5 mg, 0.15 mmol) and CuCl₂·2H₂O (17.6 mg, 0.10 mmol) at 150 °C for 9 h afforded **2j** (26.5 mg, 48%) as brown amorphous solid along with unreacted C₆₀ (16.6 mg, 46%). ¹H NMR (400 MHz, CS₂/DMSO-d₆) δ ppm 8.05 (d, *J* = 8.6 Hz, 2H), 7.94 (d, *J* = 8.6 Hz, 2H), 7.69 (d, *J* = 8.6 Hz, 2H), 7.65 (d, *J* = 8.6 Hz, 2H); ¹³C{¹H} NMR (100 MHz, CS₂/DMSO-d₆, all 1C unless indicated) δ ppm 166.76 (C=O), 148.83, 147.76, 146.88, 146.83, 146.51, 146.39, 146.21, 146.15, 146.11, 146.04, 145.87 (2C), 145.80, 145.72 (2C), 145.65, 145.54 (2C), 145.42, 145.31, 145.17, 145.11, 145.02, 144.95, 144.90 (2C), 144.72, 144.68, 144.09, 143.95, 143.87, 143.81, 142.69, 142.64, 142.55 (2C), 142.49, 142.40, 141.98, 141.96, 141.91, 141.79 (2C), 141.75, 141.72, 141.70, 141.60, 141.57, 141.32, 141.13, 139.87, 139.83, 139.78, 139.71, 138.52, 138.43, 136.97, 136.79, 131.85 (4C, aryl C), 129.09 (aryl C), 127.93 (2C, aryl C), 127.79 (2C, aryl C), 127.73 (aryl C), 125.80 (aryl C), 124.82 (aryl C), 112.22, 91.77, 81.84 (sp³-C of C₆₀), 76.24 (sp³-C of C₆₀); FT-IR ν/cm⁻¹ (KBr) 2920, 2850, 1820, 1594, 1515, 1491, 1398, 1351, 1290, 1180, 1155, 1071, 1008, 982, 906, 809, 769, 553, 524; UV-vis (CHCl₃) λ_{max} nm (log ε) 256 (5.18), 317 (4.71), 428 (3.47); MALDI-TOF MS *m/z* calcd for C₇₅H₈⁷⁹Br₂O₃ [M]⁺ 1113.8846, found 1113.8840.

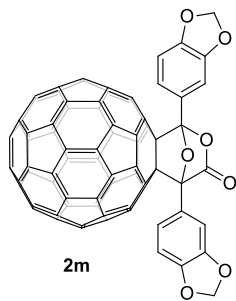


Preparation of **2k:** by following the general procedure, the reaction of C₆₀ (36.0 mg, 0.05 mmol) with **1k** (34.2 mg, 0.15 mmol) and CuCl₂·2H₂O (16.5 mg, 0.10 mmol) at 150 °C for 13 h afforded **2k** (25.4 mg, 46%) as brown amorphous solid along with unreacted C₆₀ (17.5 mg, 49%). ¹H NMR (400 MHz, C₂D₂Cl₄) δ ppm 8.30 (t, *J* = 1.8 Hz, 1H), 8.21 (t, *J* = 1.8 Hz, 1H), 8.16–8.12 (m, 1H), 8.03–7.99 (m, 1H), 7.69–7.65 (m, 1H), 7.64–7.60 (m, 1H), 7.44 (t, *J* = 7.5 Hz, 1H), 7.42 (t, *J* = 7.5 Hz, 1H); ¹³C{¹H} NMR (100 MHz, C₂D₂Cl₄, all 1C unless indicated) δ ppm 169.07 (C=O), 148.81, 147.86, 147.47, 147.40, 146.83, 146.73, 146.68 (3C), 146.59, 146.42, 146.34, 146.28, 146.26, 146.20 (2C), 146.09, 146.06, 145.93, 145.83, 145.72, 145.65, 145.60, 145.54, 145.39, 145.15, 145.11, 145.03, 144.55, 144.46, 144.37, 144.30, 143.22, 143.18, 143.05, 143.04, 143.01, 142.93, 142.49, 142.46, 142.37, 142.30 (3C), 142.25, 142.23, 142.08, 142.06, 141.87, 141.70, 140.40, 140.38, 140.33, 140.20, 138.85, 138.80, 137.71, 137.46, 134.45 (aryl C), 133.43 (aryl C), 132.34 (aryl C), 131.15 (aryl C), 130.91 (aryl C), 130.86 (aryl C), 129.53 (aryl C), 129.49 (aryl C), 125.66 (aryl C), 125.61 (aryl C), 123.31 (aryl C), 123.25 (aryl C), 112.92, 92.40, 82.24 (sp³-C of C₆₀), 76.72 (sp³-C of C₆₀); FT-IR ν/cm⁻¹ (KBr) 2924, 2847, 1821, 1511, 1422, 1348, 1294, 1268, 1185, 1041, 1018, 983, 906, 881, 778, 766, 760, 721, 692, 554, 527; UV-vis (CHCl₃) λ_{max} nm (log ε) 256 (5.09), 317 (4.62), 428 (3.41); MALDI-TOF MS *m/z* calcd for C₇₅H₈⁷⁹Br₂O₃ [M]⁺ 1113.8846, found 1113.8823.

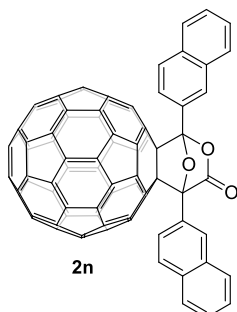


Preparation of **2l:** by following the general procedure, the reaction of C₆₀ (35.6 mg, 0.05 mmol) with **1l** (33.2 mg, 0.15 mmol) and CuCl₂·2H₂O (17.4 mg, 0.10 mmol) at 150 °C for 13 h afforded **2l** (28.6 mg, 52%) as brown amorphous solid along with unreacted C₆₀ (14.2 mg, 40%). ¹H NMR (400 MHz, 1:1 CS₂/C₂D₂Cl₄) δ ppm 8.26 (d, *J* = 2.0 Hz, 1H), 8.16 (d, *J* = 2.0 Hz, 1H), 8.04 (dd, *J* = 8.3, 2.0 Hz, 1H), 7.91 (dd, *J* = 8.3, 2.0 Hz, 1H), 7.64 (d, *J* = 8.3 Hz, 1H), 7.62 (d, *J* = 8.3 Hz, 1H); ¹³C{¹H} NMR (100 MHz, 1:1 CS₂/C₂D₂Cl₄, all 1C unless indicated) δ ppm 168.25 (C=O), 148.30, 147.41, 147.34 (2C), 146.67, 146.62 (2C), 146.53, 146.37, 146.35, 146.30, 146.20 (2C), 146.15, 146.06, 146.03, 145.98, 145.93, 145.84, 145.82, 145.66, 145.59, 145.53, 145.47, 145.27,

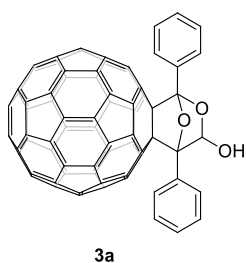
144.98, 144.95, 144.77, 144.48, 144.37, 144.29, 144.21, 143.16, 143.13, 143.01, 142.99, 142.96, 142.87, 142.40, 142.39, 142.26 (2C), 142.22, 142.19, 142.16 (2C), 142.04, 142.02, 141.74, 141.57, 140.41 (2C), 140.38, 140.30, 138.85, 138.79, 137.63, 137.40, 135.85 (aryl C), 134.81 (aryl C), 133.79 (aryl C), 133.73 (aryl C), 131.33 (aryl C), 131.27 (aryl C), 130.23 (aryl C), 129.02 (aryl C), 128.55 (2C, aryl C), 126.15 (aryl C), 126.03 (aryl C), 112.47, 92.02, 82.00 (sp^3 -C of C_{60}), 76.46 (sp^3 -C of C_{60}); FT-IR ν/cm^{-1} (KBr) 2923, 2853, 1817, 1508, 1474, 1427, 1386, 1353, 1301, 1247, 1180, 1137, 1033, 1020, 984, 909, 881, 813, 775, 548, 524; UV-vis (CHCl_3) λ_{\max} nm ($\log \epsilon$) 256 (5.13), 317 (4.67), 428 (3.40); MALDI-TOF MS m/z calcd for $\text{C}_{75}\text{H}_6^{35}\text{Cl}_4\text{O}_3$ [M]⁻ 1093.9077, found 1093.9064.



Preparation of 2m: by following the general procedure, the reaction of C_{60} (35.9 mg, 0.05 mmol) with **1m** (29.4 mg, 0.15 mmol) and $\text{CuCl}_2 \cdot 2\text{H}_2\text{O}$ (16.8 mg, 0.10 mmol) at 150 °C for 14 h afforded **2m** (17.0 mg, 33%) as brown amorphous solid along with unreacted C_{60} (18.0 mg, 50%). ¹H NMR (400 MHz, $\text{C}_2\text{D}_2\text{Cl}_4$) δ ppm 7.66 (dd, $J = 8.2, 1.8$ Hz, 1H), 7.61 (d, $J = 1.7$ Hz, 1H), 7.54 (dd, $J = 8.2, 1.8$ Hz, 1H), 7.47 (d, $J = 1.7$ Hz, 1H), 6.95 (d, $J = 1.8$ Hz, 1H), 6.93 (d, $J = 1.8$ Hz, 1H), 6.02 (s, 2H), 5.99 (s, 2H); ¹³C{¹H} NMR (100 MHz, $\text{C}_2\text{D}_2\text{Cl}_4$, all 1C unless indicated) δ ppm 169.79 (C=O), 149.70, 149.59, 148.77, 148.71, 148.13 (2C, aryl C), 147.32, 147.30, 147.26, 147.17, 146.59 (2C), 146.53 (2C), 146.45 (2C), 146.26, 146.18, 146.11, 146.05, 145.87, 145.84, 145.70, 145.60, 145.56, 145.49, 145.45 (2C), 145.38, 145.35, 145.33, 145.06, 144.48, 144.36, 144.30, 144.21, 143.10, 143.03, 142.88 (3C), 142.80, 142.37 (2C), 142.34, 142.25, 142.19, 142.15 (2C), 142.08, 141.93, 141.89, 141.86, 141.66, 140.18 (2C), 140.11, 140.00, 138.63, 138.57, 137.41, 137.15, 124.02 (aryl C), 122.62 (aryl C), 121.15 (aryl C), 120.98 (aryl C), 113.43, 109.04 (aryl C), 108.98 (aryl C), 107.33 (aryl C), 107.13 (aryl C), 102.19, 101.97, 92.88, 82.43 (sp^3 -C of C_{60}), 77.10 (sp^3 -C of C_{60}); FT-IR ν/cm^{-1} (KBr) 2920, 2847, 1809, 1574, 1505, 1445, 1358, 1299, 1260, 1233, 1182, 1108, 1039, 933, 805, 526, 461; UV-vis (CHCl_3) λ_{\max} nm ($\log \epsilon$) 256 (5.05), 316 (4.62), 428 (3.58); MALDI-TOF MS m/z calcd for $\text{C}_{77}\text{H}_{10}\text{O}_7$ [M]⁻ 1046.0432, found 1046.0419.

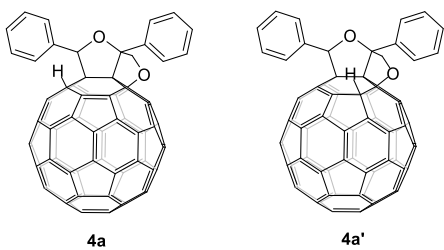


Preparation of **2n:** by following the general procedure, the reaction of C₆₀ (35.6 mg, 0.05 mmol) with **1n** (30.3 mg, 0.15 mmol) and CuCl₂·2H₂O (17.0 mg, 0.10 mmol) at 140 °C for 10 h afforded **2n** (23.2 mg, 44%) as brown amorphous solid along with unreacted C₆₀ (18.3 mg, 51%). ¹H NMR (400 MHz, CS₂/DMSO-*d*₆) δ ppm 8.48 (s, 1H), 8.35 (s, 1H), 8.03 (dd, *J* = 8.6, 1.7 Hz, 1H), 7.91 (dd, *J* = 8.6, 1.7 Hz, 1H), 7.78–7.69 (m, 4H), 7.65–7.58 (m, 2H), 7.34–7.24 (m, 4H); ¹³C{¹H} NMR (100 MHz, CS₂/DMSO-*d*₆, all 1C unless indicated) δ ppm 167.08 (C=O), 149.15, 148.09, 146.88, 146.76, 146.47, 146.42, 145.89, 145.84, 145.78, 145.75, 145.68, 145.62, 145.45, 145.39, 145.30, 145.24, 145.18 (2C), 144.96, 144.85, 144.77 (2C), 144.70, 144.63 (3C), 144.56, 144.46, 143.71, 143.62, 143.50 (2C), 142.26 (2C), 142.11 (2C), 142.08, 141.99, 141.68, 141.63, 141.61, 141.52, 141.41, 141.39, 141.32 (2C), 141.20, 141.16, 141.04, 140.83, 139.46, 139.41, 139.30, 139.22, 138.20, 138.13, 136.68, 136.44, 133.44 (aryl C), 132.93 (aryl C), 132.21 (aryl C), 131.97 (aryl C), 128.29 (aryl C), 128.17 (aryl C), 128.16 (aryl C), 128.08 (aryl C), 127.50 (aryl C), 127.42 (aryl C), 127.37 (aryl C), 127.17 (aryl C), 126.74 (aryl C), 126.57 (aryl C), 126.30 (aryl C), 126.11 (2C, aryl C), 125.97 (aryl C), 123.11 (aryl C), 122.58 (aryl C), 112.46, 92.01, 82.04 (sp³-C of C₆₀), 76.54 (sp³-C of C₆₀); FT-IR ν/cm⁻¹ (KBr) 3052, 2920, 1810, 1599, 1508, 1427, 1360, 1335, 1294, 1176, 1129, 1089, 1039, 1013, 952, 890, 852, 810, 742, 552, 525, 475; UV-vis (CHCl₃) λ_{max} nm (log ε) 257 (5.04), 315 (4.56), 429 (3.46); MALDI-TOF MS *m/z* calcd for C₈₃H₁₄O₃ [M]⁺ 1058.0948, found 1058.0944.



To a stirred solution of **2a** (9.6 mg, 0.01 mmol) in *ortho*-dichlorobenzene (2 mL) under nitrogen atmosphere at room temperature was added diisobutyl aluminium hydride (DIBAL-H) (0.02 mL, 1.5 mol/L solution in toluene, 0.03 mmol). After being stirred for 15 min, the reaction mixture was quenched with acetic acid and then filtered through a silica gel plug to remove any insoluble material. After evaporation in vacuo, the residue was separated on a silica gel column with CS₂/dichloromethane (DCM) (4:1) as the eluent to give the product **3a** (8.0 mg, 86%) as brown amorphous solid. ¹H NMR (400 MHz, 1:1 CS₂/CDCl₃) δ ppm 8.19 (s, 1H), 8.12–8.06 (m, 2H), 7.72 (s, 1H), 7.61–

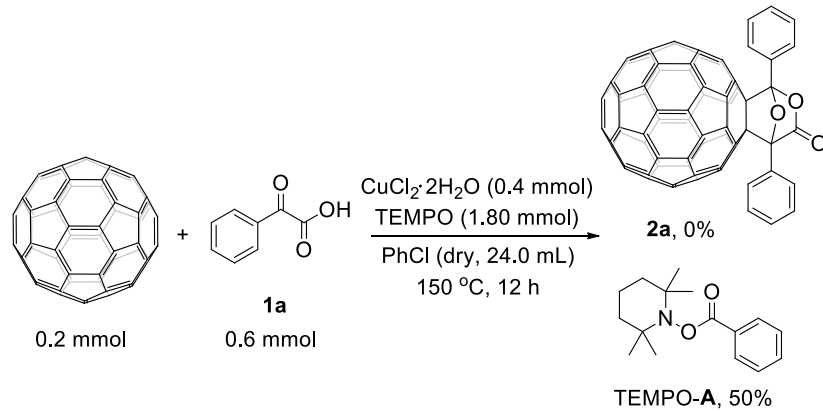
7.39 (m, 6H), 6.90 (d, J = 11.9 Hz, 1H), 2.97 (d, J = 11.9 Hz, 1H, OH); $^{13}\text{C}\{\text{H}\}$ NMR (100 MHz, 1:1 CS₂/CDCl₃, all 1C unless indicated) δ ppm 151.70, 150.30, 149.69, 148.41, 147.19, 147.11, 147.05, 146.94, 146.46, 146.36, 146.32, 146.24, 146.12 (2C), 145.95, 145.92, 145.83, 145.78, 145.55, 145.53, 145.41 (2C), 145.39 (2C), 145.35, 145.29, 145.28, 145.12, 144.47 (2C), 144.37, 144.08, 143.06, 143.00, 142.80, 142.73 (2C), 142.62, 142.30 (2C), 142.24, 142.21, 142.08, 142.05, 142.03 (2C), 141.87, 141.72, 141.68, 141.64, 140.00, 139.91, 139.86, 139.67, 138.90, 138.32, 136.70, 136.49, 133.22 (aryl C), 132.49 (aryl C), 129.79 (aryl C), 129.18 (aryl C), 129.05 (aryl C), 128.63 (aryl C), 128.42 (2C, aryl C), 127.67 (aryl C), 127.11 (aryl C), 126.98 (2C, aryl C), 113.03, 99.28, 96.70, 83.81 (sp³-C of C₆₀), 77.37 (sp³-C of C₆₀); FT-IR ν/cm^{-1} (KBr) 3529, 2908, 1508, 1444, 1422, 1351, 1297, 1261, 1181, 1135, 1066, 1015, 993, 925, 906, 851, 825, 739, 717, 695, 527; UV-vis (CHCl₃) λ_{max} nm (log ϵ) 256 (5.04), 313 (4.55), 429 (3.44), 695 (3.31); MALDI-TOF MS m/z calcd for C₇₅H₁₂O₃ [M]⁺ 960.0792, found 960.0798.



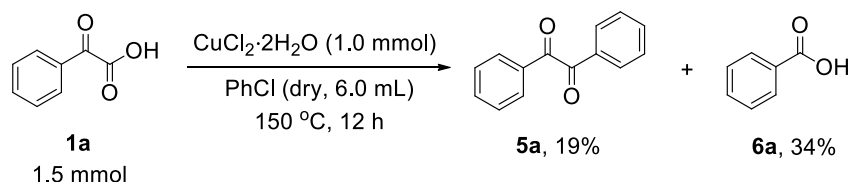
To a stirred solution of **2a** (48.0 mg, 0.05 mmol) in *ortho*-dichlorobenzene (10 mL) under nitrogen atmosphere at 0 °C was added DIBAL-H (0.226 mL, 1.0 mol/L in *n*-hexane, 0.226 mmol). After being stirred for 3 h, the reaction mixture was treated with triethylsilane (Et₃SiH) (0.036 mL, 0.225 mmol) and ethylaluminum dichloride (EtAlCl₂) (114.4 mg, 25 wt% in *n*-hexane, 0.225 mmol) dropwise, and the resultant mixture was stirred at 0 °C for 4 h. The reaction mixture was quenched with triethylamine and then filtered through a silica gel plug to remove any insoluble material. After evaporation in vacuo, the residue was separated on a silica gel column with CS₂ as the eluent to give products **4a** (29.4 mg, 62%) and **4a'** (7.5 mg, 16%) as brown amorphous solids. **4a**: ^1H NMR (400 MHz, CS₂/DMSO-*d*₆) δ ppm 7.59 (d, J = 7.3 Hz, 2H), 7.29 (d, J = 7.2 Hz, 2H), 7.19 (t, J = 7.5 Hz, 2H), 7.15–7.04 (m, 4H), 6.35 (s, 1H), 6.22 (s, 1H), 4.86 (d, J = 11.4 Hz, 1H), 4.42 (d, J = 11.4 Hz, 1H); $^{13}\text{C}\{\text{H}\}$ NMR (100 MHz, CS₂/DMSO-*d*₆, all 1C unless indicated) δ ppm 150.39, 149.62, 148.52, 148.36, 148.18 (2C), 147.82, 147.46, 147.21, 146.42, 146.36, 146.15 (2C), 145.84 (2C), 145.56, 145.50, 144.96, 144.59, 144.54, 144.41, 144.13, 143.98, 143.92, 143.68, 143.60 (5C), 143.48, 143.40 (2C), 143.32, 142.88 (2C), 142.60 (2C), 142.14 (2C), 141.79, 141.74, 141.69, 141.58, 141.50 (2C), 141.19, 141.10, 140.48, 140.43, 140.25, 139.78, 137.44, 136.68, 136.12, 135.78, 135.63 (aryl C), 134.98 (aryl C), 128.19 (aryl C), 128.12 (2C, aryl C), 127.92 (4C, aryl C), 127.61 (aryl C), 126.67 (2C, aryl C), 97.61, 97.39 (sp³-C of C₆₀), 89.20, 80.15 (sp³-C of C₆₀), 76.88, 74.31 (sp³-C of C₆₀), 59.65 (sp³-C of C₆₀); FT-IR ν/cm^{-1} (KBr) 2914, 2853, 1511, 1454, 1150, 1125, 1079, 1024, 983, 900, 872, 780, 751, 715, 701, 572, 526; UV-vis (CHCl₃) λ_{max} nm (log ϵ) 257 (5.05), 335 (4.47), 429 (3.74); MALDI-TOF MS m/z calcd for C₇₅H₁₄O₂ [M]⁺ 946.0999, found 946.0992. **4a'**: ^1H

NMR (400 MHz, CS₂/DMSO-*d*₆) δ ppm 8.02 (d, *J* = 7.8 Hz, 2H), 7.78 (d, *J* = 7.4 Hz, 2H), 7.37 (t, *J* = 7.4 Hz, 2H), 7.34–7.23 (m, 3H), 7.18 (t, *J* = 7.2 Hz, 1H), 6.78 (s, 1H), 6.34 (s, 1H), 5.63 (d, *J* = 9.7 Hz, 1H), 5.07 (d, *J* = 9.7 Hz, 1H); ¹³C{¹H} NMR (100 MHz, CS₂/DMSO-*d*₆, all 1C unless indicated) δ ppm 150.53, 148.29, 148.08, 147.94, 147.40, 147.36, 147.33, 146.79, 146.41, 146.37, 146.23, 146.18, 146.03, 145.84, 145.78, 145.72, 145.18, 145.11, 144.62, 144.38, 144.10 (2C), 144.00, 143.97, 143.76, 143.71 (2C), 143.68, 143.65, 143.62, 143.57, 143.45, 143.42 (2C), 142.89, 142.87, 142.82, 142.54, 142.42, 142.22, 142.18 (2C), 142.01, 141.88, 141.79, 141.64, 141.25, 141.23, 140.77, 140.16, 140.00 (aryl C), 139.94, 137.70, 137.68, 136.70, 135.89 (aryl C), 135.58, 134.21, 128.40 (aryl C), 128.18 (2C, aryl C), 127.88 (2C, aryl C), 127.66 (aryl C), 126.98 (2C, aryl C), 125.88 (2C, aryl C), 97.59, 96.21 (*sp*³-C of C₆₀), 88.82, 79.43 (*sp*³-C of C₆₀), 74.69, 73.86 (*sp*³-C of C₆₀), 57.96 (*sp*³-C of C₆₀); FT-IR ν/cm⁻¹ (KBr) 2914, 2847, 1511, 1490, 1447, 1421, 1281, 1258, 1190, 1142, 1088, 1044, 981, 917, 904, 871, 751, 697, 615, 566, 544, 525; UV-vis (CHCl₃) λ_{max} nm (log ε) 258 (5.01), 333 (4.44), 428 (3.72); MALDI-TOF MS *m/z* calcd for C₇₅H₁₄O₂ [M]⁺ 946.0999, found 946.0985.

5. Control experiments



A mixture of C₆₀ (144.0 mg, 0.2 mmol), **1a** (90.4 mg, 0.6 mmol), CuCl₂·2H₂O (67.8 mg, 0.4 mmol), and 2,2,6,6-tetramethyl-1-piperidinyloxy (TEMPO) (281.5 mg, 1.8 mmol) was dissolved in anhydrous chlorobenzene (24.0 mL), and the reaction was performed in a sealed tube. Then the solution was vigorously stirred in an oil bath at 150 °C for 12 h. The resulting solution was evaporated in vacuo, and the residue was then separated on a silica gel column with CS₂ as the eluent to give the recovered C₆₀ (140.0 mg, 97%). Finally, TEMPO-A (79.0 mg, 50%) was separated out using petroleum ether/ethyl acetate (10:1) as the eluent. TEMPO-A: ¹H NMR (400 MHz, CDCl₃) δ ppm 8.08 (d, *J* = 7.8 Hz, 2H), 7.58 (t, *J* = 7.2 Hz, 1H), 7.47 (t, *J* = 7.6 Hz, 2H), 1.84–1.65 (m, 3H), 1.63–1.57 (m, 2H), 1.50–1.43 (m, 1H), 1.28 (s, 6H), 1.12 (s, 6H).



A mixture of **1a** (225.5 mg, 1.5 mmol) and CuCl₂·2H₂O (169.7 mg, 1.0 mmol) was dissolved in anhydrous chlorobenzene (6.0 mL), and the reaction was performed in a sealed tube. Then the solution was stirred in an oil bath at 150 °C for 12 h. The resulting solution was evaporated in vacuo, and the residue was then separated on a silica gel column with petroleum ether/ethyl acetate (10/1) as the eluent to give **5a** (29.4 mg, 19%). Finally, **6a** (62.4 mg, 34%) and the unreacted **1a** (87.6 mg, 39%) were separated out using petroleum ether/ethyl acetate (3:1) as the eluent. **5a**:² ¹H NMR (400 MHz, CDCl₃) δ ppm 8.03–7.94 (m, 4H), 7.67 (tt, *J* = 7.4, 1.3 Hz, 2H), 7.52 (t, *J* = 7.8 Hz, 4H); **6a**:³ ¹H NMR (400 MHz, CDCl₃) δ ppm 12.15 (s, 1H), 8.18–8.09 (m, 2H), 7.63 (tt, *J* = 7.4, 1.3 Hz, 1H), 7.49 (t, *J* = 7.7 Hz, 2H).

6. Device fabrication

Indium-doped tin oxide (ITO) patterned glass substrates were cleaned by sequential ultrasonic treatment with detergent, deionized water, acetone and isopropanol in an ultrasonic bath for 15 min, respectively. Next, the cleaned ITO substrates were treated with UV/O₃ for 15 min. Subsequently, 65 μL of SnO₂ precursor solution (2.67% in water) was spin-coated on the cleaned ITO substrate at 4000 rpm for 30 s, which was annealed at 170 °C for 30 min. After cooling down to room temperature, the SnO₂ coated ITO glass was further treated with UV/O₃ for 3 min before spin-coating of the solution of **4a** (0.3 mg/mL in chlorobenzene). 25 μL of the **4a** solution was spin-coated on the top of the SnO₂ layer at 4000 rpm for 30 s. Next, 25 μL of perovskite precursor solution (1.2 M CH₃NH₃I and 1.2 M PbI₂ in 700 μL DMF and 300 μL DMSO) was spin-coated on the fullerene layer at 3500 rpm for 30 s, with slowly dropping 200 μL of anhydrous chlorobenzene onto the substrate at 10 s after starting the spin-coating process, followed up with annealing at 100 °C for 10 min. For 2,2',7,7'-tetrakis (*N,N*-di-pmethoxyphenylamine)-9,9'-spirobifluorene (Spiro-OMeTAD) hole transporting layer, Spiro-OMeTAD in chlorobenzene solution (72.3 mg/mL) was employed with the additives containing 17.5 μL bis(trifluoromethane) sulfonimide lithium salt (Li-TFSI)/acetonitrile (520 mg/mL), 29 μL 4-*tert*-butylpyridine (TBP), and 29 μL tris(2-(1*H*-pyrazol-1-yl)-4-*tert*-butylpyridine)cobalt(III) tris(bis(trifluoromethylsulfonyl) imide)) (FK209)/acetonitrile (300 mg/mL), and spin-coated by solution process at 4000 rpm for 30 s. Finally, an 80-nm-thick of Ag anode was fabricated by thermal deposition at a constant evaporation rate of 0.05 nm s⁻¹ under the pressure of 10⁻⁶ Torr.

Table S2. Photovoltaic parameters of the n-type perovskite solar cells without overcoating layer and using **4a** as the overcoating layer of ETL under 1 sun (AM 1.5 G, 100 mW cm⁻²)^a.

Overcoating layer	V _{oc} (V)	J _{sc} (mA/cm ²)	FF (%)	PCE (%)	R _s (Ω·cm ²)	R _{sh} (Ω·cm ²)
-	1.07 ± 0.01 (1.07)	22.38 ± 1.08 (21.56)	71.83 ± 4.52 (75.35)	17.21 ± 0.28 (17.44)	4.6	76.1
4a	1.09 ± 0.01 (1.09)	23.11±0.54 (23.28)	71.50 ± 2.11 (73.05)	18.04 ± 0.46 (18.49)	5.0	1008.7

^aThe data were from reverse scan and averaged over 6 devices in the same batch. The best device performance were shown in brackets.

It should be noted that we also attempted to use products **2a** and **3a** as the overcoating layer. Although **2a** was soluble in 1,2-dichlorobenzene and carbon disulfide, its solubility in chlorobenzene was too low to be applied in the perovskite solar cell. When **3a** was the overcoating layer, no improvement in power conversion efficiency (PCE) was observed.

7. NMR spectra of compounds **2a–n**, **3a**, **4a**, **4a'**, TEMPO-A, **5a** and **6a**

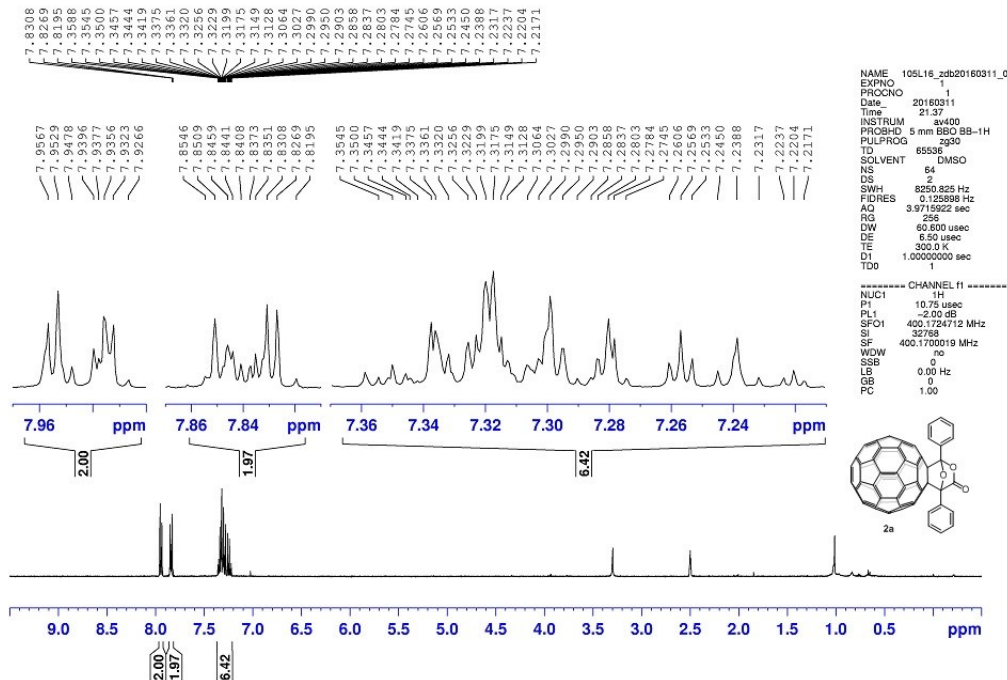


Figure S1. ¹H NMR (400 MHz, CS₂/DMSO-*d*₆) of **2a**.

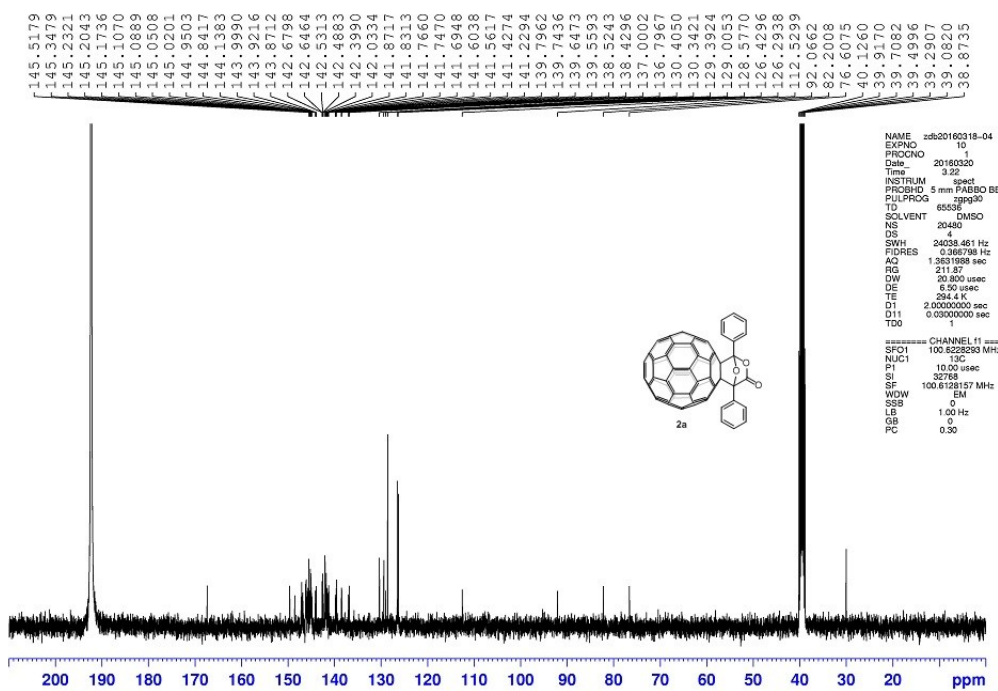


Figure S2. $^{13}\text{C}\{\text{H}\}$ NMR (100 MHz, $\text{CS}_2/\text{DMSO}-d_6$) of **2a**.

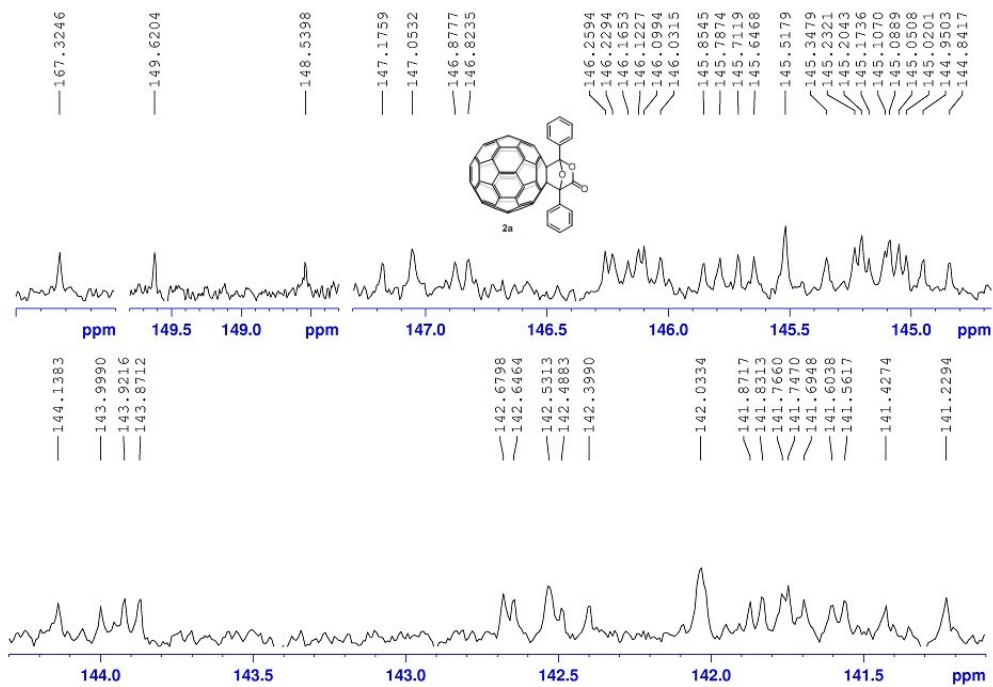


Figure S3. Expanded $^{13}\text{C}\{\text{H}\}$ NMR (100 MHz, $\text{CS}_2/\text{DMSO}-d_6$) of **2a**.

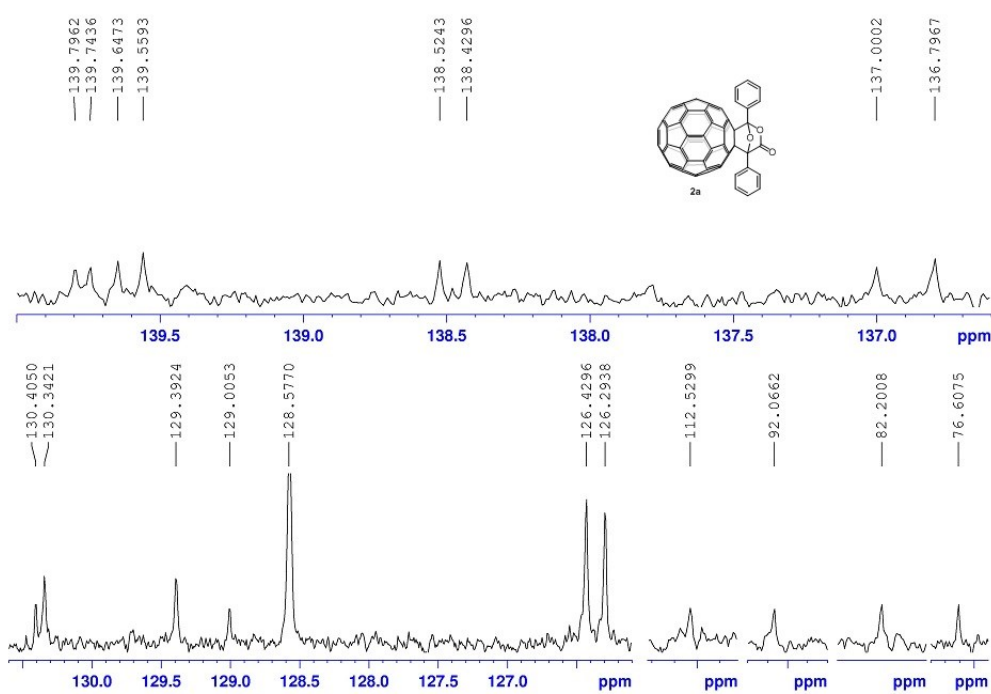


Figure S4. Expanded $^{13}\text{C}\{\text{H}\}$ NMR (100 MHz, $\text{CS}_2/\text{DMSO}-d_6$) of **2a**.

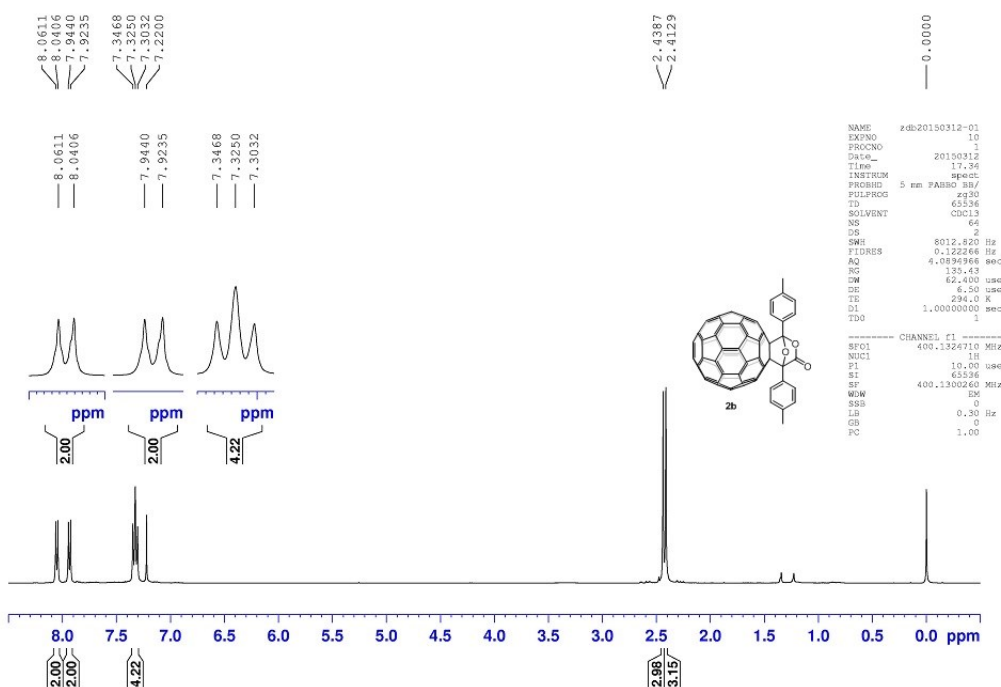


Figure S5. ^1H NMR (400 MHz, 1:1 $\text{CS}_2/\text{CDCl}_3$) of **2b**.

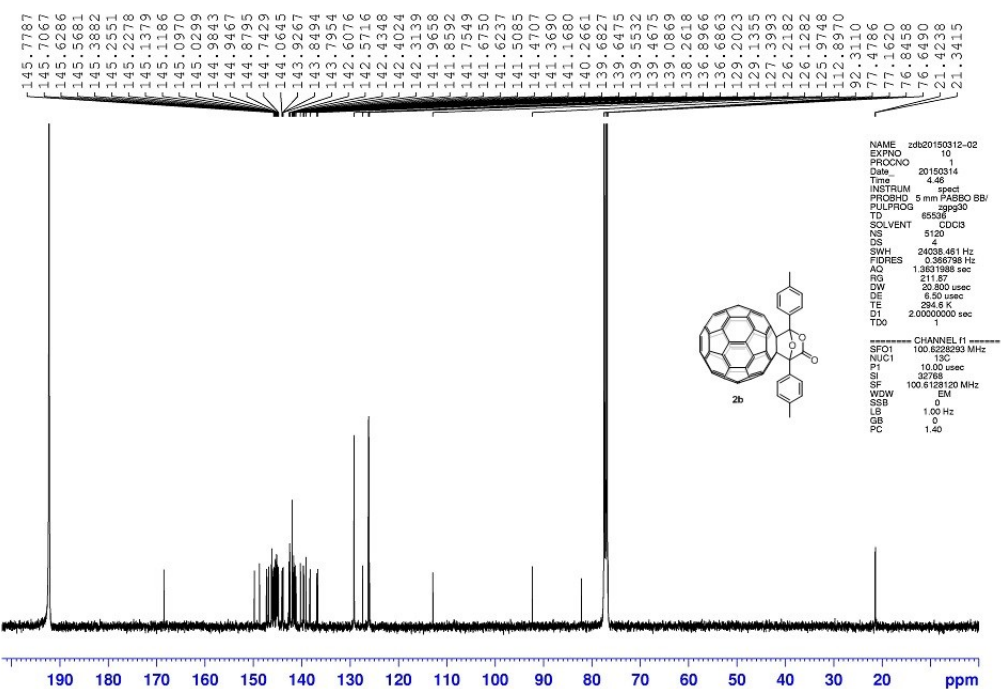


Figure S6. $^{13}\text{C}\{\text{H}\}$ NMR (100 MHz, 1:1 CS₂/CDCl₃) of **2b**.

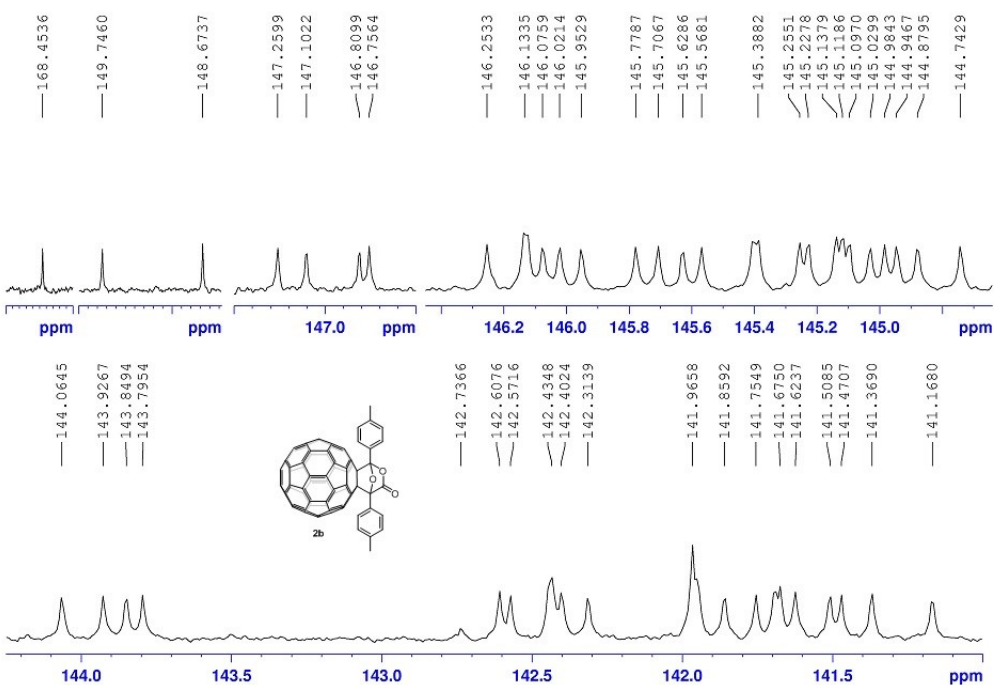


Figure S7. Expanded $^{13}\text{C}\{\text{H}\}$ NMR (100 MHz, 1:1 CS₂/CDCl₃) of **2b**.

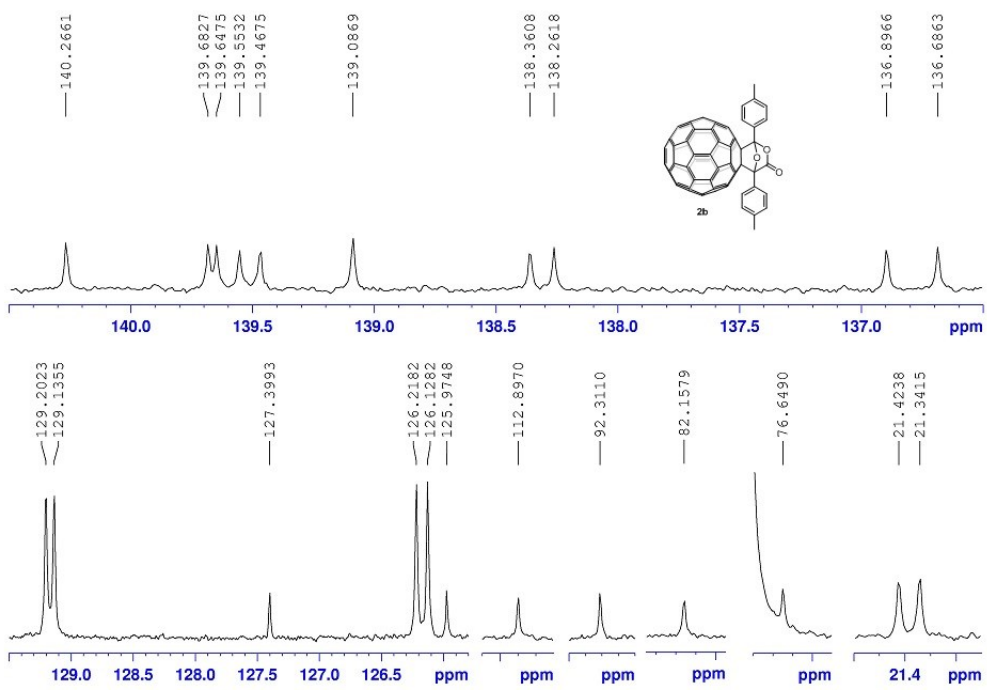


Figure S8. Expanded $^{13}\text{C}\{\text{H}\}$ NMR (100 MHz, 1:1 $\text{CS}_2/\text{CDCl}_3$) of **2b**.

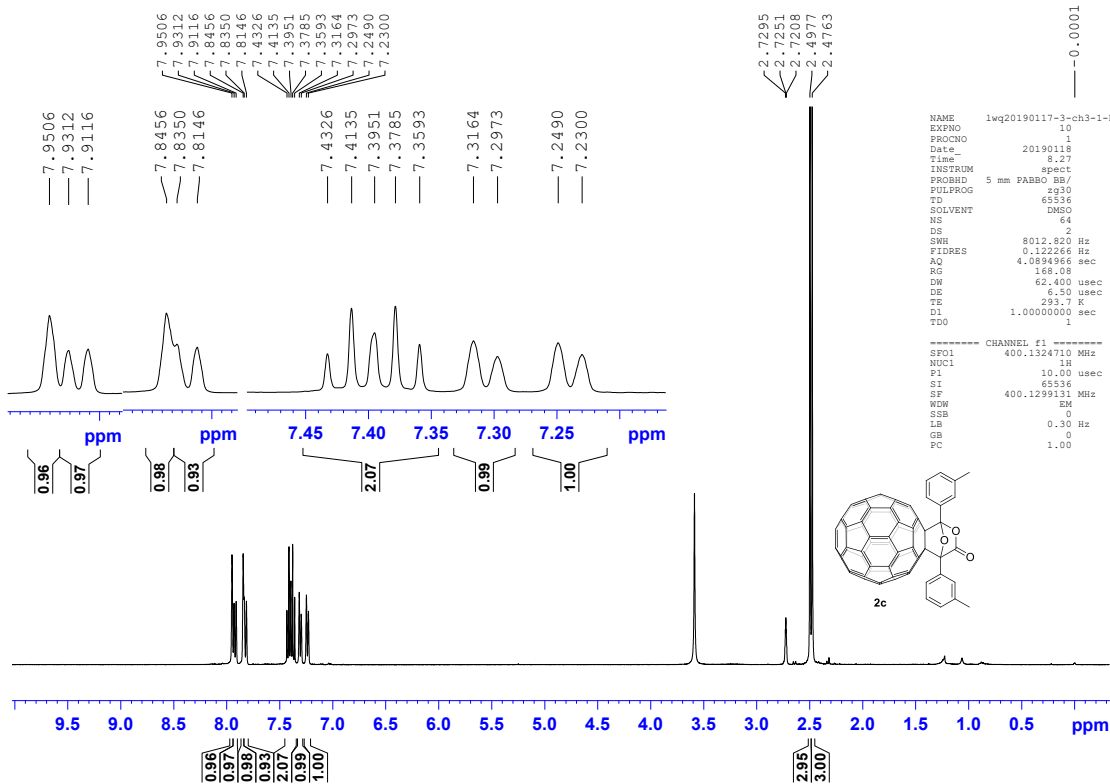


Figure S9. ^1H NMR (400 MHz, $\text{CS}_2/\text{DMSO}-d_6$) of **2c**.

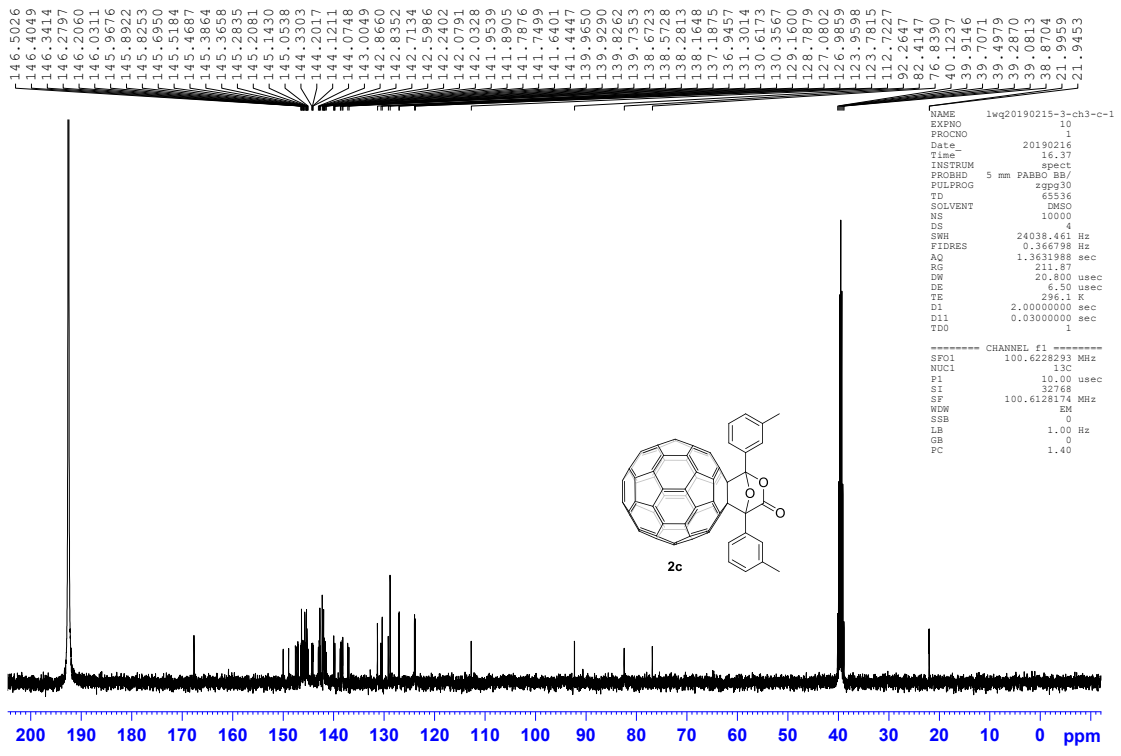


Figure S10. $^{13}\text{C}\{\text{H}\}$ NMR (100 MHz, $\text{CS}_2/\text{DMSO}-d_6$) of **2c**.

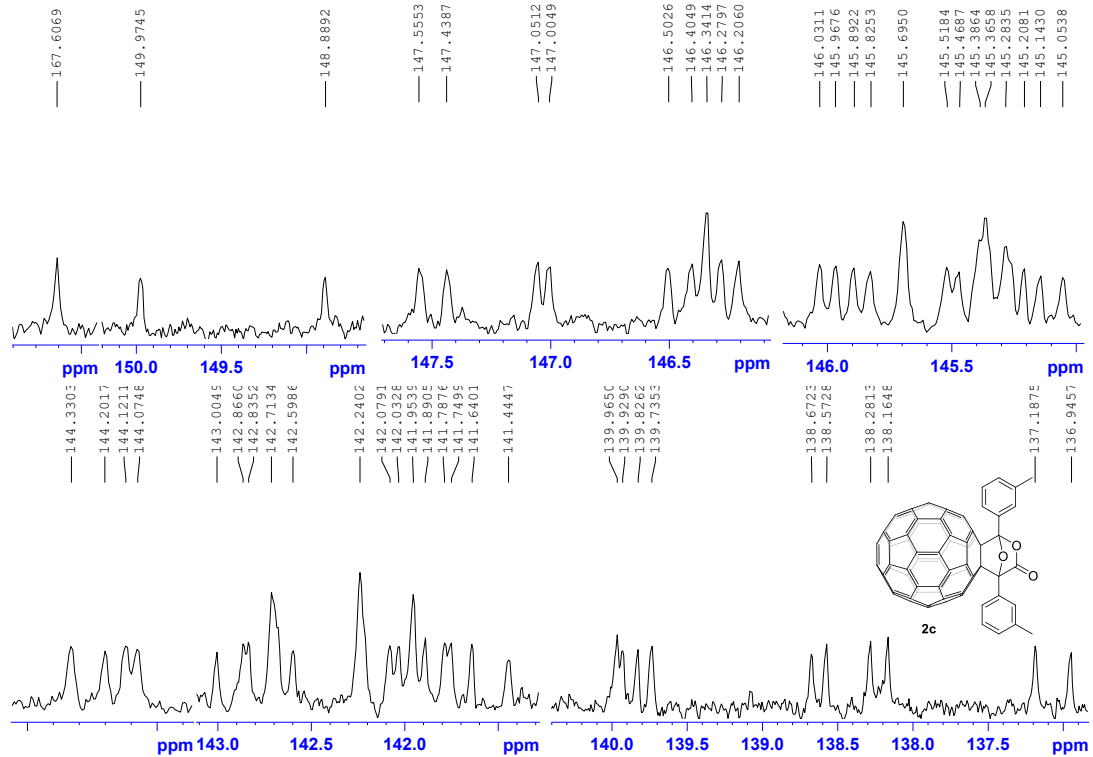


Figure S11. Expanded $^{13}\text{C}\{\text{H}\}$ NMR (100 MHz, $\text{CS}_2/\text{DMSO}-d_6$) of **2c**.

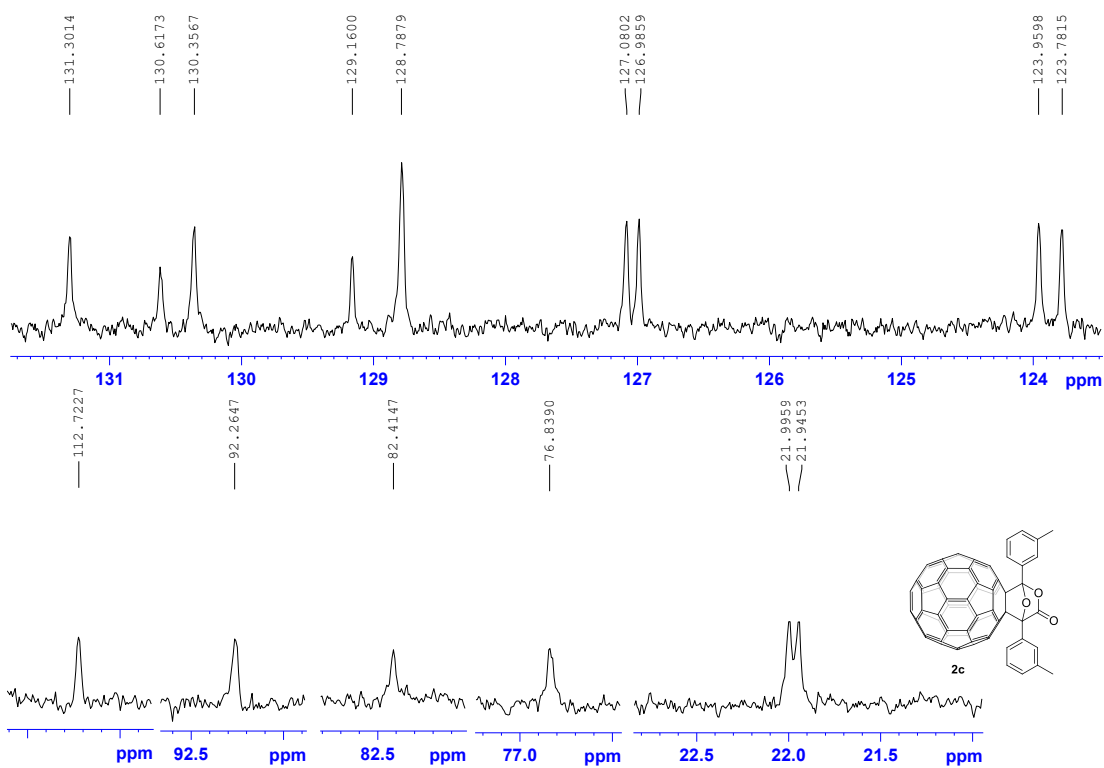


Figure S12. Expanded $^{13}\text{C}\{\text{H}\}$ NMR (100 MHz, $\text{CS}_2/\text{DMSO}-d_6$) of **2c**.

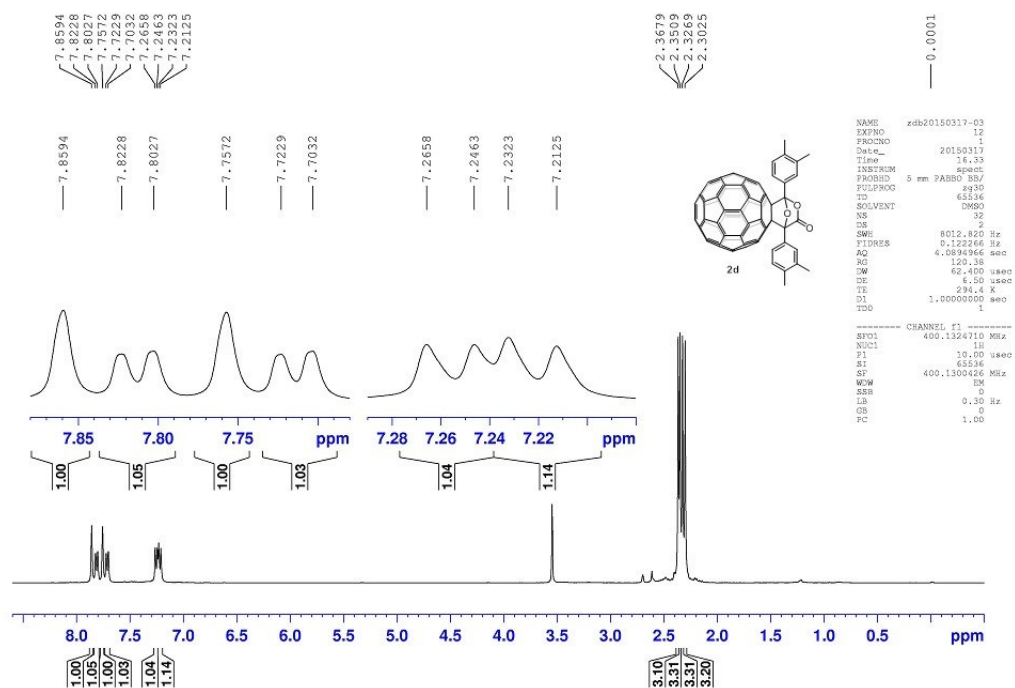


Figure S13. ^1H NMR (400 MHz, $\text{CS}_2/\text{DMSO}-d_6$) of **2d**.

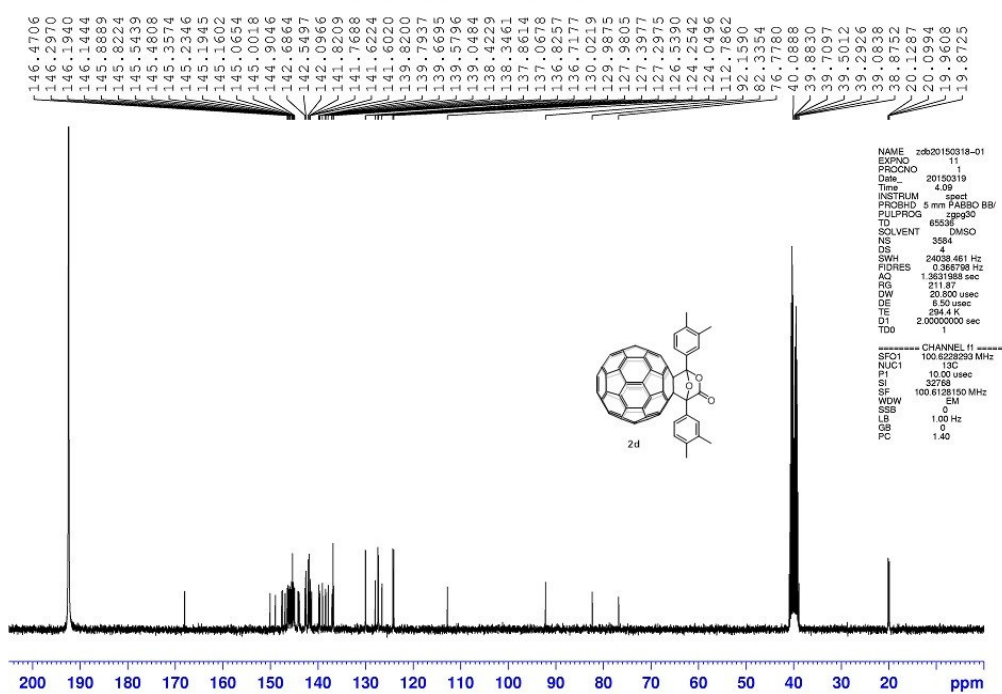


Figure S14. $^{13}\text{C}\{^1\text{H}\}$ NMR (100 MHz, $\text{CS}_2/\text{DMSO}-d_6$) of **2d**.

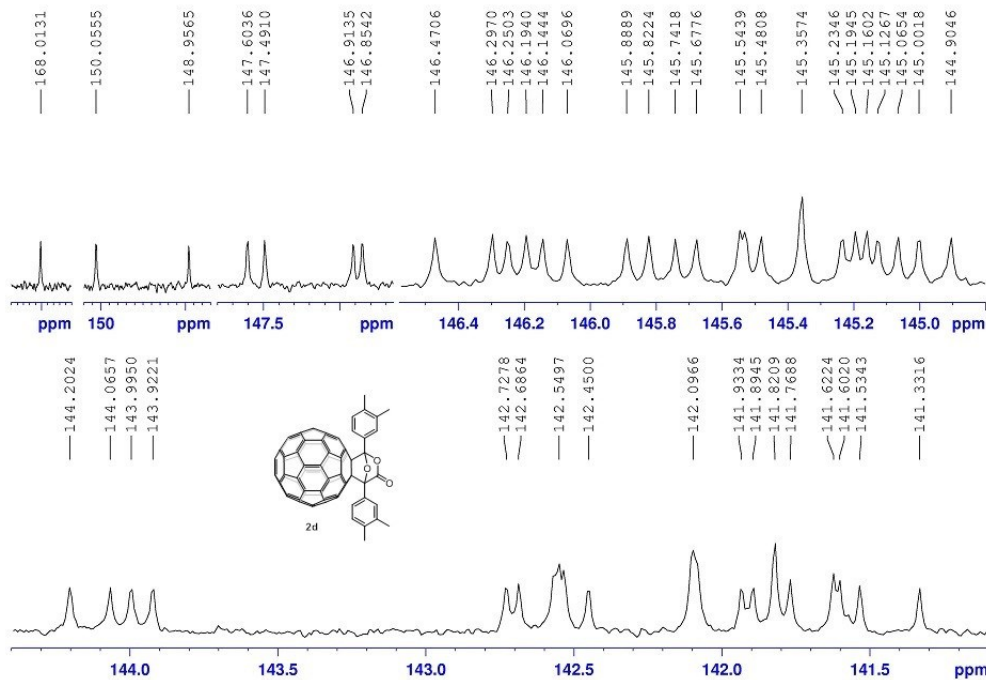


Figure S15. Expanded $^{13}\text{C}\{^1\text{H}\}$ NMR (100 MHz, $\text{CS}_2/\text{DMSO}-d_6$) of **2d**.

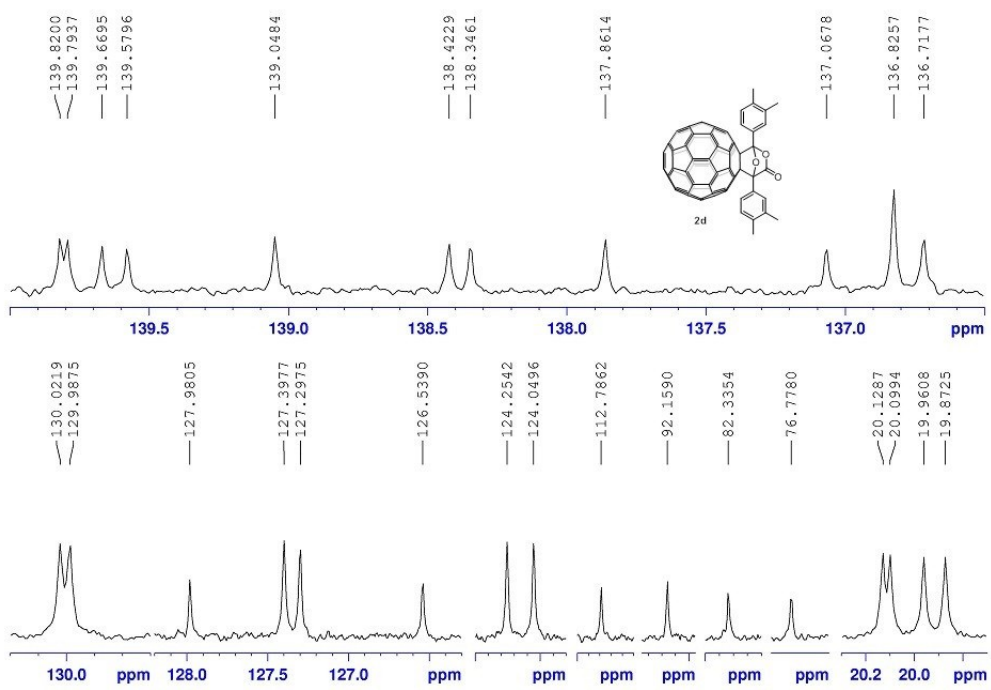


Figure S16. Expanded $^{13}\text{C}\{^1\text{H}\}$ NMR (100 MHz, $\text{CS}_2/\text{DMSO}-d_6$) of **2d**.

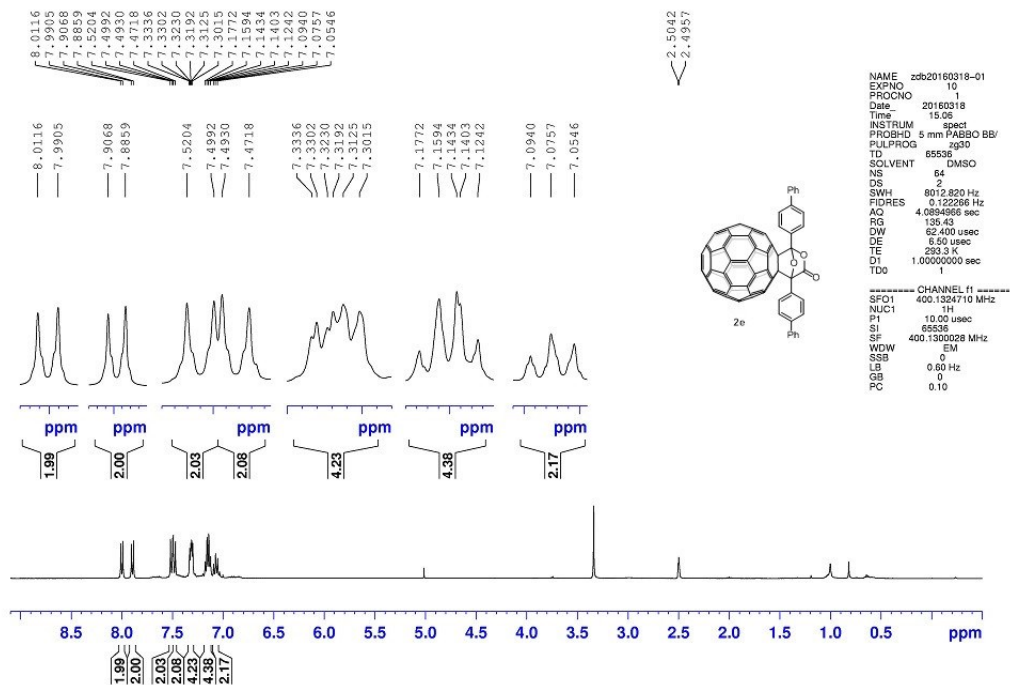


Figure S17. ^1H NMR (400 MHz, $\text{CS}_2/\text{DMSO}-d_6$) of **2e**.

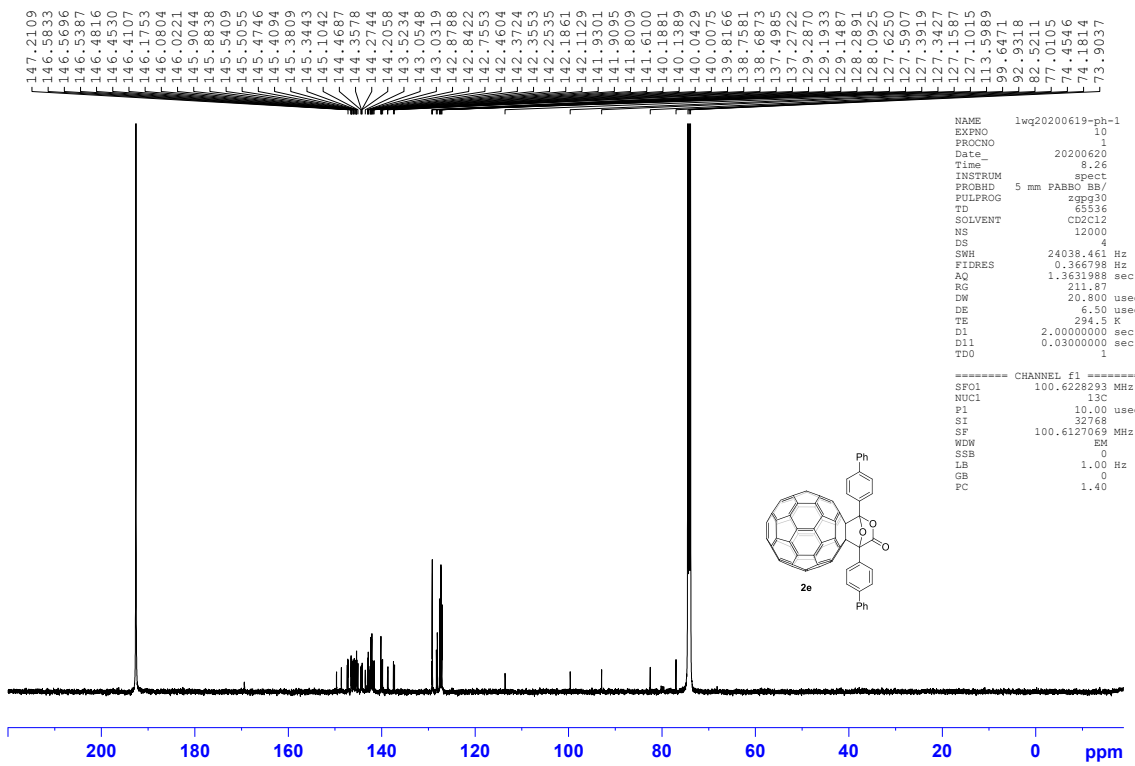


Figure S18. $^{13}\text{C}\{\text{H}\}$ NMR (100 MHz, 1:1 CS₂/C₂D₂Cl₄) of **2e**.

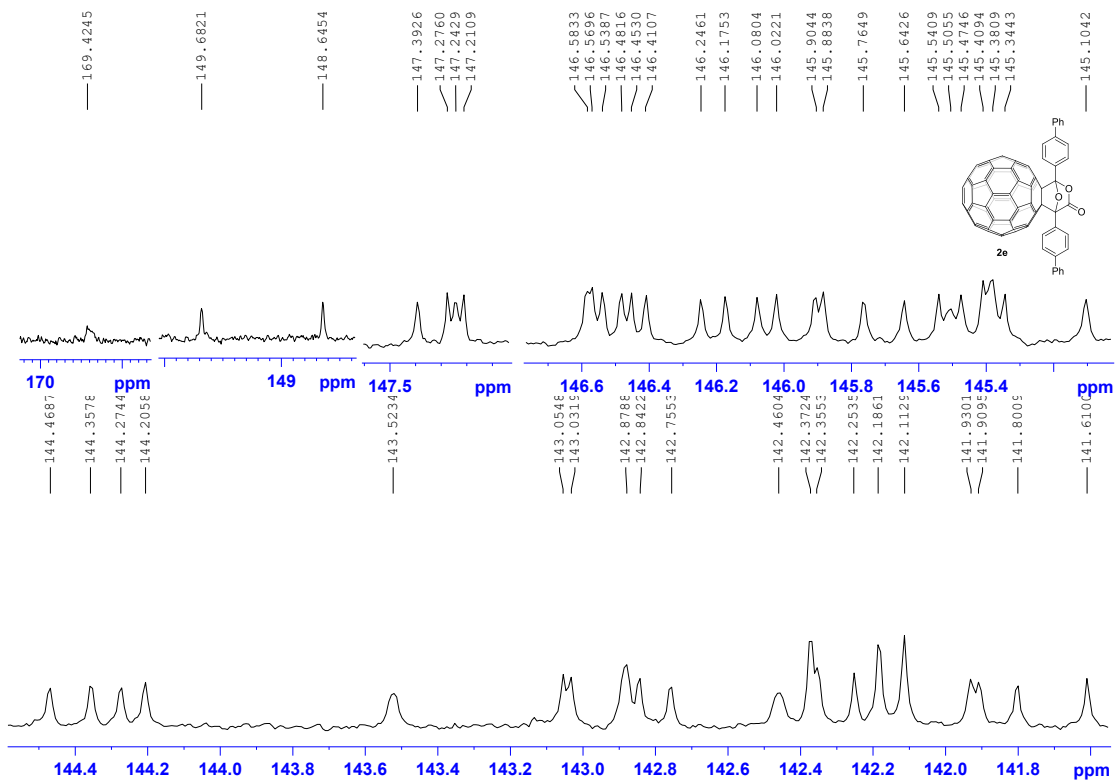


Figure S19. Expanded $^{13}\text{C}\{\text{H}\}$ NMR (100 MHz, 1:1 $\text{CS}_2/\text{C}_2\text{D}_2\text{Cl}_4$) of **2e**.

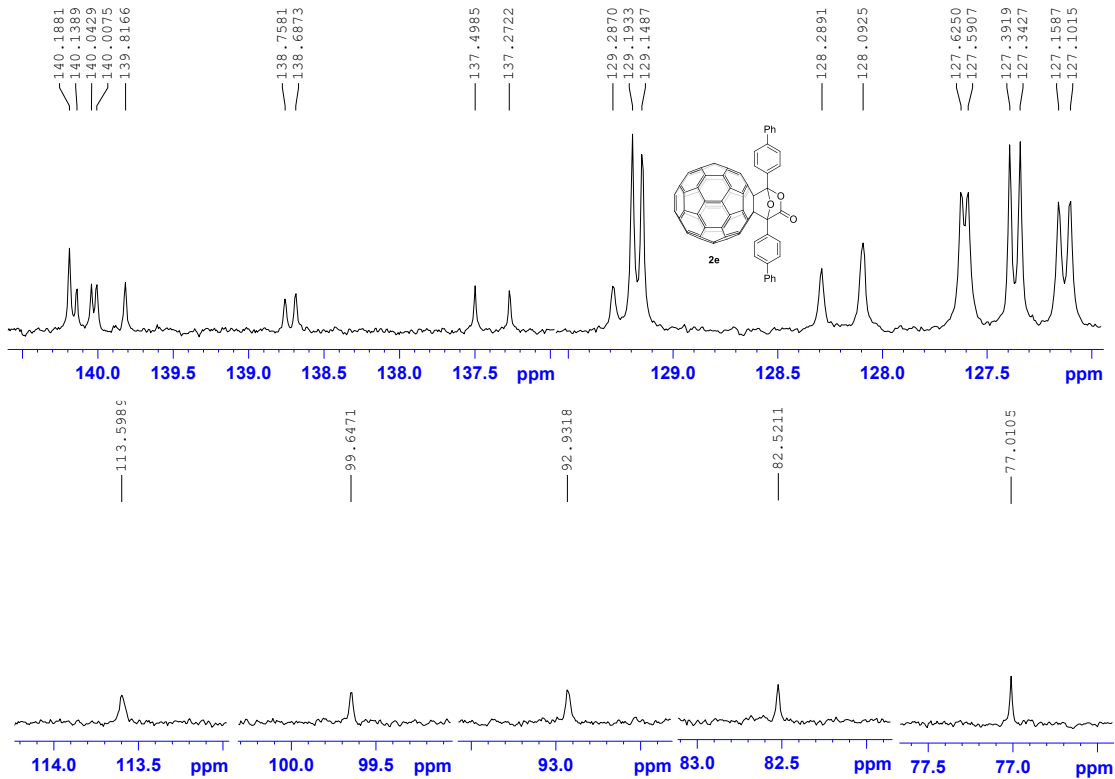


Figure S20. Expanded $^{13}\text{C}\{\text{H}\}$ NMR (100 MHz, 1:1 $\text{CS}_2/\text{C}_2\text{D}_2\text{Cl}_4$) of **2e**.

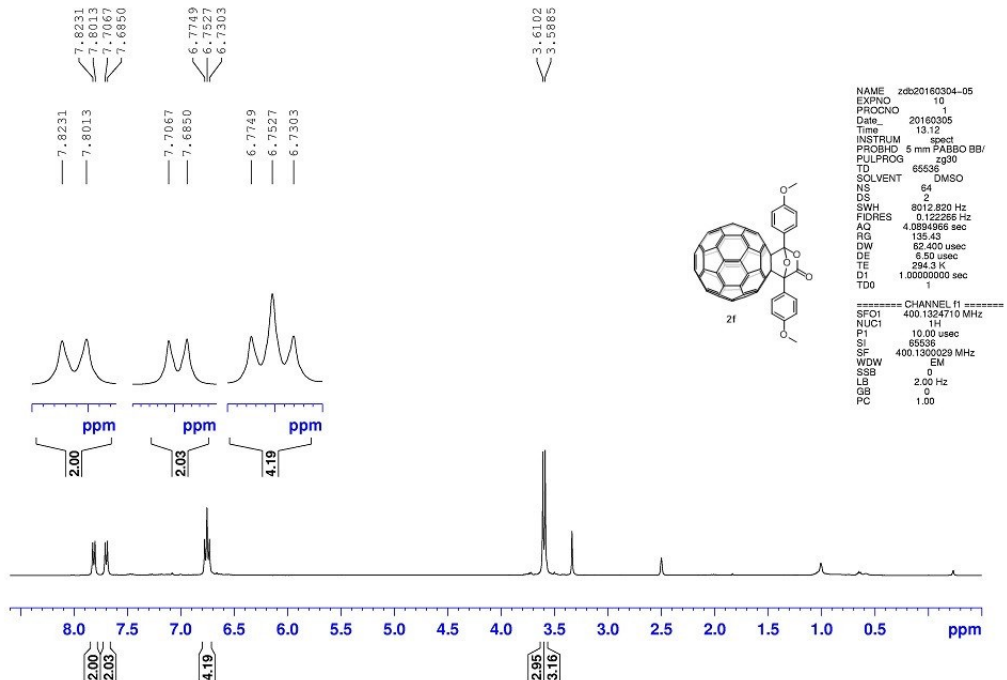


Figure S21. ^1H NMR (400 MHz, $\text{CS}_2/\text{DMSO}-d_6$) of **2f**.

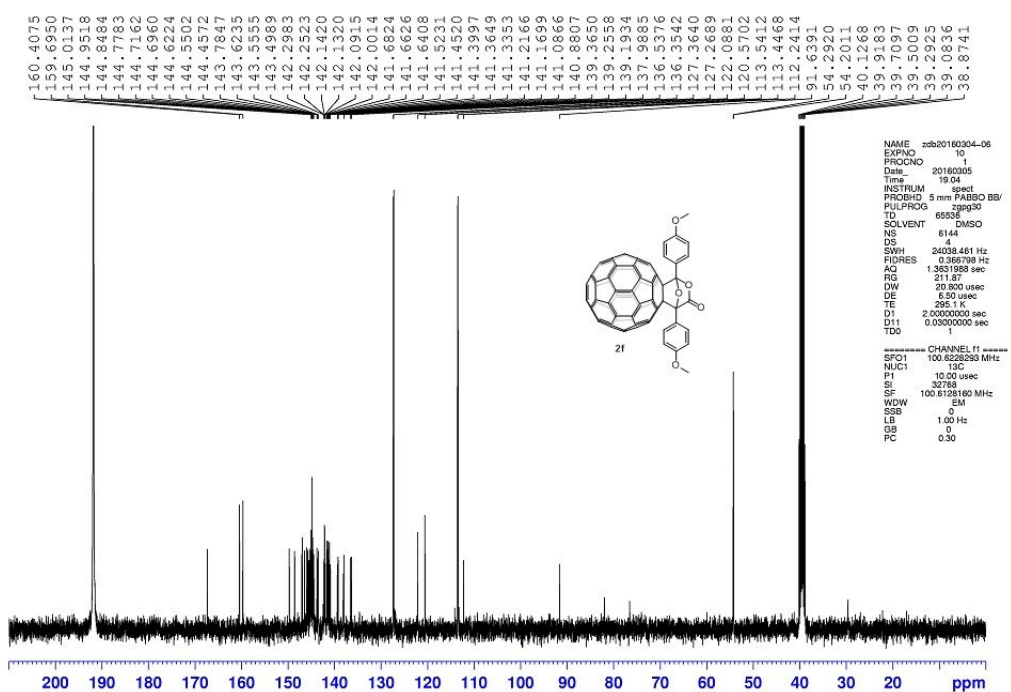


Figure S22. $^{13}\text{C}\{\text{H}\}$ NMR (100 MHz, $\text{CS}_2/\text{DMSO}-d_6$) of **2f**.

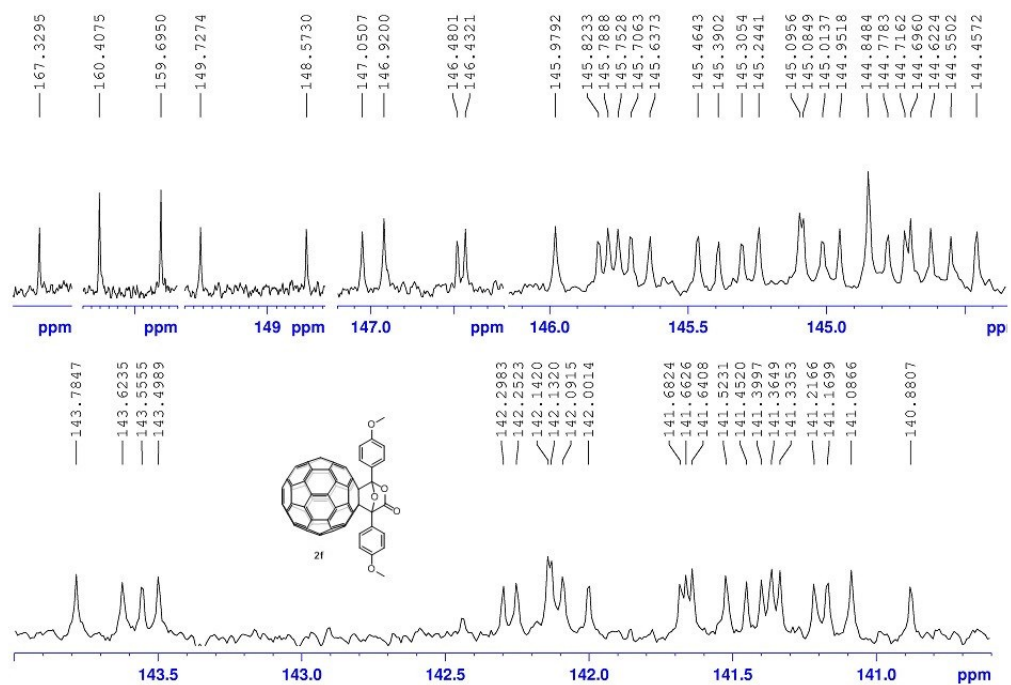


Figure S23. Expanded $^{13}\text{C}\{\text{H}\}$ NMR (100 MHz, $\text{CS}_2/\text{DMSO}-d_6$) of **2f**.

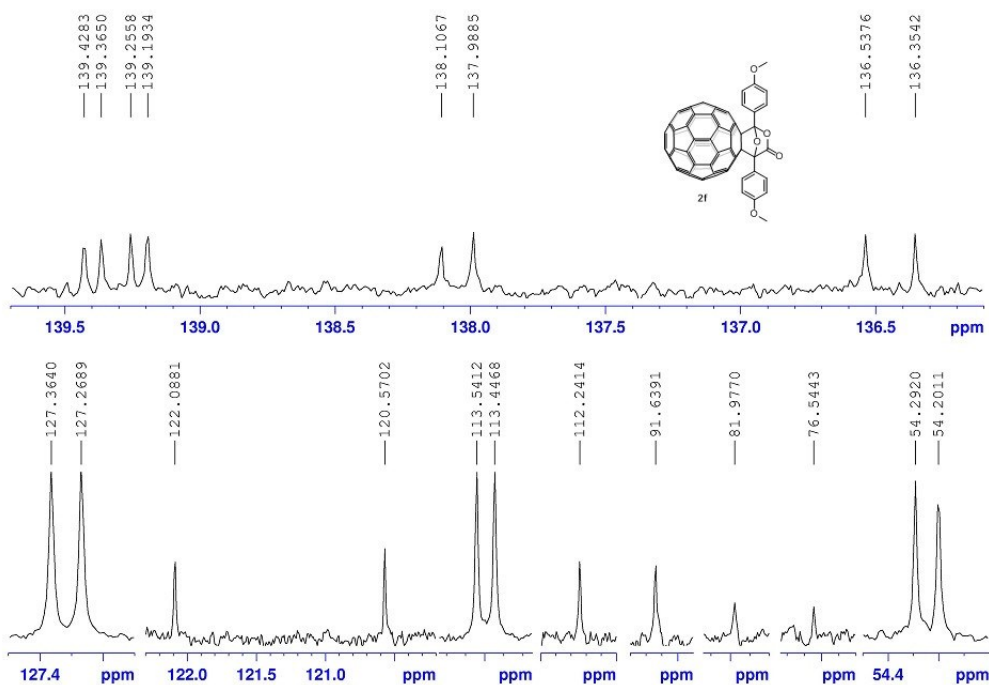


Figure S24. Expanded $^{13}\text{C}\{\text{H}\}$ NMR (100 MHz, $\text{CS}_2/\text{DMSO}-d_6$) of **2f**.

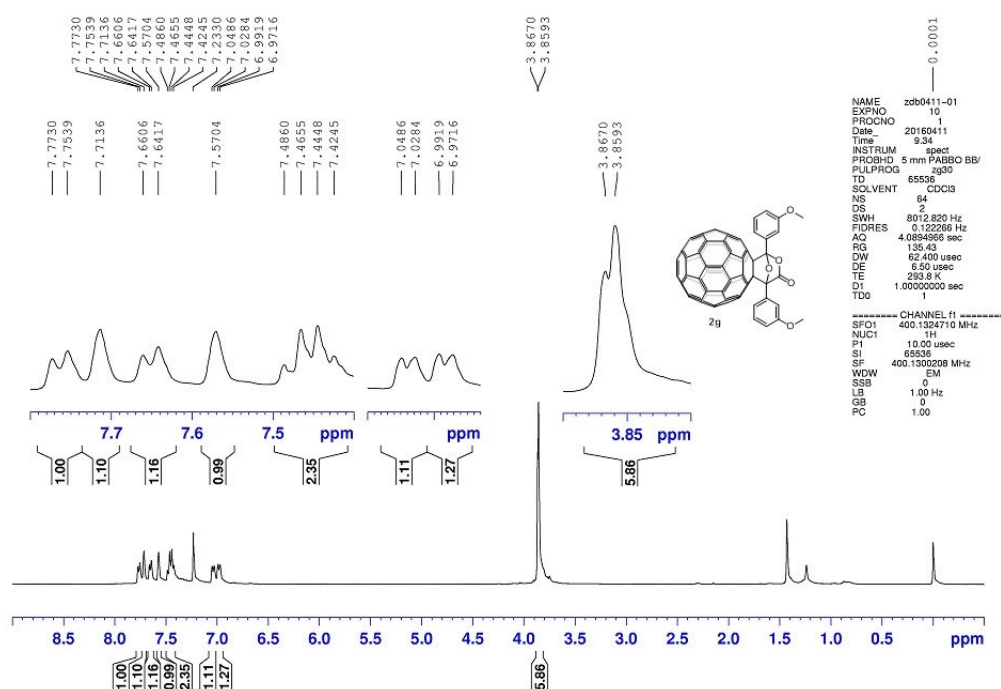


Figure S25. ^1H NMR (400 MHz, 1:1 CS₂/CDCl₃) of **2g**.

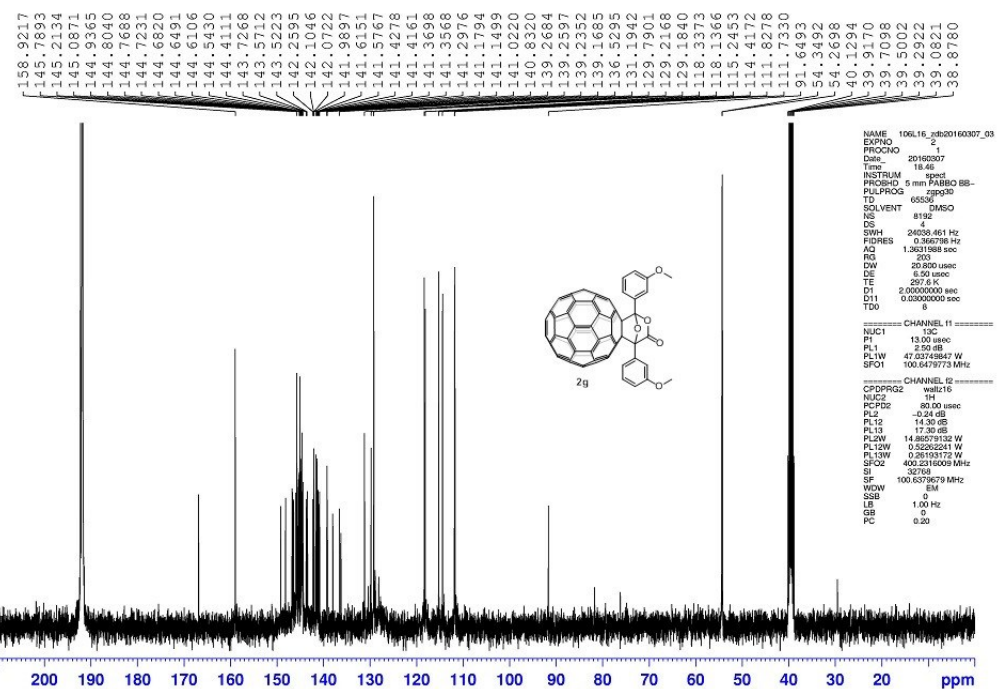


Figure S26. $^{13}\text{C}\{^1\text{H}\}$ NMR (100 MHz, 1:1 CS₂/CDCl₃) of **2g**.

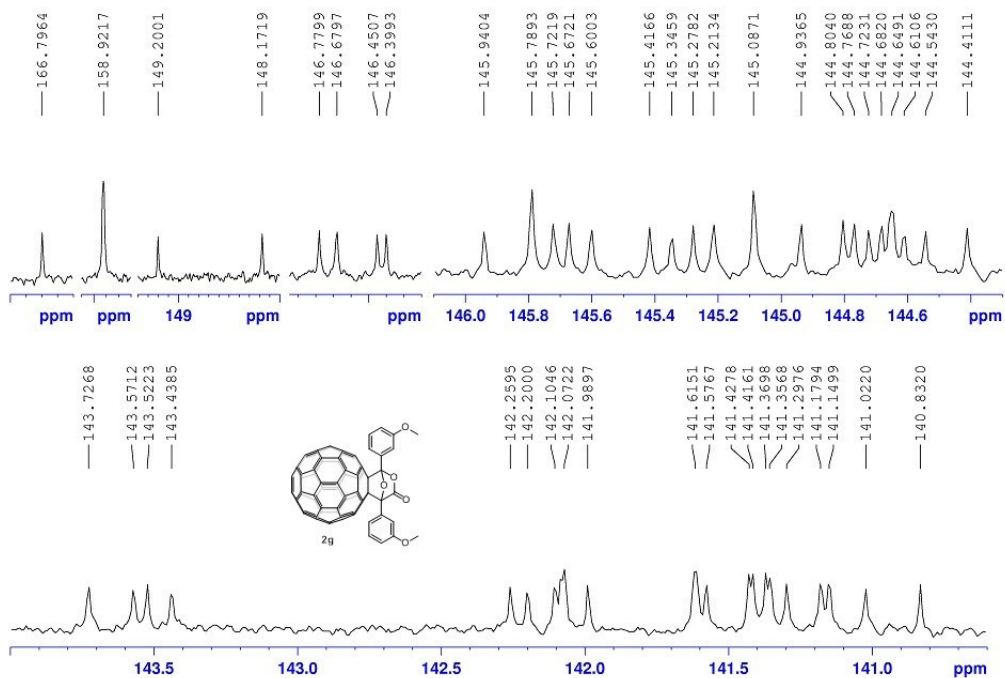


Figure S27. Expanded $^{13}\text{C}\{^1\text{H}\}$ NMR (100 MHz, 1:1 CS₂/CDCl₃) of **2g**.

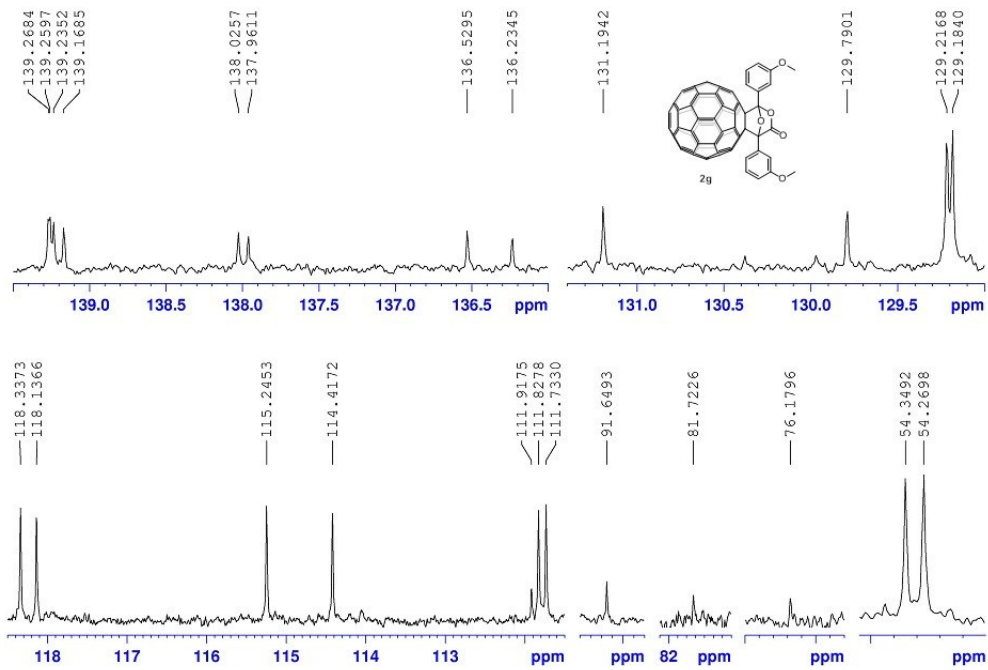


Figure S28. Expanded $^{13}\text{C}\{\text{H}\}$ NMR (100 MHz, 1:1 $\text{CS}_2/\text{CDCl}_3$) of **2g**.

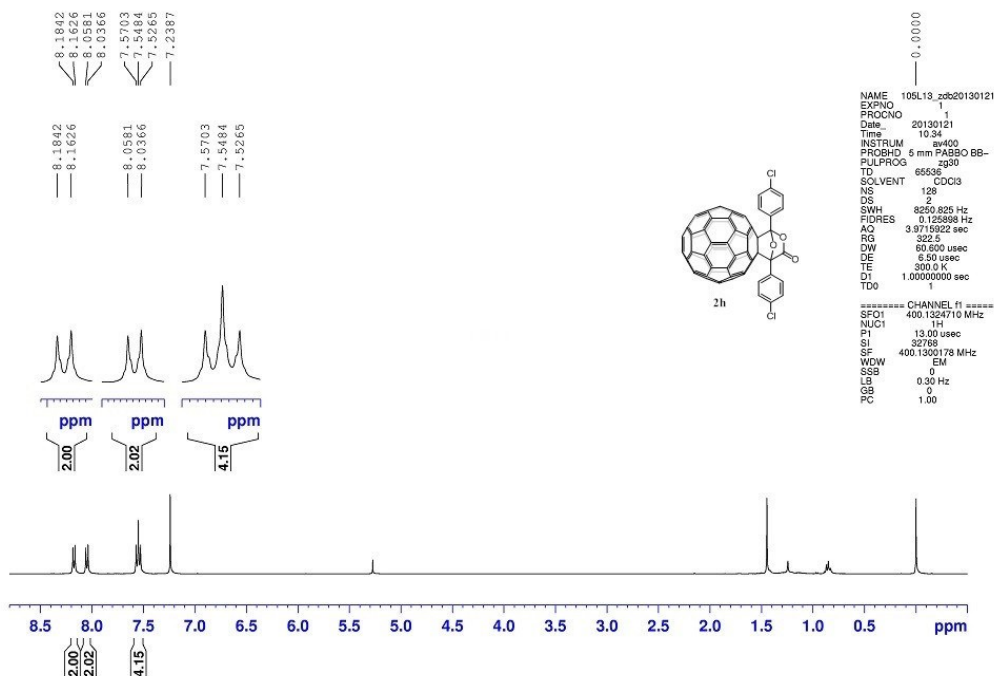


Figure S33 ^1H NMR (400 MHz, 1:1 CS₂/CDCl₃) of **2h**.

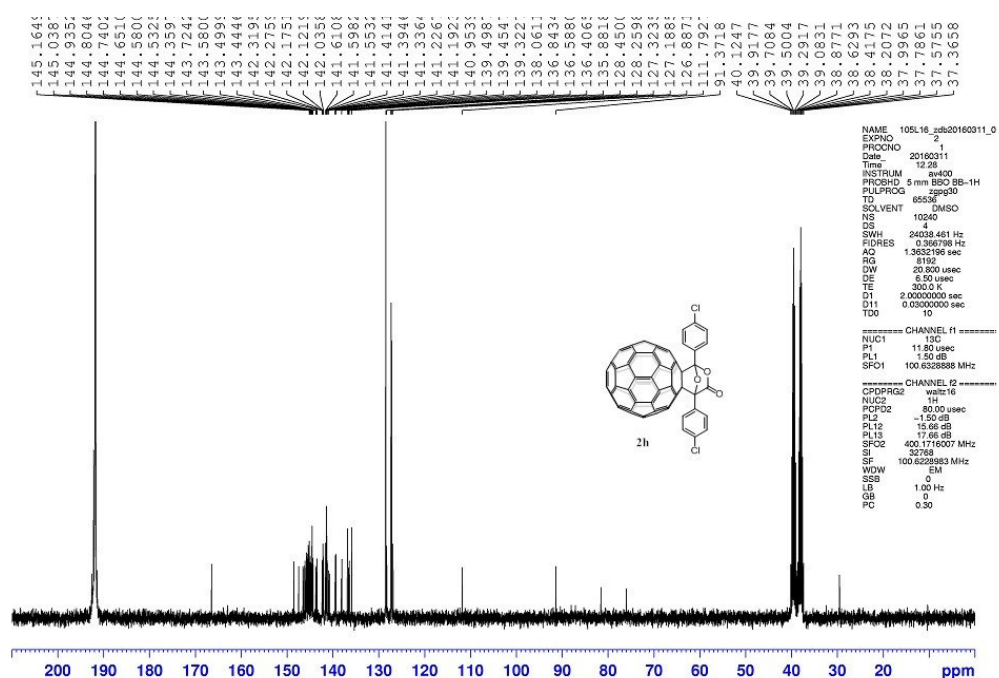


Figure S34. $^{13}\text{C}\{^1\text{H}\}$ NMR (100 MHz, $\text{CS}_2/\text{DMSO}-d_6$) of **2h**.

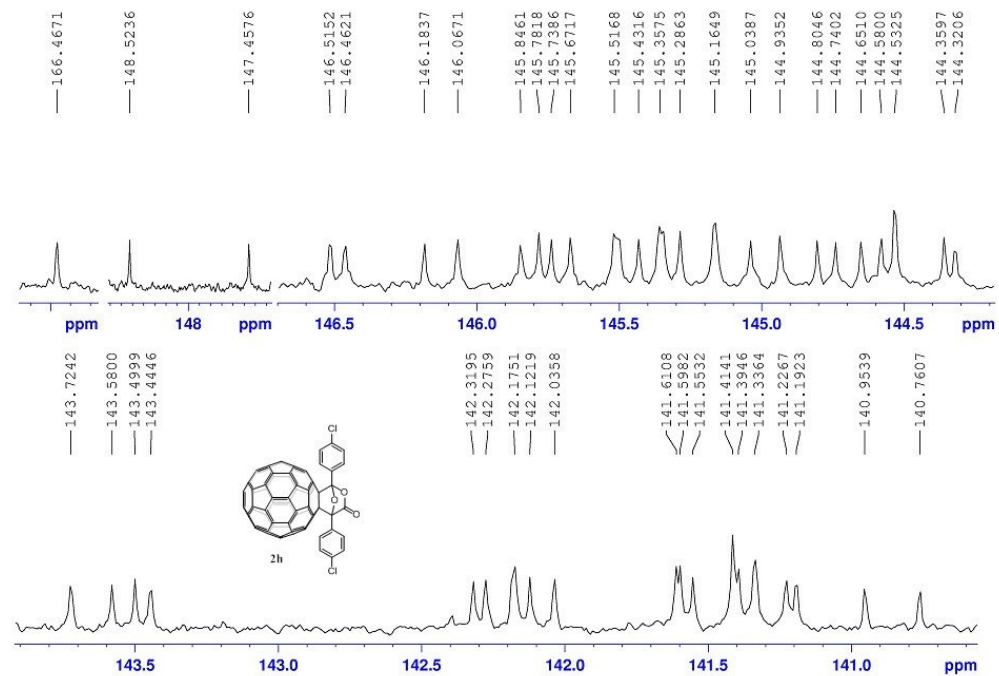


Figure S35. Expanded $^{13}\text{C}\{^1\text{H}\}$ NMR (100 MHz, $\text{CS}_2/\text{DMSO}-d_6$) of **2h**.

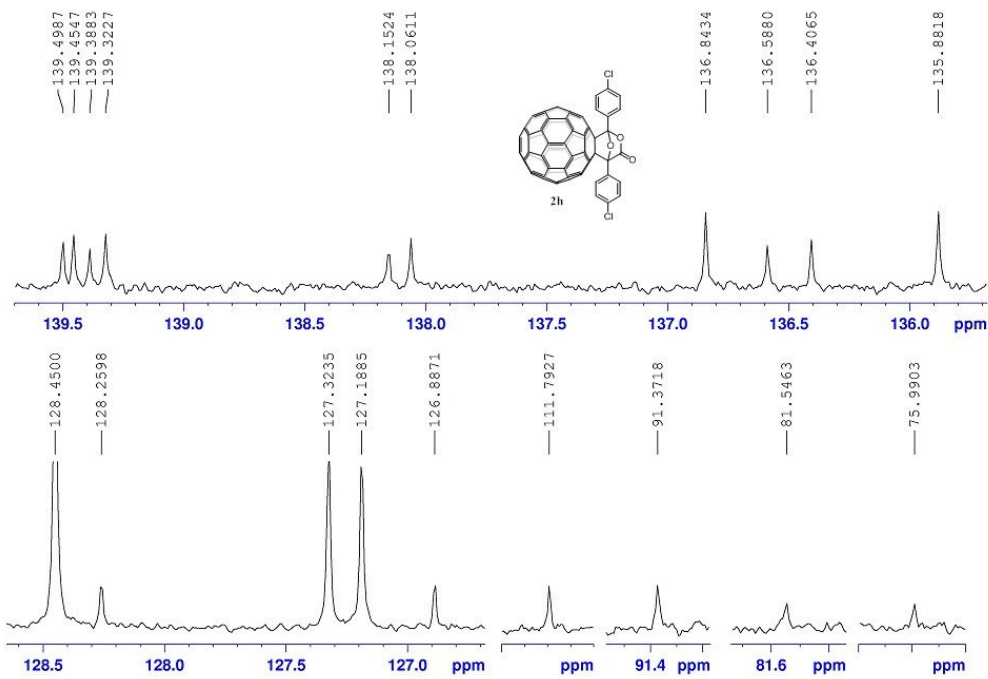


Figure S36. Expanded $^{13}\text{C}\{\text{H}\}$ NMR (100 MHz, $\text{CS}_2/\text{DMSO}-d_6$) of **2h**.

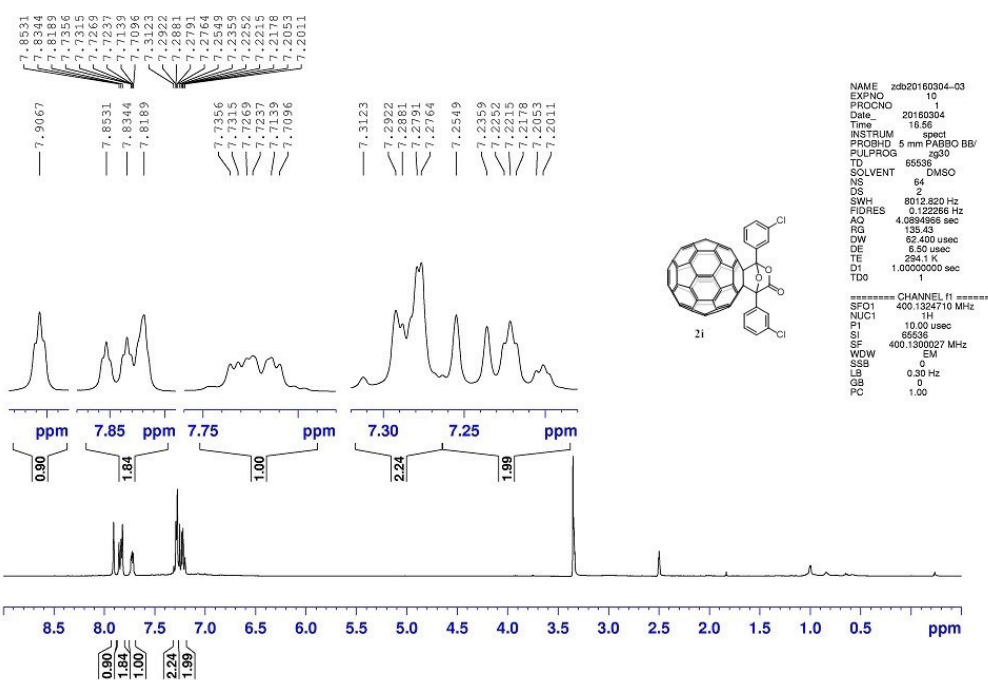


Figure S29. ^1H NMR (400 MHz, $\text{CS}_2/\text{DMSO}-d_6$) of **2i**.

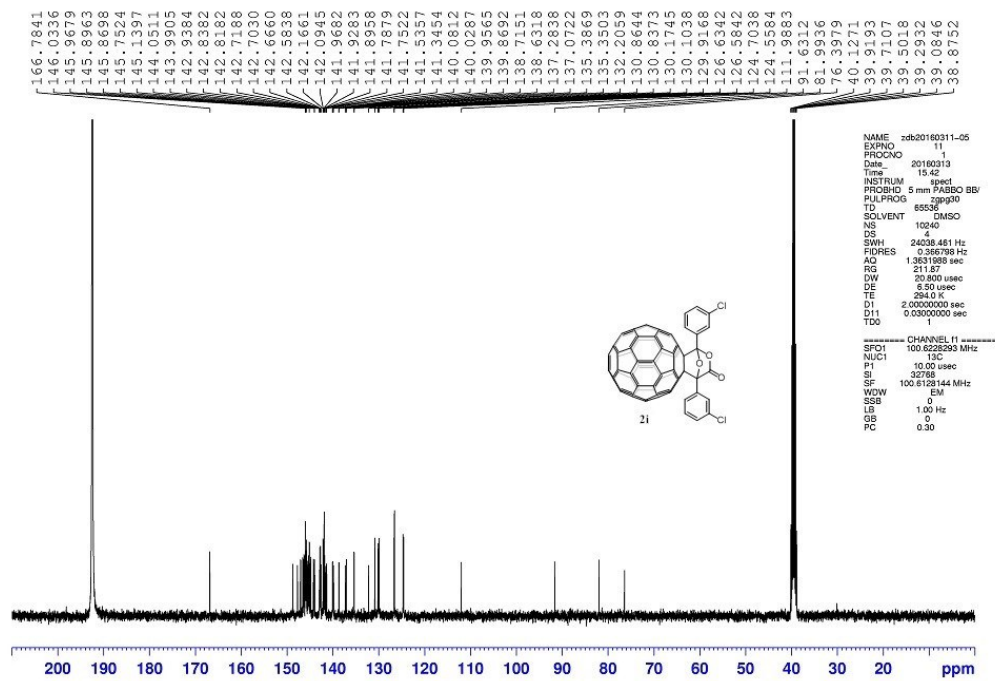


Figure S30. $^{13}\text{C}\{\text{H}\}$ NMR (100 MHz, $\text{CS}_2/\text{DMSO}-d_6$) of **2i**.

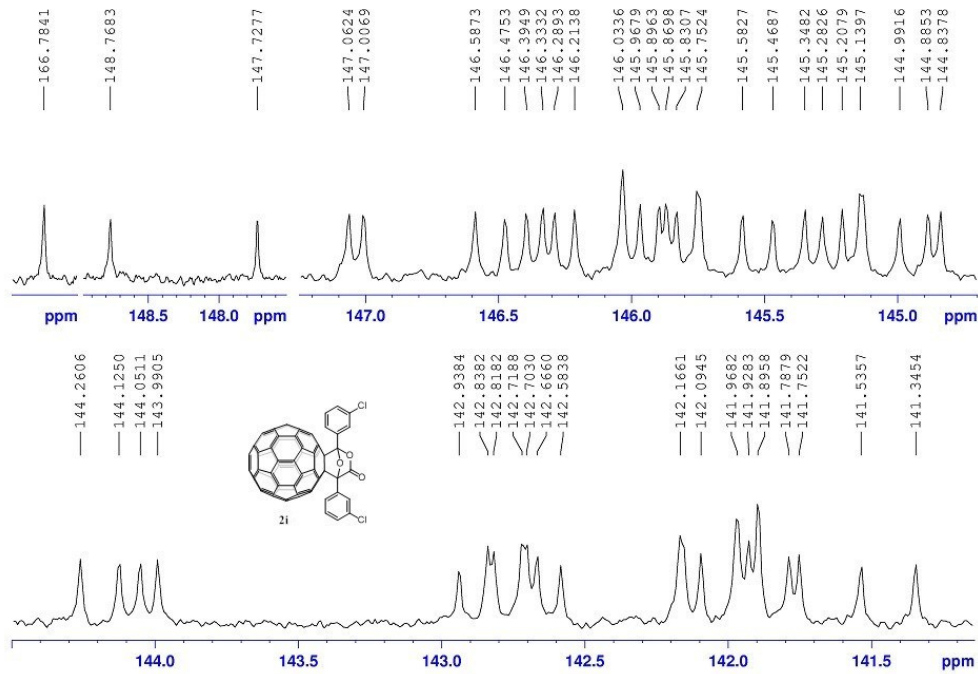


Figure S31. Expanded $^{13}\text{C}\{\text{H}\}$ NMR (100 MHz, $\text{CS}_2/\text{DMSO}-d_6$) of **2i**.

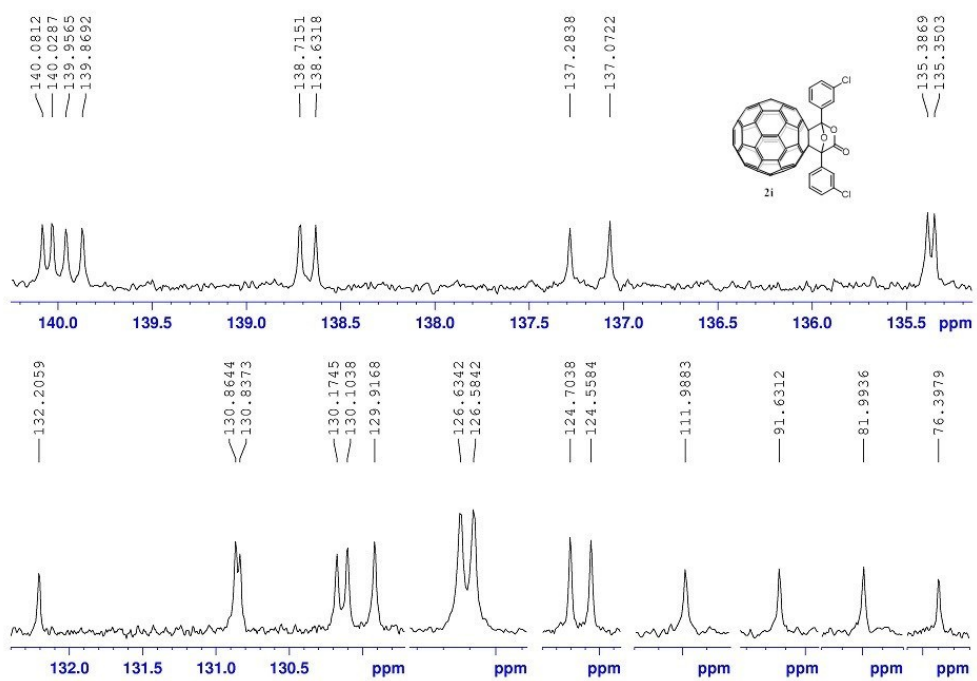


Figure S32. Expanded $^{13}\text{C}\{\text{H}\}$ NMR (100 MHz, $\text{CS}_2/\text{DMSO}-d_6$) of **2i**.

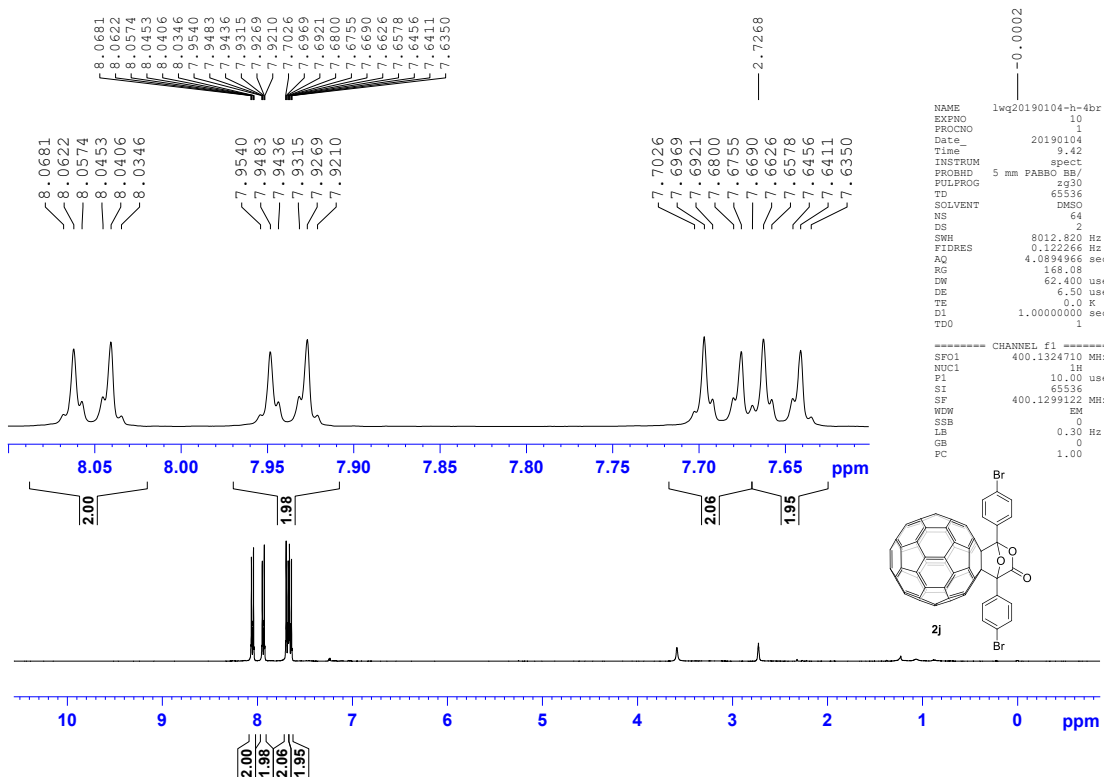


Figure S41. ^1H NMR (400 MHz, $\text{CS}_2/\text{DMSO}-d_6$) of **2j**.

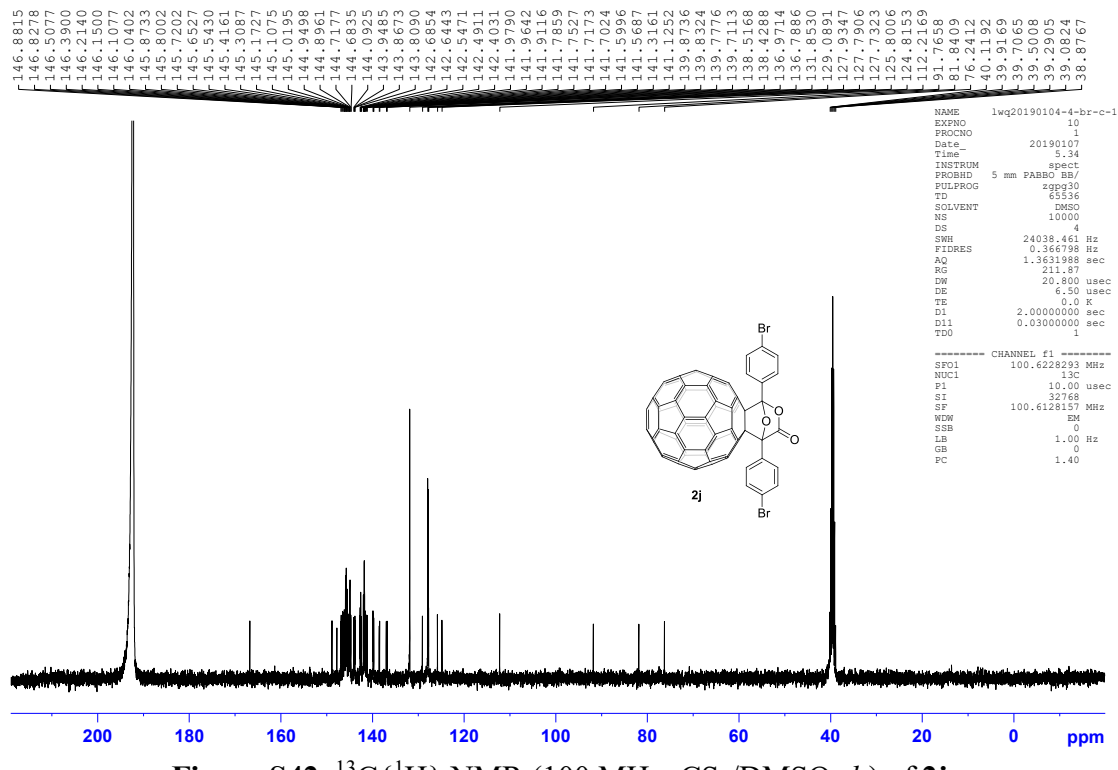


Figure S42. $^{13}\text{C}\{\text{H}\}$ NMR (100 MHz, $\text{CS}_2/\text{DMSO}-d_6$) of **2j**.

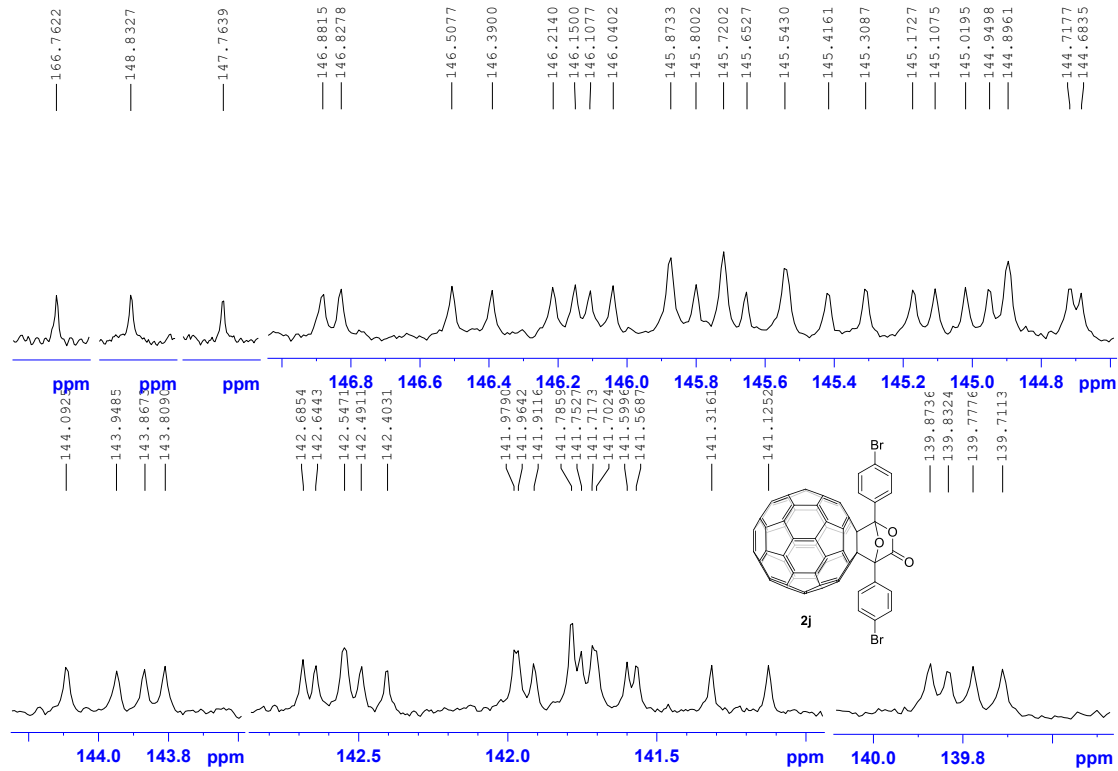


Figure S43. Expanded $^{13}\text{C}\{\text{H}\}$ NMR (100 MHz, $\text{CS}_2/\text{DMSO}-d_6$) of **2j**.

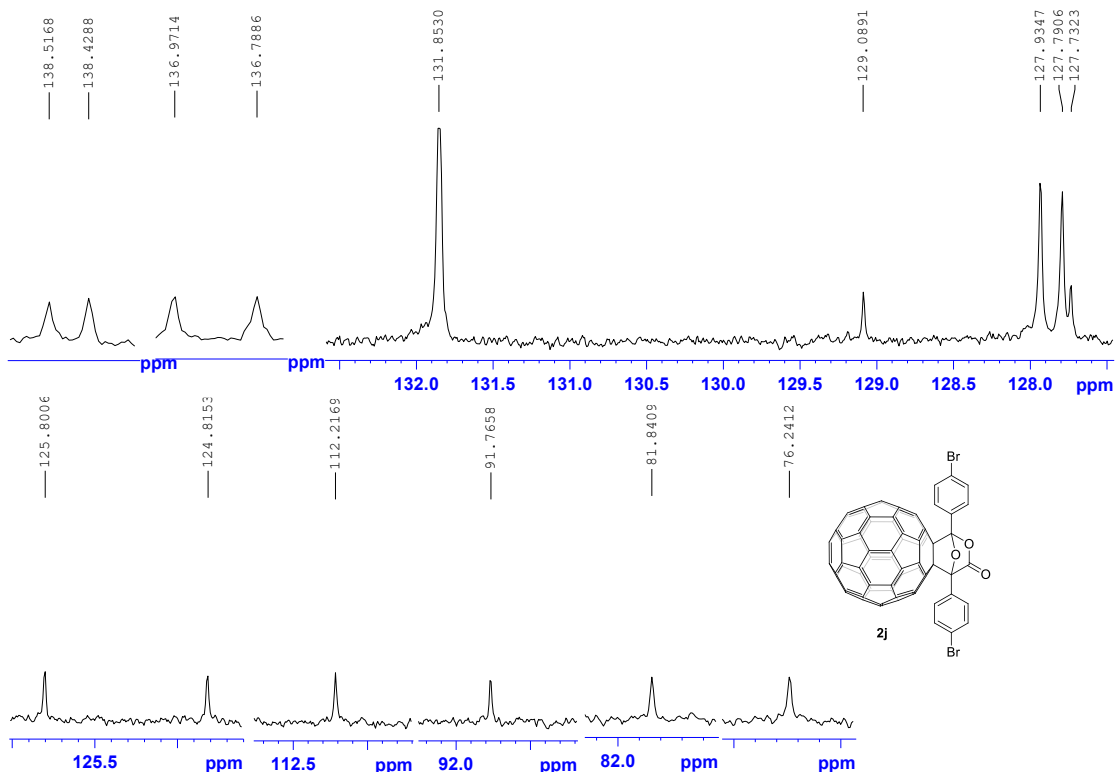


Figure S44. Expanded $^{13}\text{C}\{\text{H}\}$ NMR (100 MHz, $\text{CS}_2/\text{DMSO}-d_6$) of **2j**.

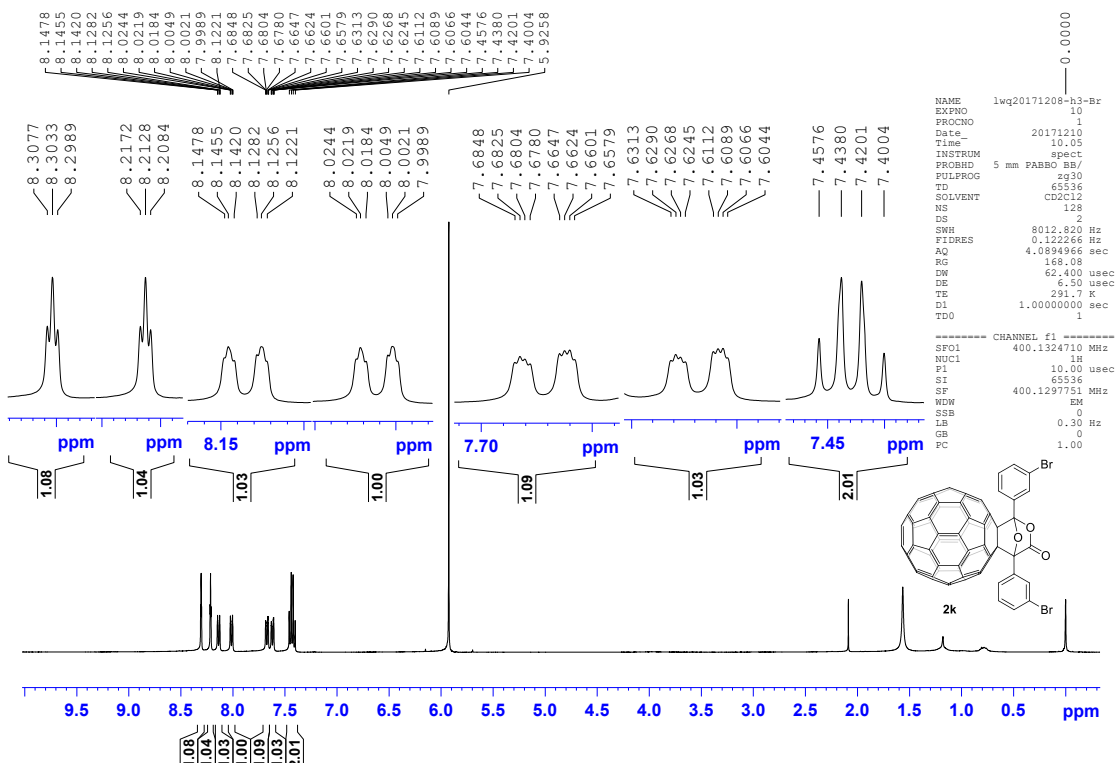


Figure S37. ^1H NMR (400 MHz, $\text{C}_2\text{D}_2\text{Cl}_4$) of **2k**.

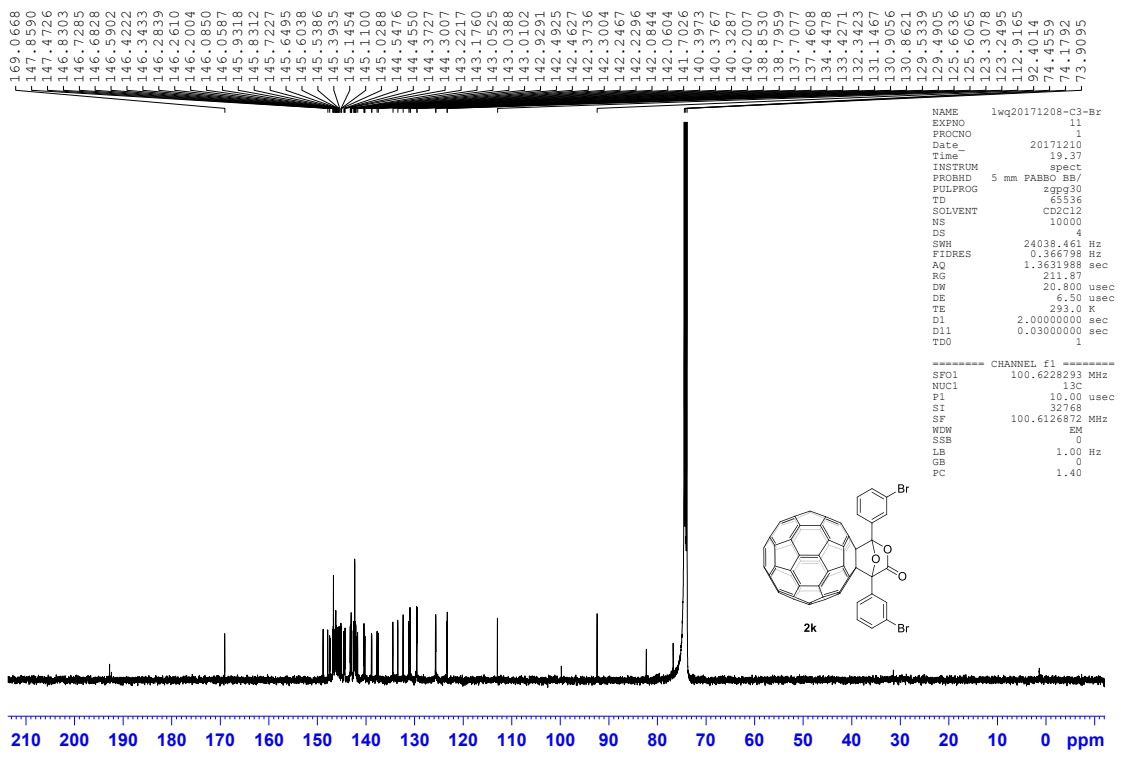


Figure S38. $^{13}\text{C}\{\text{H}\}$ NMR (100 MHz, $\text{C}_2\text{D}_2\text{Cl}_4$) of **2k**.

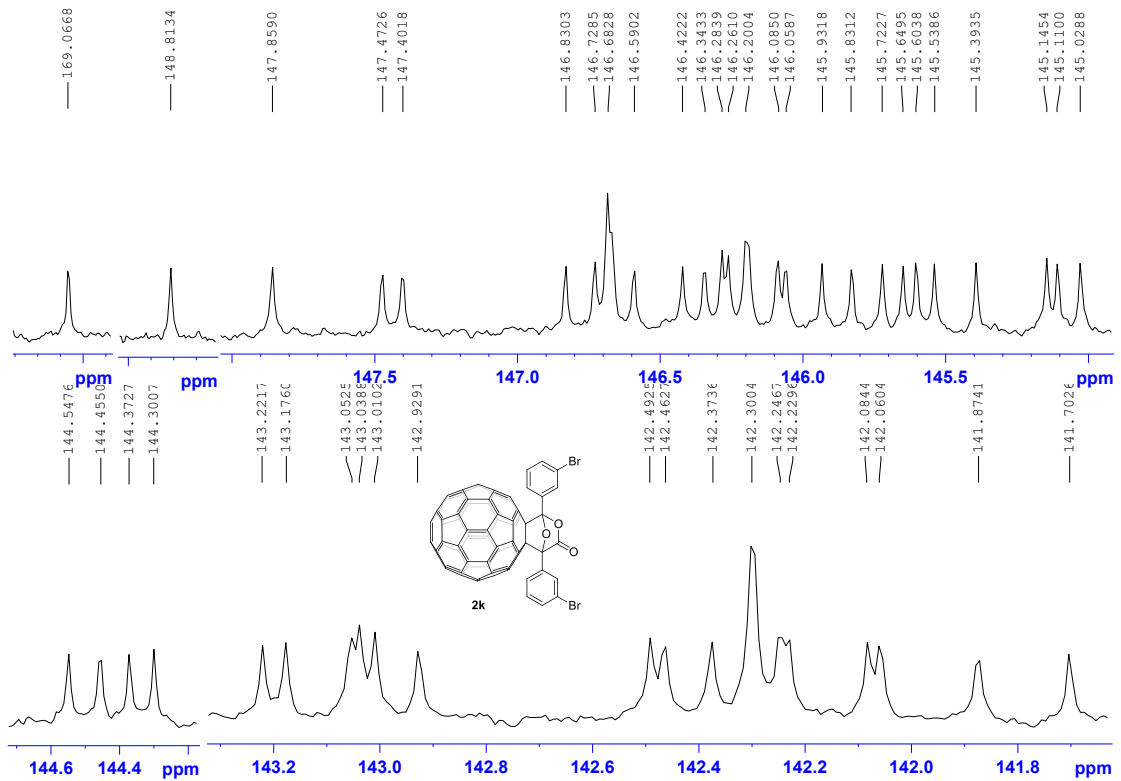


Figure S39. Expanded $^{13}\text{C}\{\text{H}\}$ NMR (100 MHz, $\text{C}_2\text{D}_2\text{Cl}_4$) of **2k**.

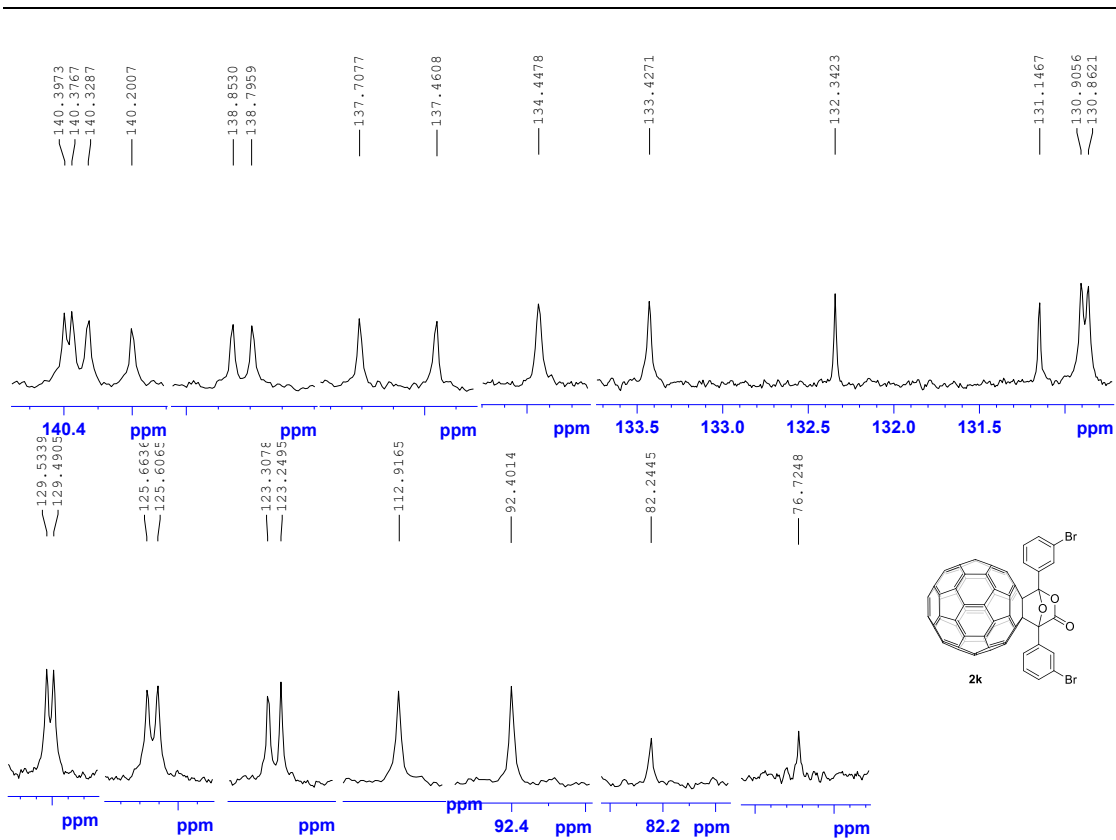


Figure S40. Expanded $^{13}\text{C}\{\text{H}\}$ NMR (100 MHz, $\text{C}_2\text{D}_2\text{Cl}_4$) of **2k**.

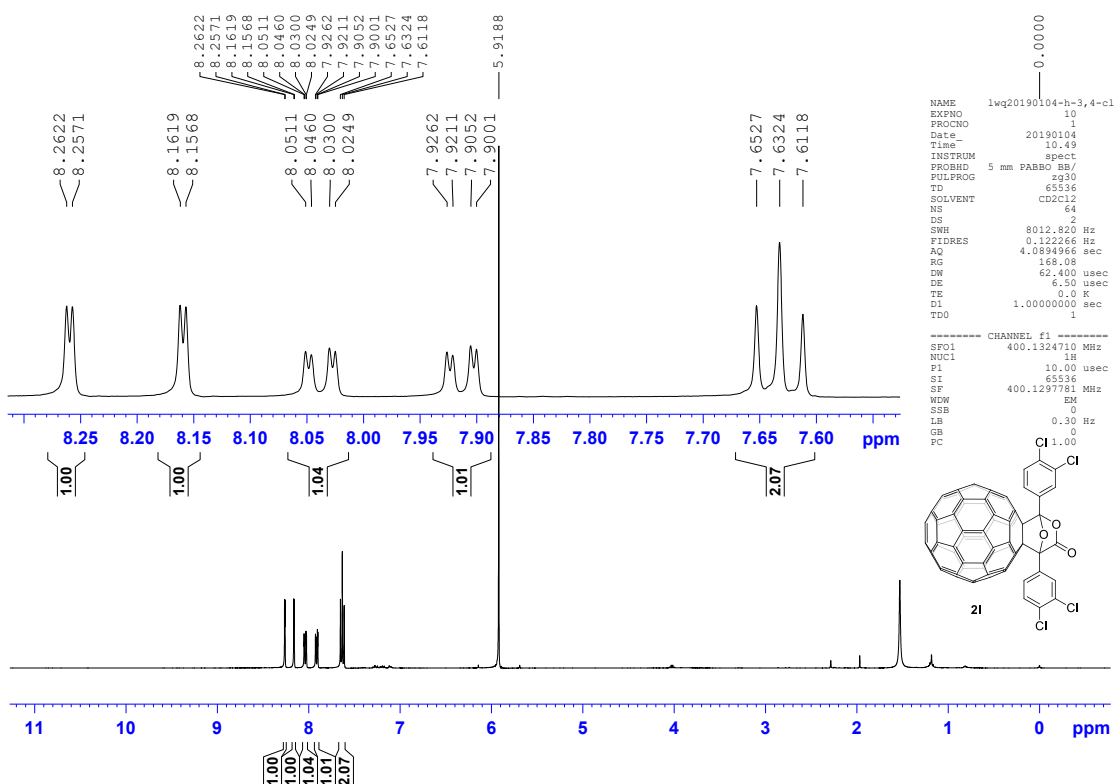


Figure S45. ^1H NMR (400 MHz, 1:1 $\text{CS}_2/\text{C}_2\text{D}_2\text{Cl}_4$) of **2l**.

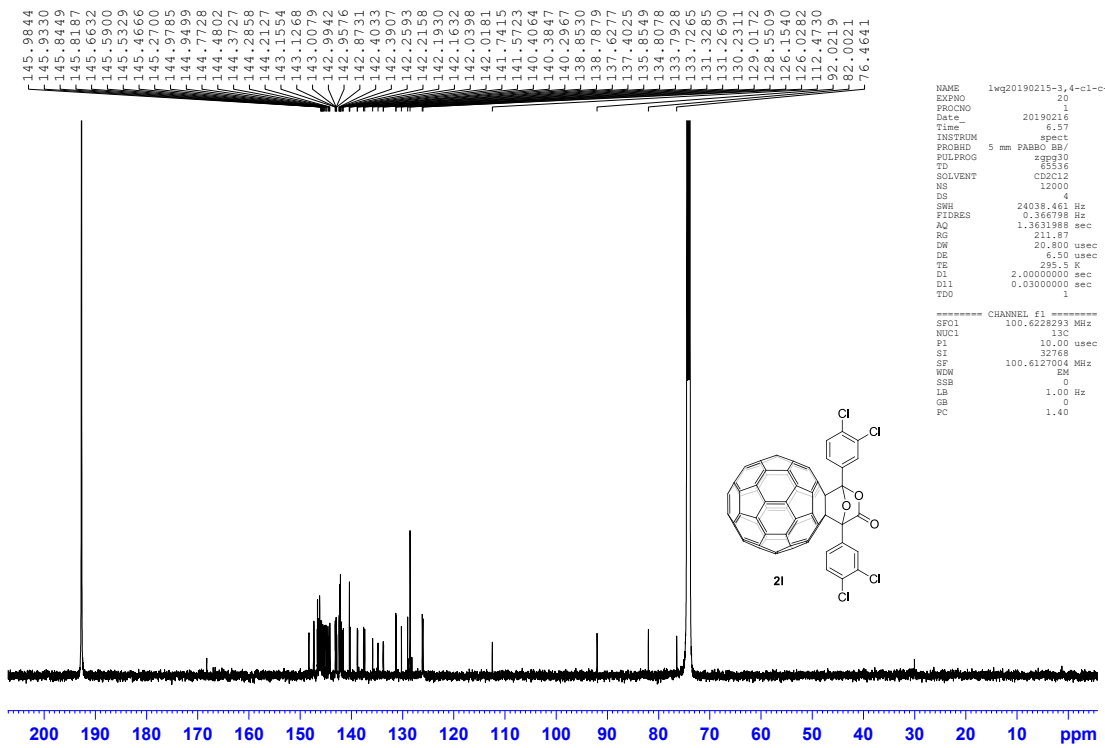


Figure S46. $^{13}\text{C}\{\text{H}\}$ NMR (100 MHz, 1:1 CS₂/C₂D₂Cl₄) of **2l**.

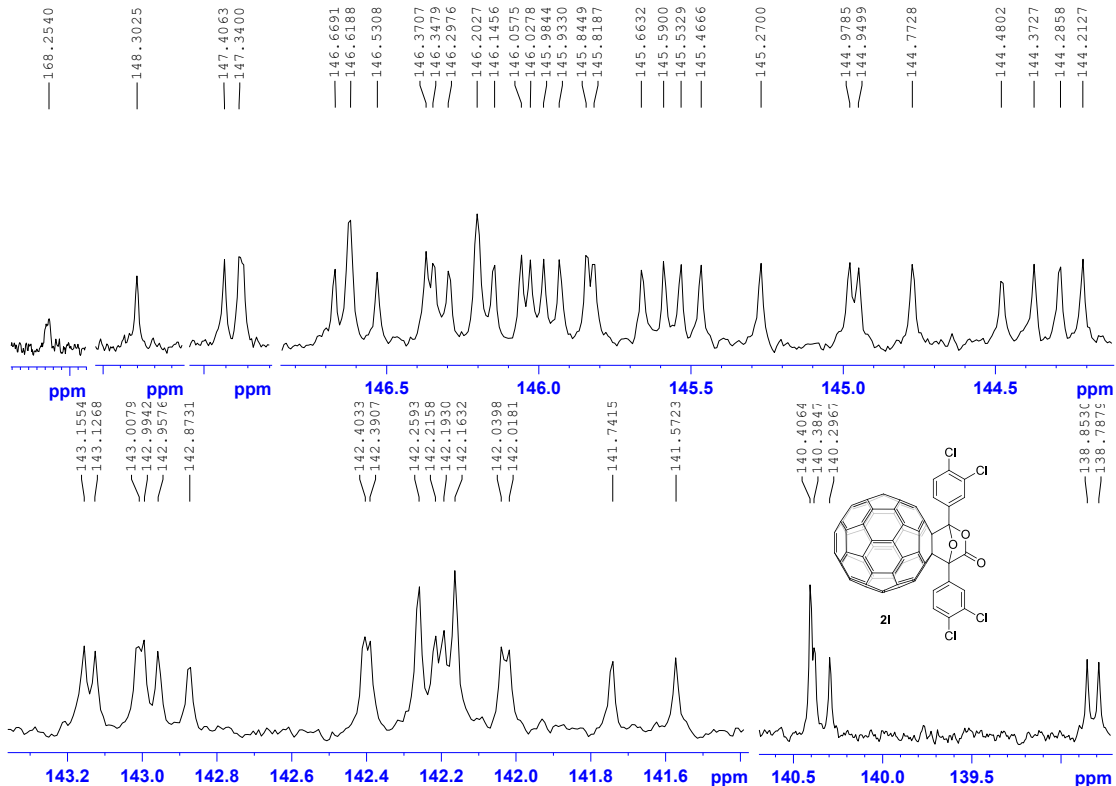


Figure S47. Expanded $^{13}\text{C}\{^1\text{H}\}$ NMR (100 MHz, 1:1 $\text{CS}_2/\text{C}_2\text{D}_2\text{Cl}_4$) of **2l**.

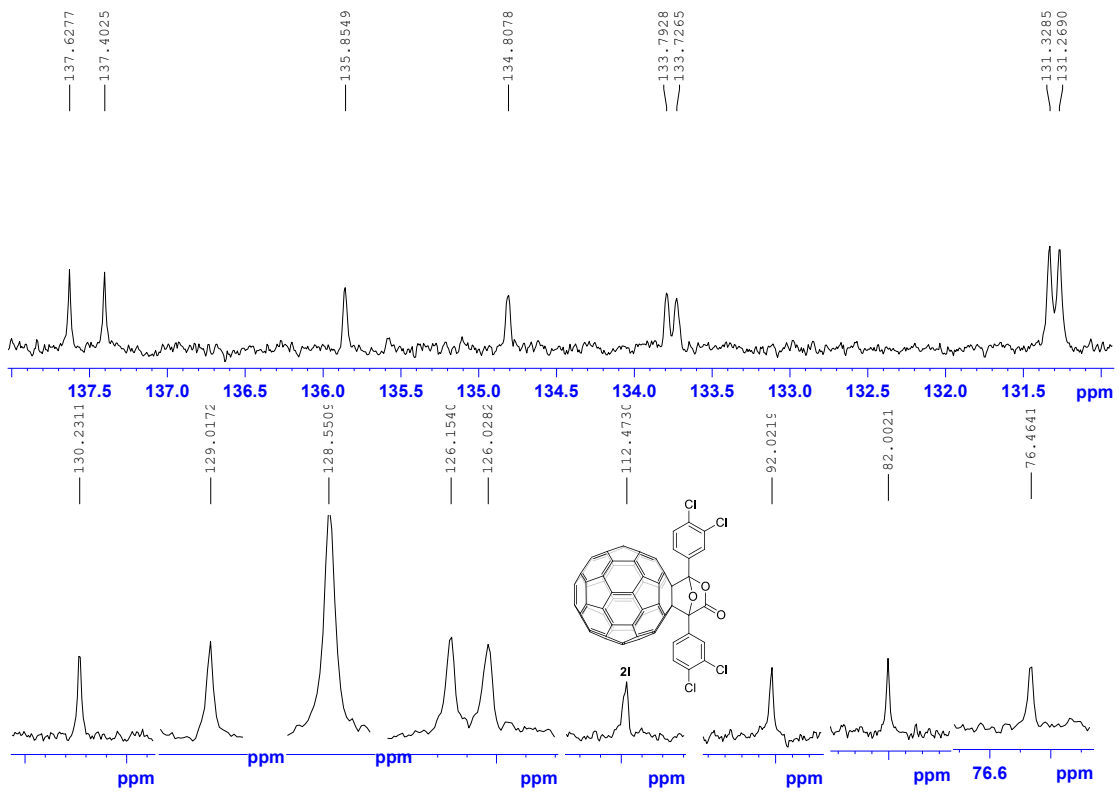


Figure S48. Expanded $^{13}\text{C}\{\text{H}\}$ NMR (100 MHz, 1:1 $\text{CS}_2/\text{C}_2\text{D}_2\text{Cl}_4$) of **2l**.

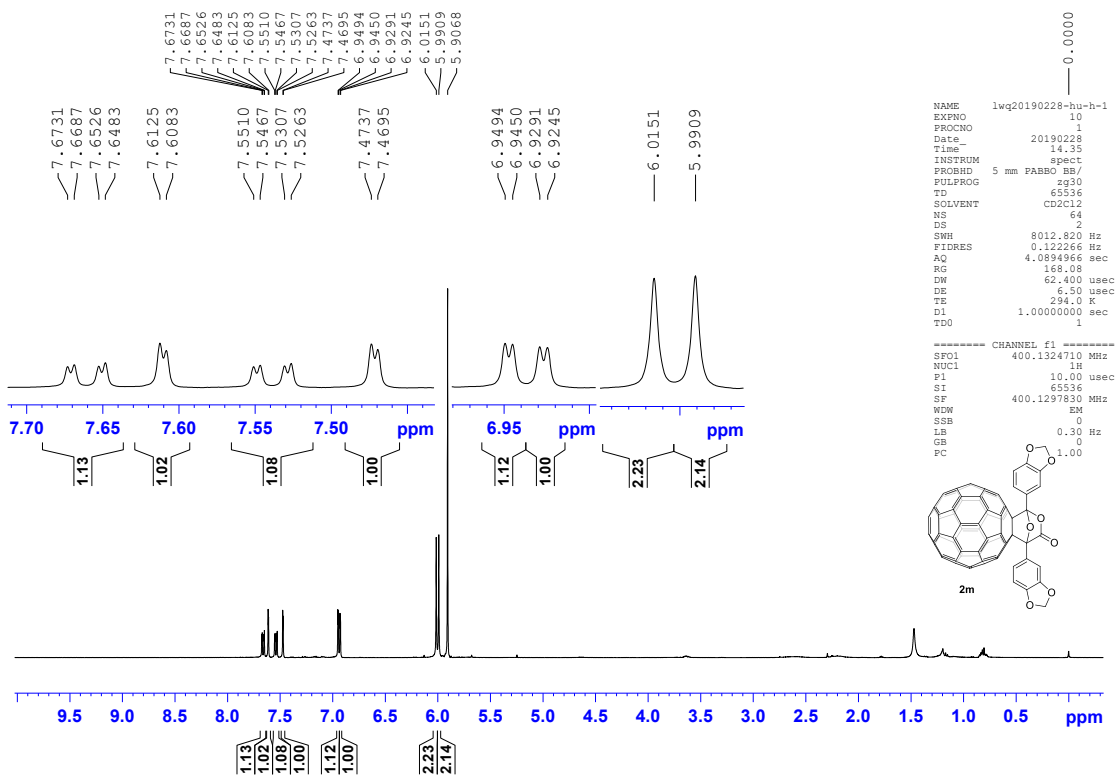


Figure S49. ^1H NMR (400 MHz, $\text{C}_2\text{D}_2\text{Cl}_4$) of **2m**.

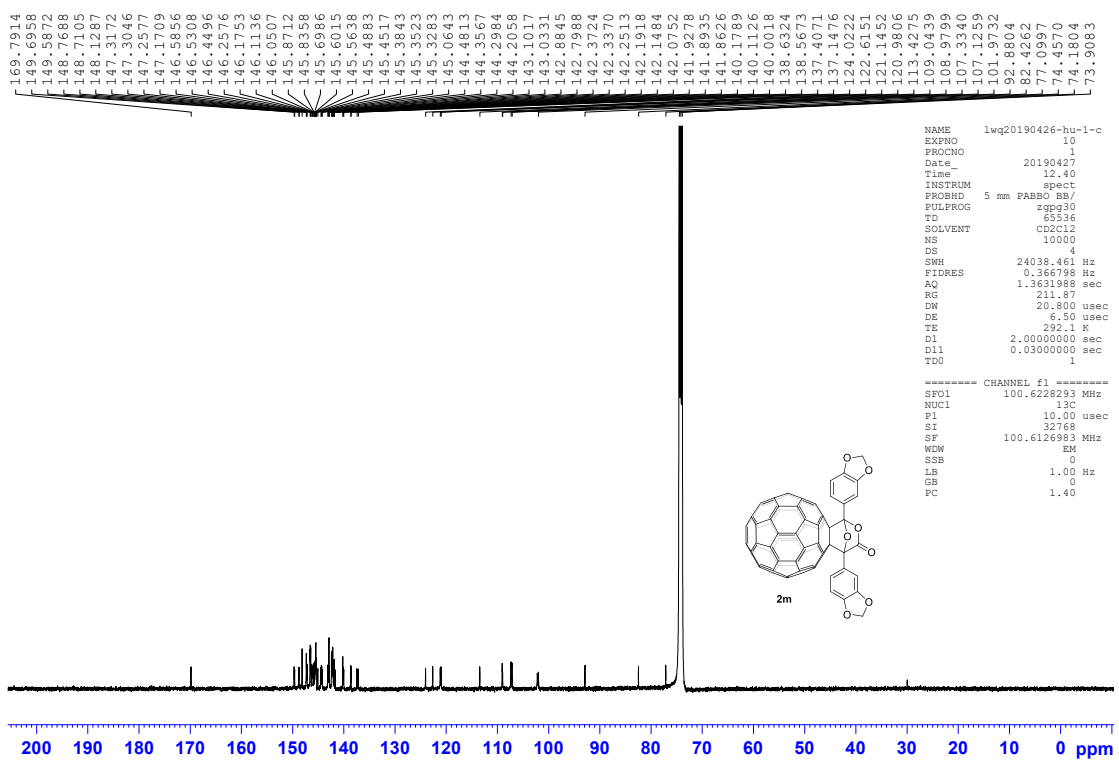


Figure S50. $^{13}\text{C}\{\text{H}\}$ NMR (100 MHz, $\text{C}_2\text{D}_2\text{Cl}_4$) of **2m**.

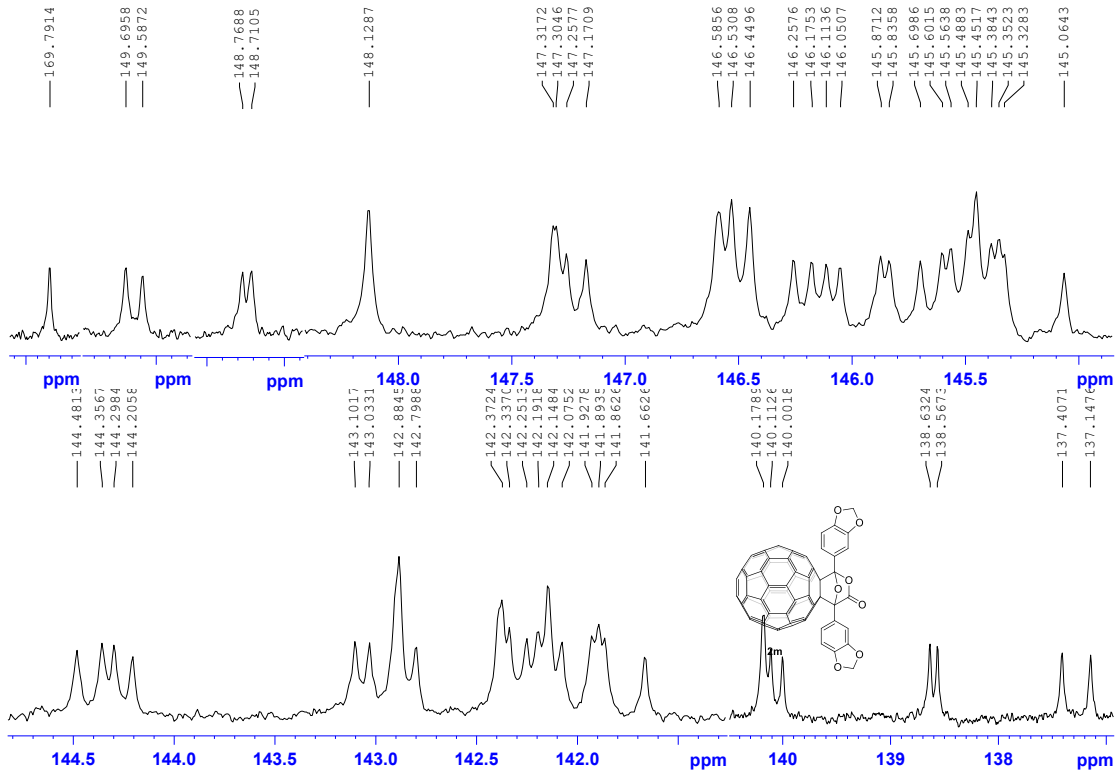


Figure S51. Expanded $^{13}\text{C}\{\text{H}\}$ NMR (100 MHz, $\text{C}_2\text{D}_2\text{Cl}_4$) of **2m**.

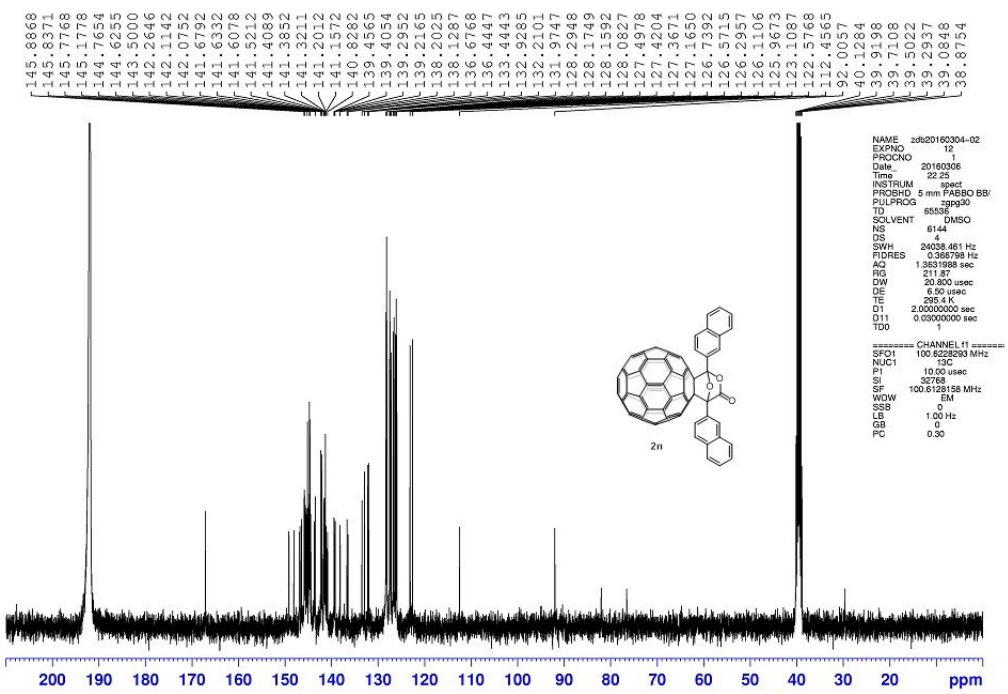


Figure S54. $^{13}\text{C}\{^1\text{H}\}$ NMR (100 MHz, $\text{CS}_2/\text{DMSO}-d_6$) of **2n**.

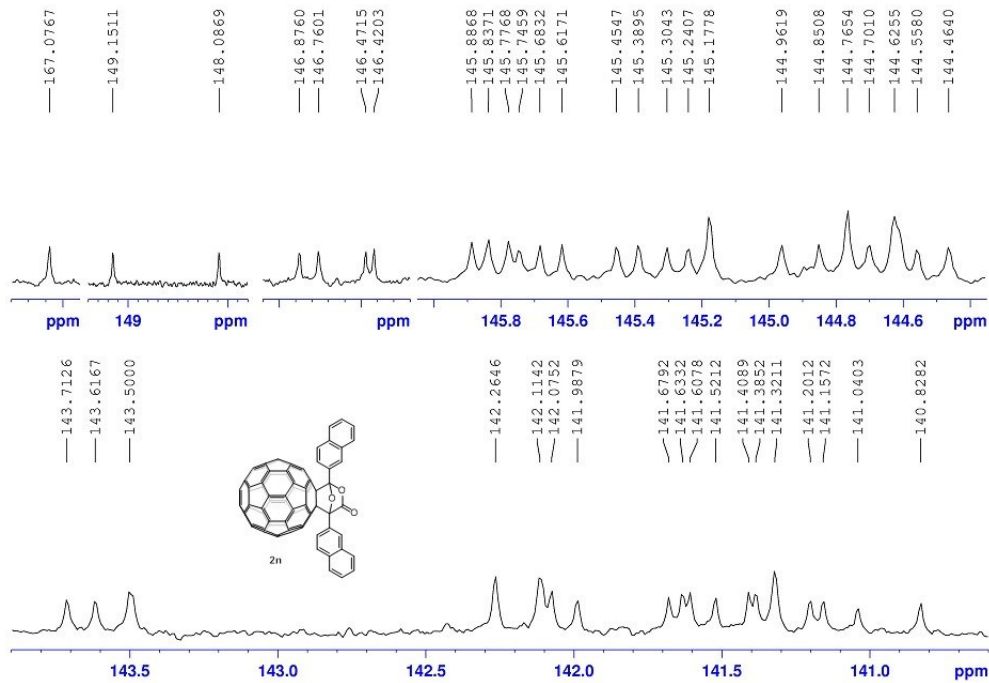


Figure S55. Expanded $^{13}\text{C}\{^1\text{H}\}$ NMR (100 MHz, $\text{CS}_2/\text{DMSO}-d_6$) of **2n**.

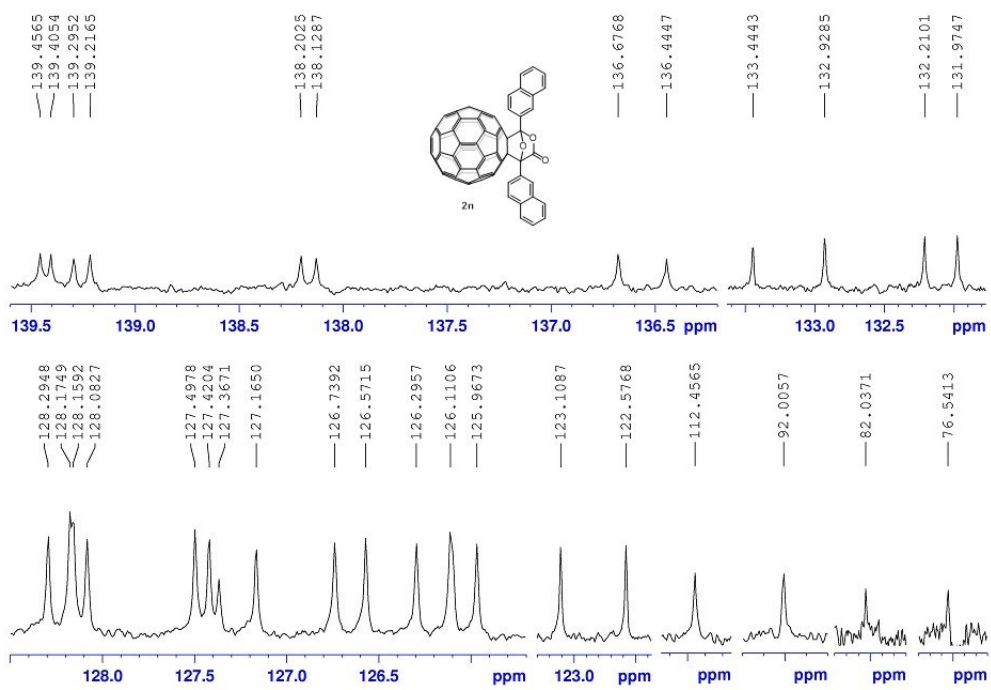


Figure S56. Expanded $^{13}\text{C}\{\text{H}\}$ NMR (100 MHz, $\text{CS}_2/\text{DMSO}-d_6$) of **2n**.

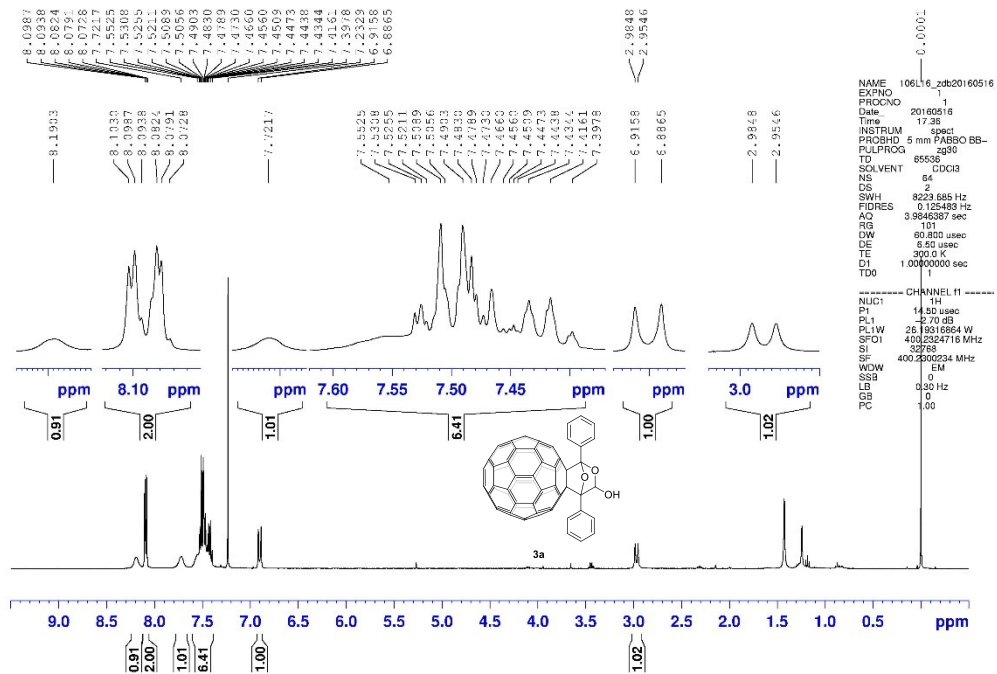


Figure S57. ^1H NMR (400 MHz, 1:1 CS₂/CDCl₃) of **3a**.

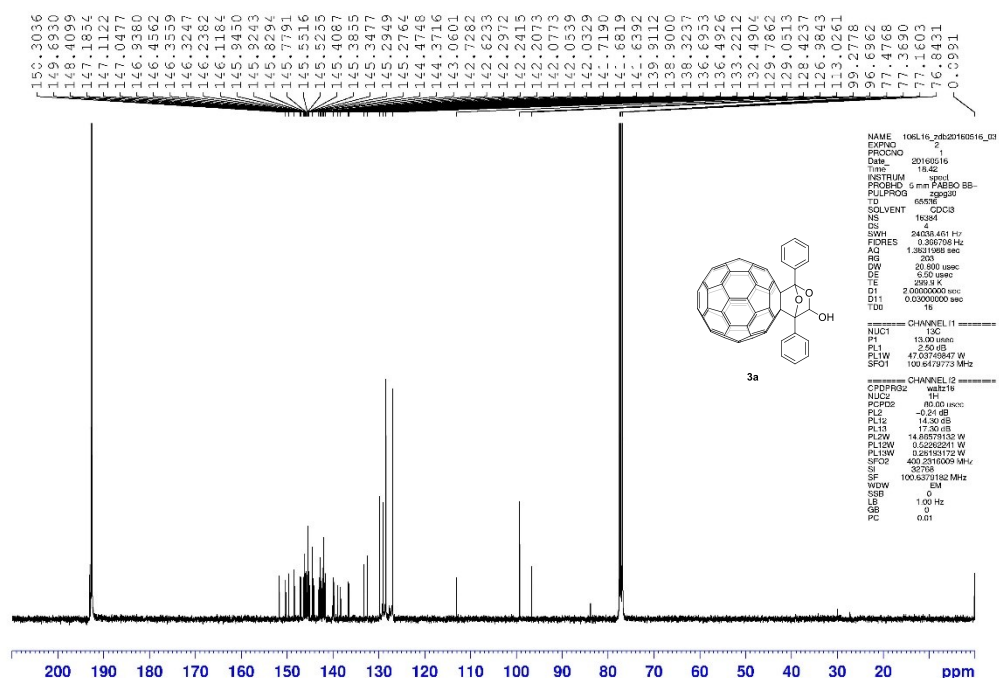


Figure S58. $^{13}\text{C}\{^1\text{H}\}$ NMR (100 MHz, 1:1 CS₂/CDCl₃) of **3a**.

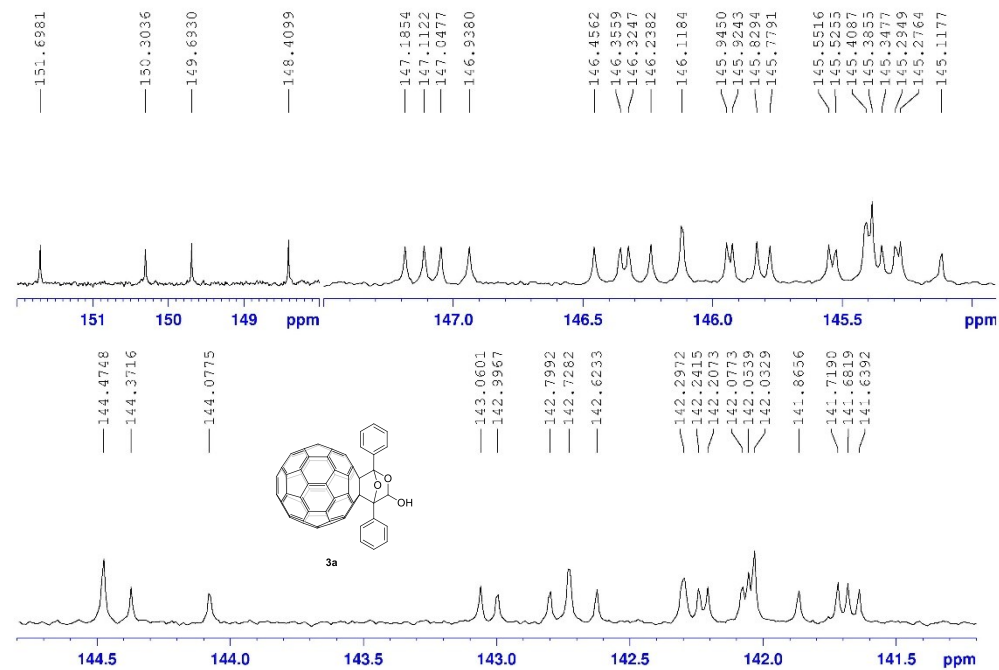


Figure S59. Expanded $^{13}\text{C}\{^1\text{H}\}$ NMR (100 MHz, 1:1 CS₂/CDCl₃) of **3a**.

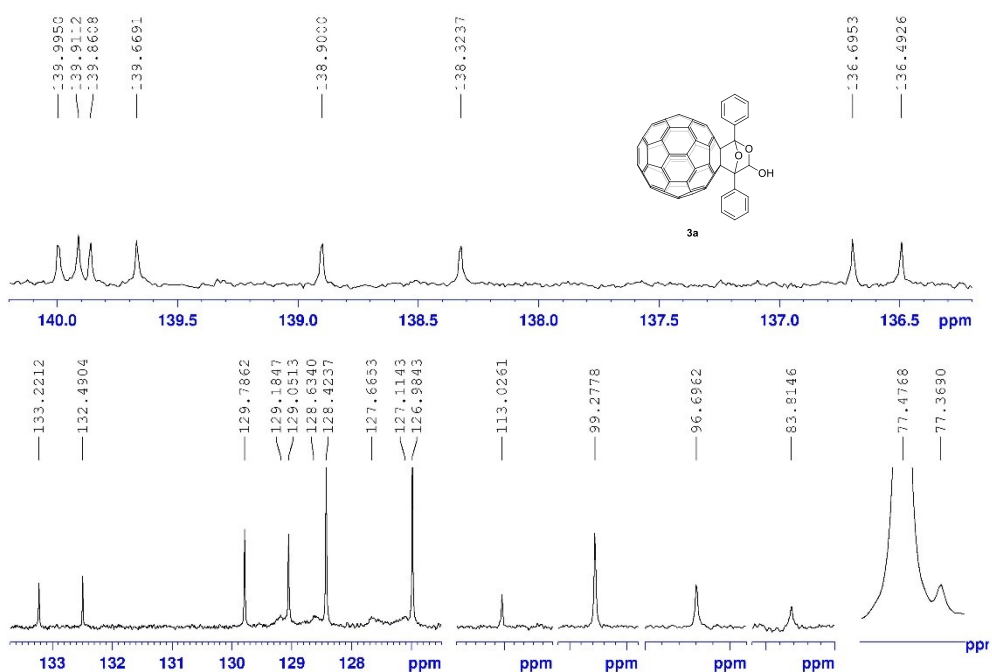


Figure S60. Expanded $^{13}\text{C}\{^1\text{H}\}$ NMR (100 MHz, 1:1 CS₂/CDCl₃) of **3a**.

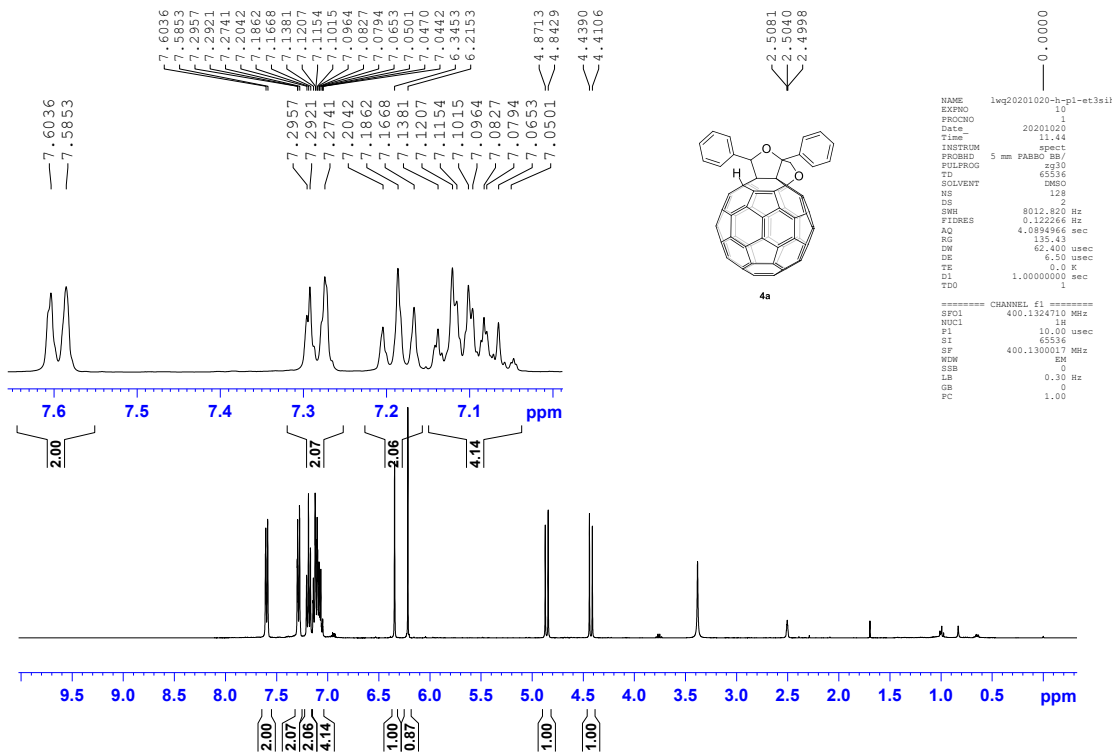


Figure S61. ^1H NMR (400 MHz, CS₂/DMSO-*d*₆) of **4a**.

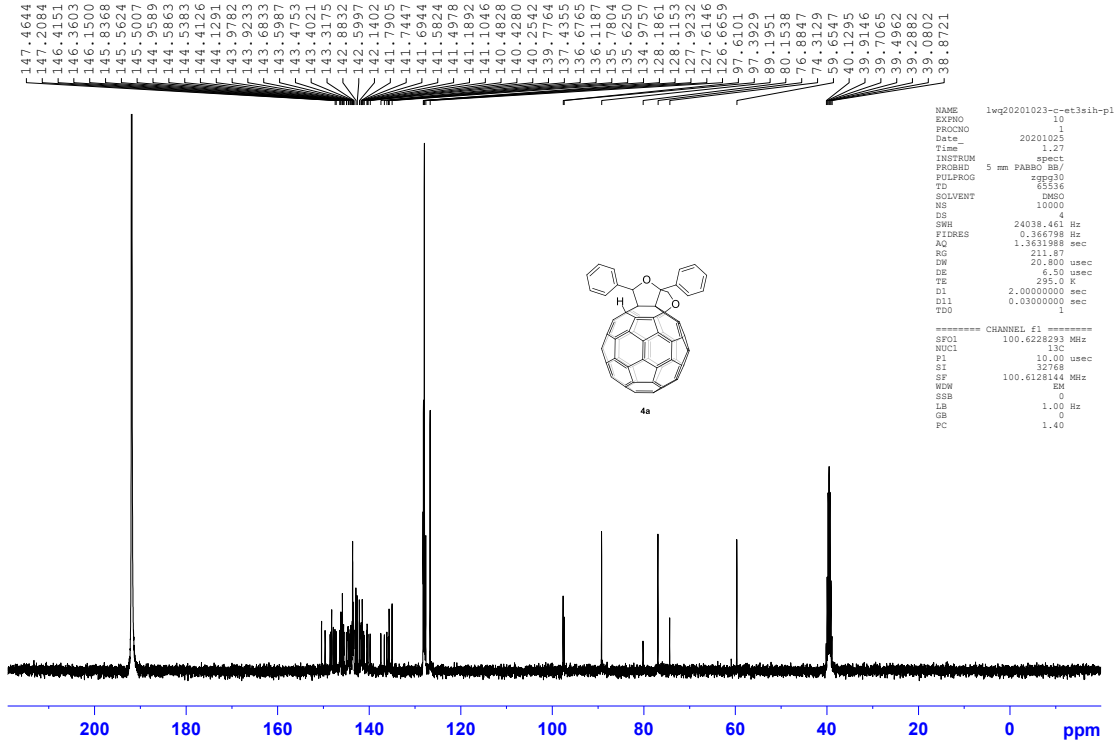


Figure S62. $^{13}\text{C}\{^1\text{H}\}$ NMR (100 MHz, $\text{CS}_2/\text{DMSO}-d_6$) of **4a**.

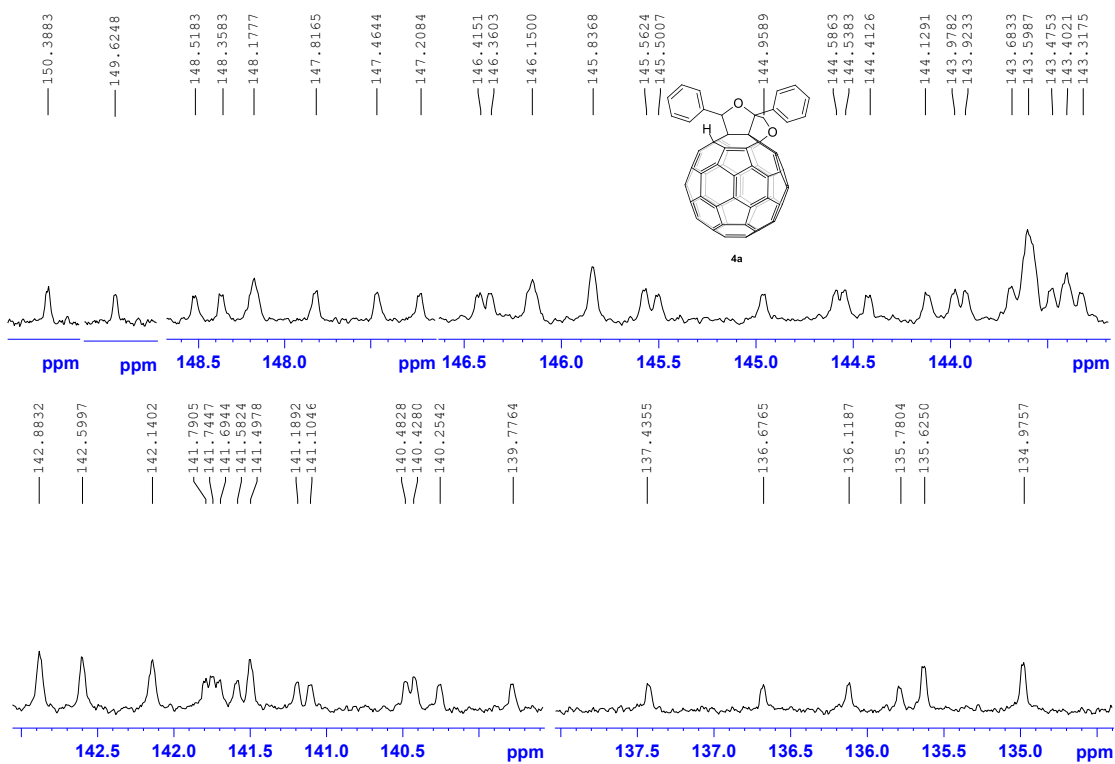


Figure S63. Expanded $^{13}\text{C}\{^1\text{H}\}$ NMR (100 MHz, $\text{CS}_2/\text{DMSO}-d_6$) of **4a**.

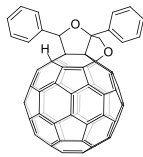
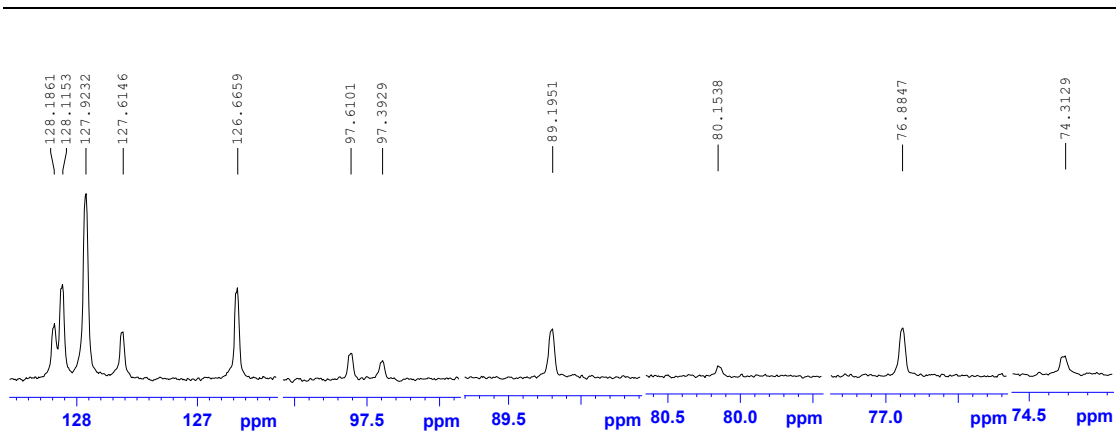


Figure S64. Expanded $^{13}\text{C}\{^1\text{H}\}$ NMR (100 MHz, $\text{CS}_2/\text{DMSO}-d_6$) of **4a**.

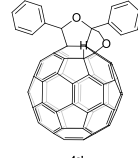
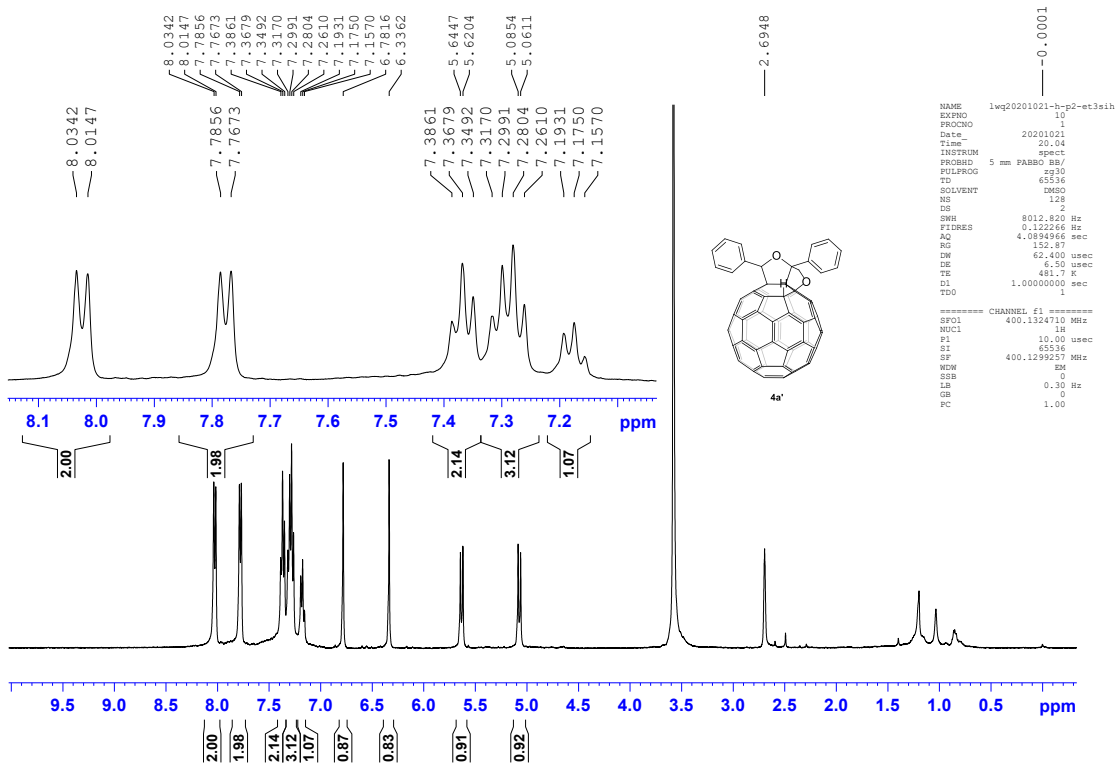


Figure S65. ^1H NMR (400 MHz, $\text{CS}_2/\text{DMSO}-d_6$) of **4a'**.

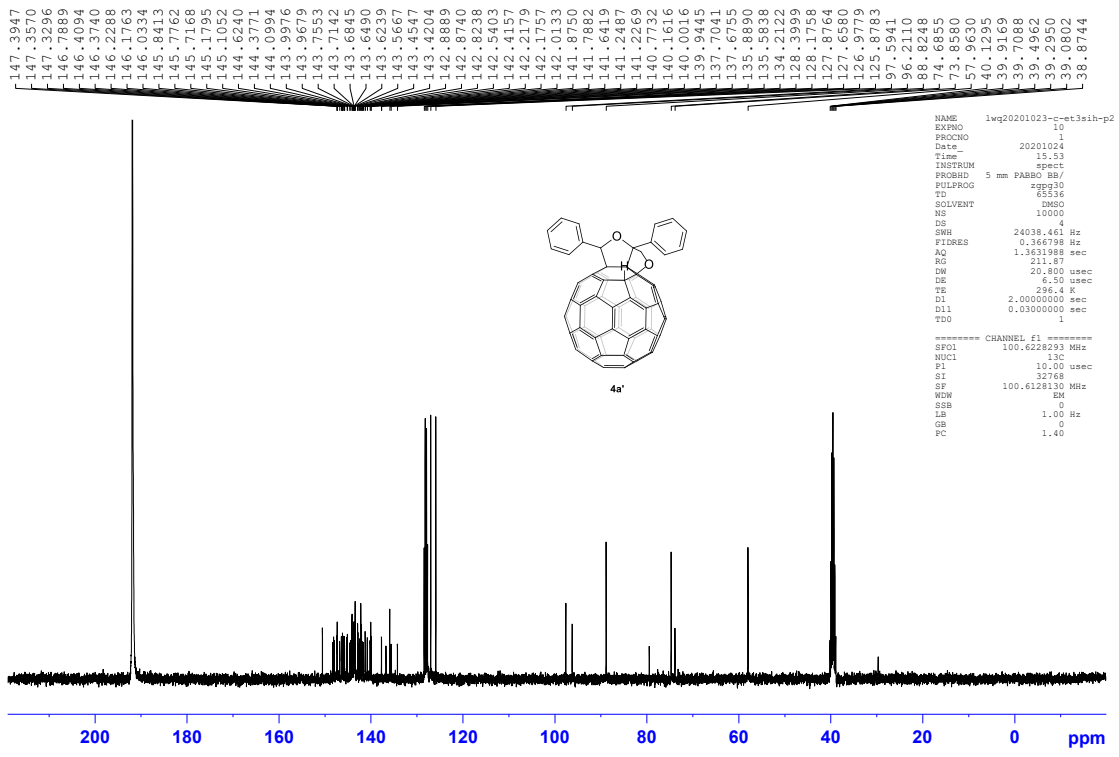


Figure S66. $^{13}\text{C}\{\text{H}\}$ NMR (100 MHz, $\text{CS}_2/\text{DMSO}-d_6$) of **4a'**.

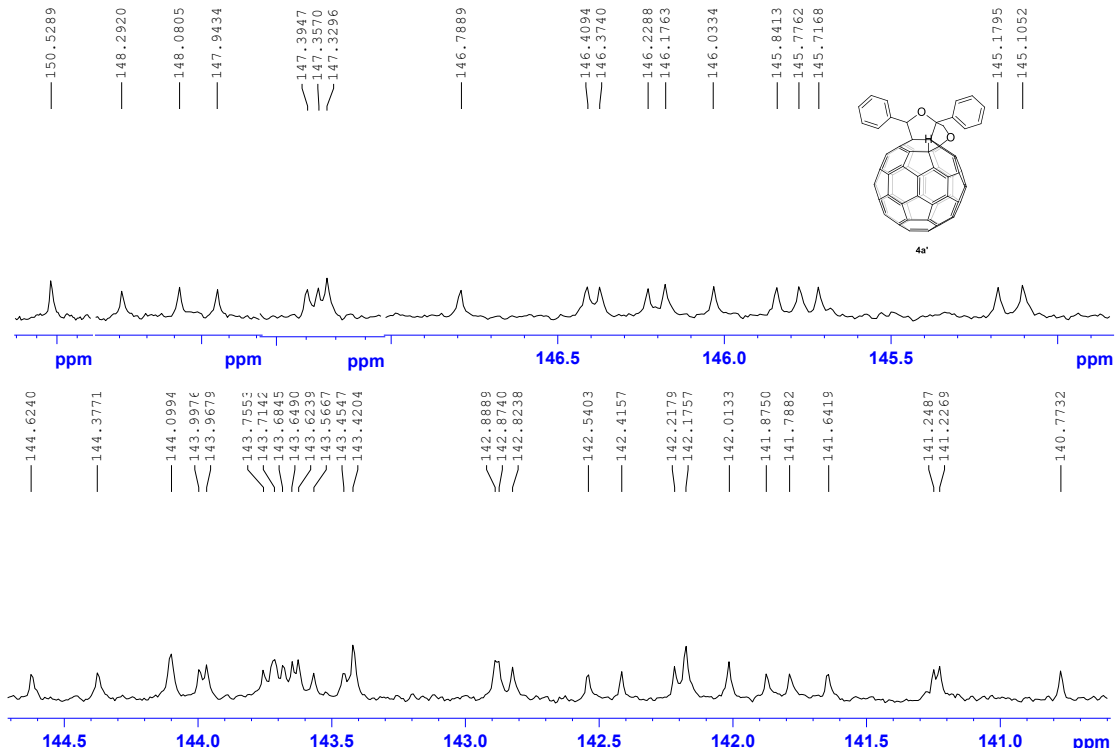


Figure S67. Expanded $^{13}\text{C}\{\text{H}\}$ NMR (100 MHz, $\text{CS}_2/\text{DMSO}-d_6$) of **4a'**.

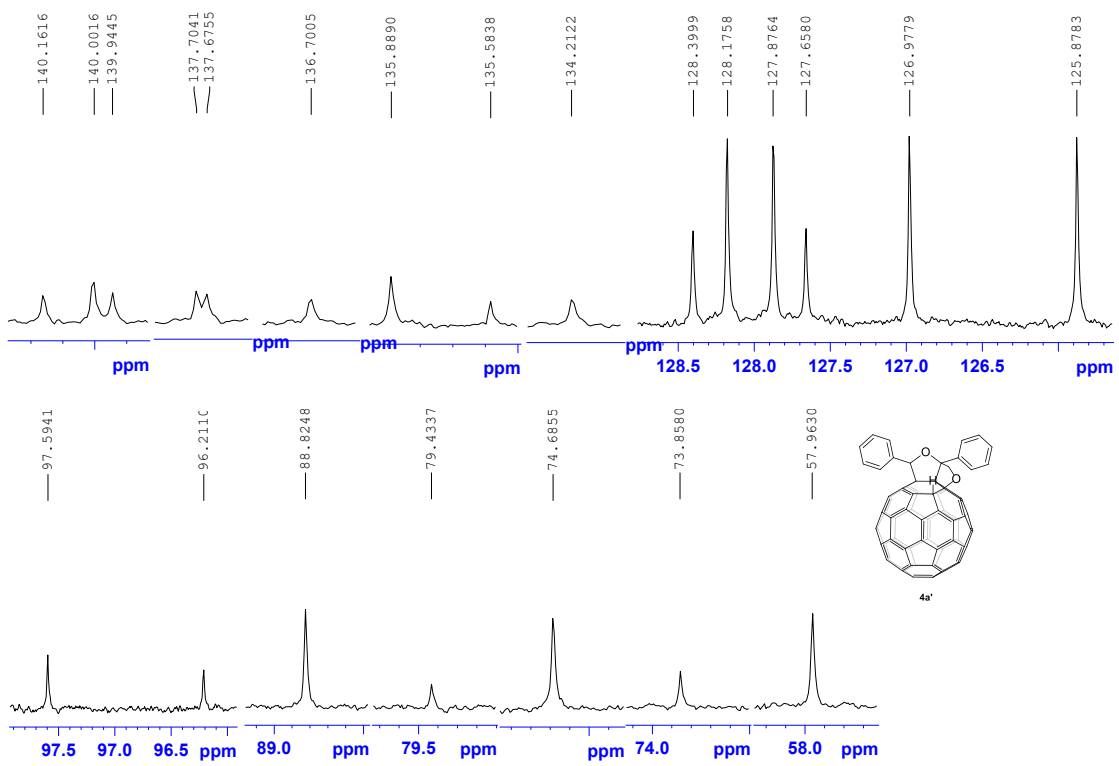


Figure S68. Expanded $^{13}\text{C}\{\text{H}\}$ NMR (100 MHz, $\text{CS}_2/\text{DMSO}-d_6$) of **4a'**.

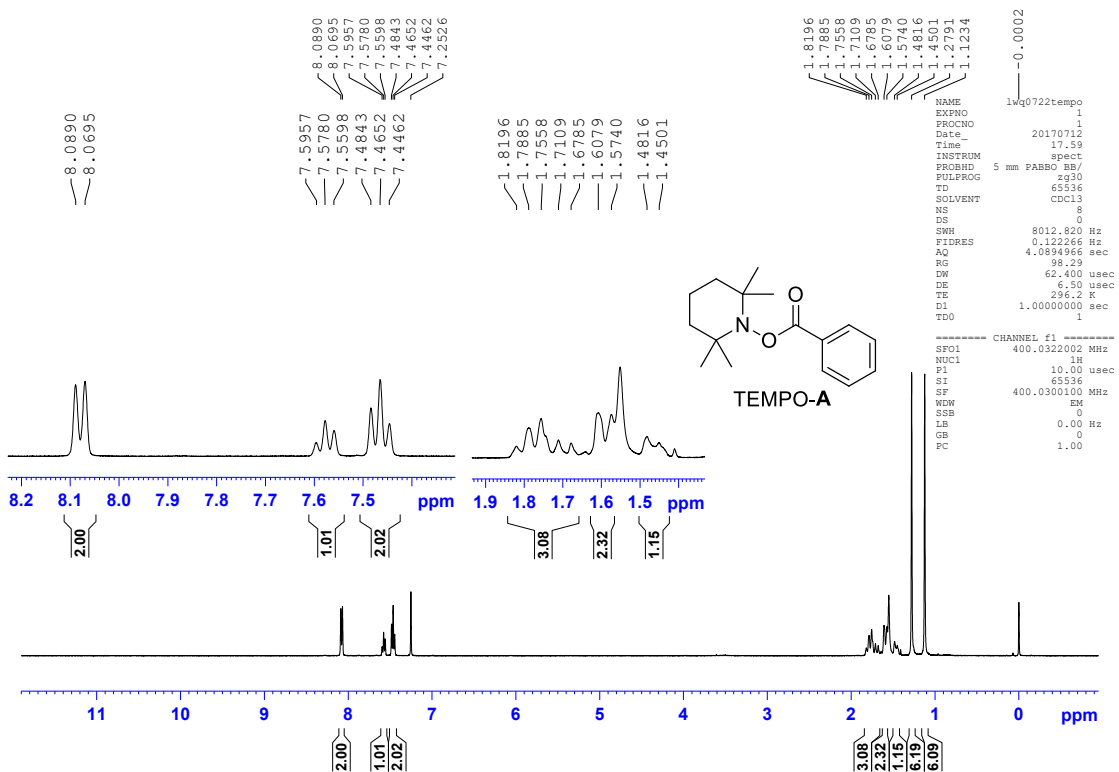


Figure S69. ^1H NMR (400 MHz, CDCl_3) of TEMPO-A.

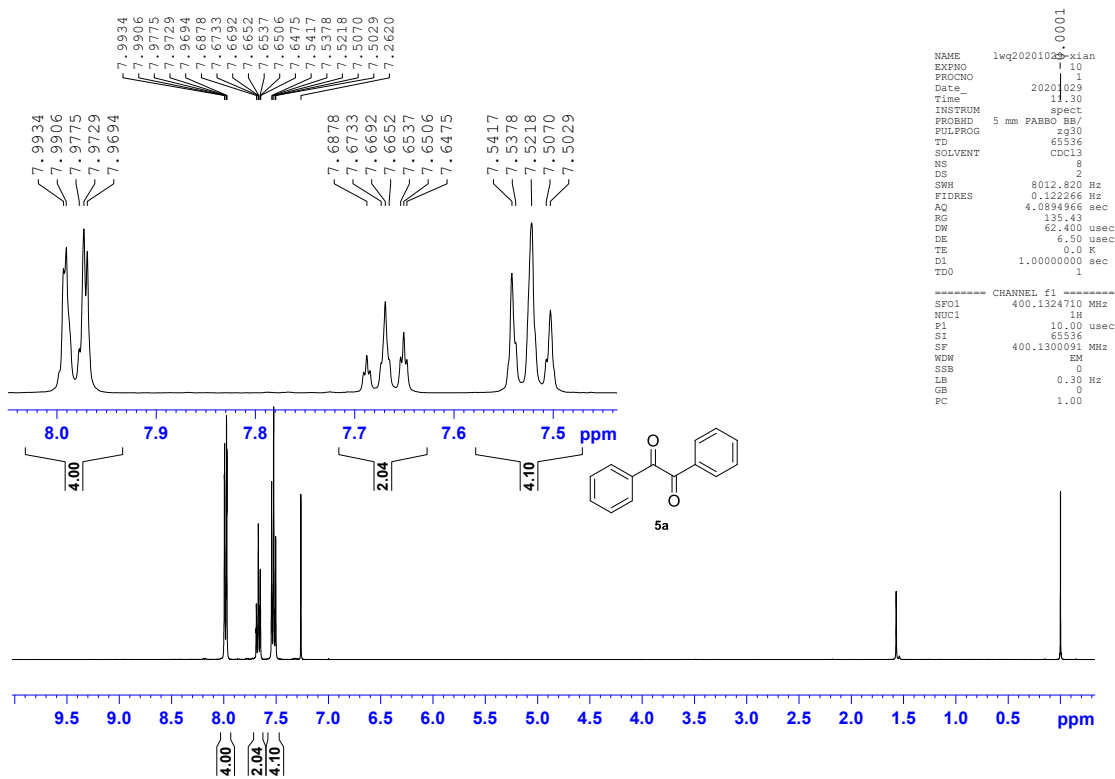


Figure S70. ¹H NMR (400 MHz, CDCl₃) of **5a**.

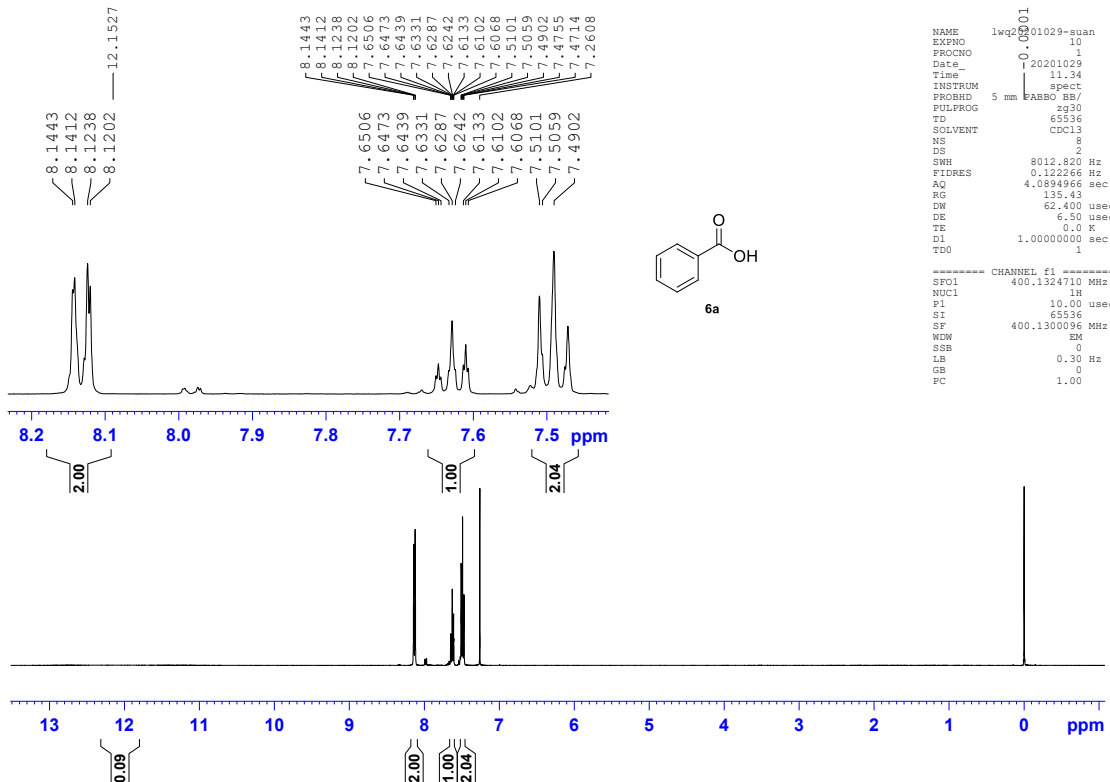


Figure S71. ¹H NMR (400 MHz, CDCl₃) of **6a**.

8. UV-vis spectra of compounds 2a–n, 3a, 4a and 4a'

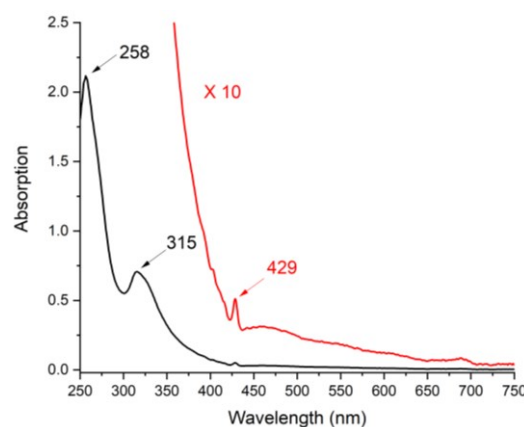


Figure S72. UV-vis absorption of compound 2a.

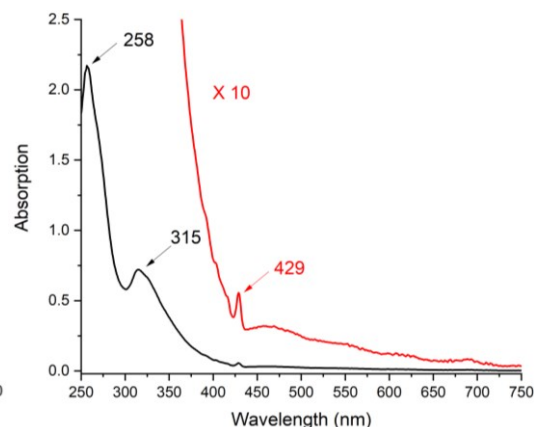


Figure S73. UV-vis absorption of compound 2b.

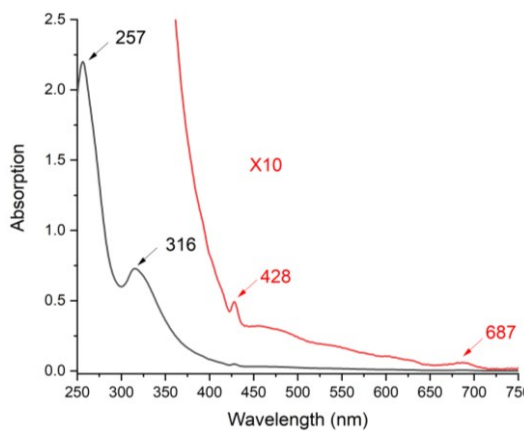


Figure S74. UV-vis absorption of compound 2c.

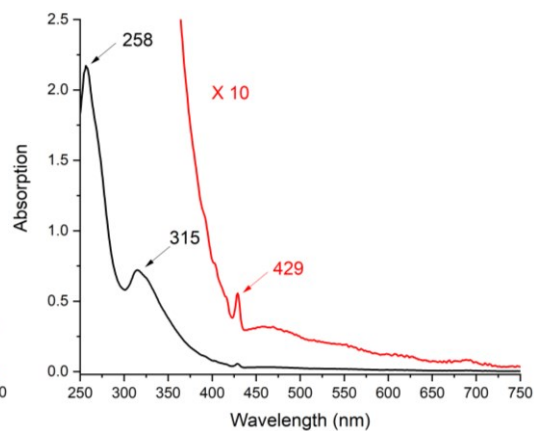


Figure S75. UV-vis absorption of compound 2d.

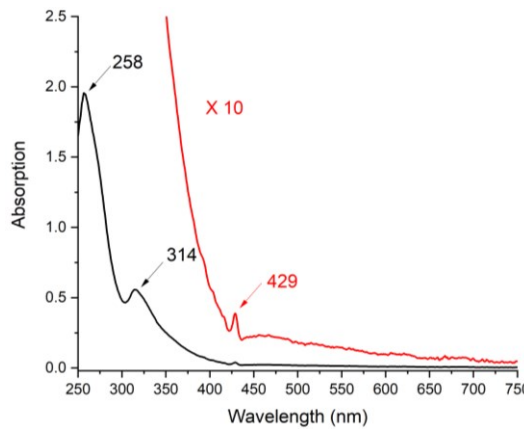


Figure S76. UV-vis absorption of compound 2e.

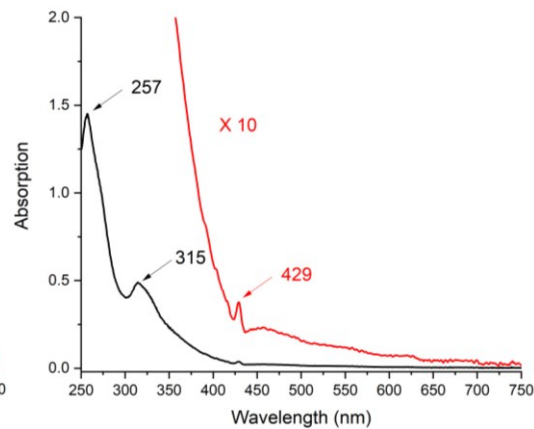


Figure S77. UV-vis absorption of compound 2f.

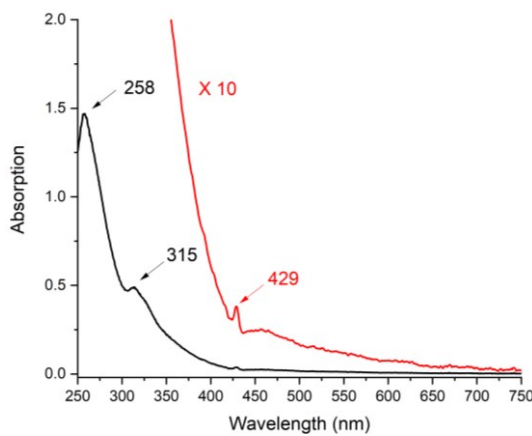


Figure S78. UV-vis absorption of compound **2g**.

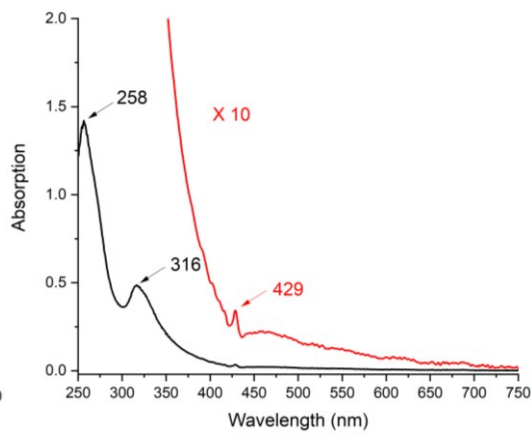


Figure S79. UV-vis absorption of compound **2h**.

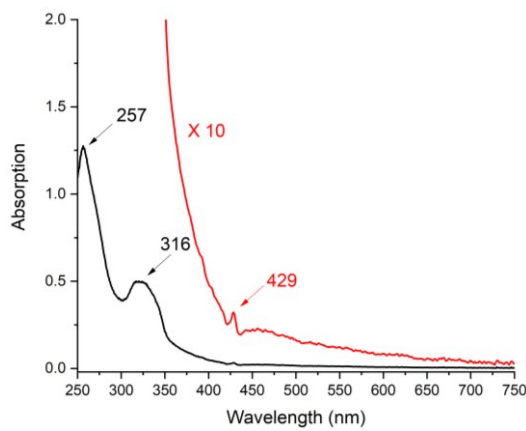


Figure S80. UV-vis absorption of compound **2i**.

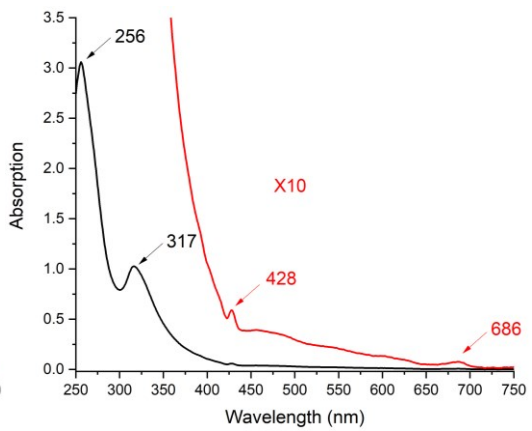


Figure S81. UV-vis absorption of compound **2j**.

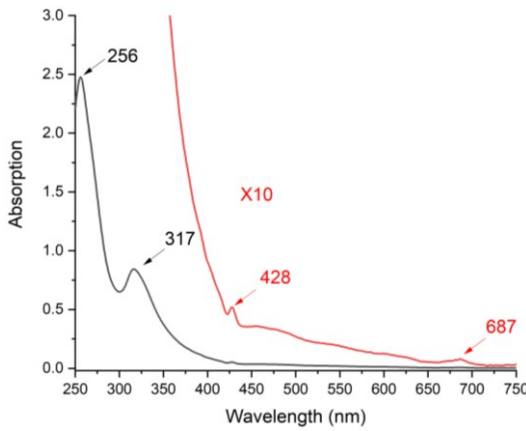


Figure S82. UV-vis absorption of compound **2k**.

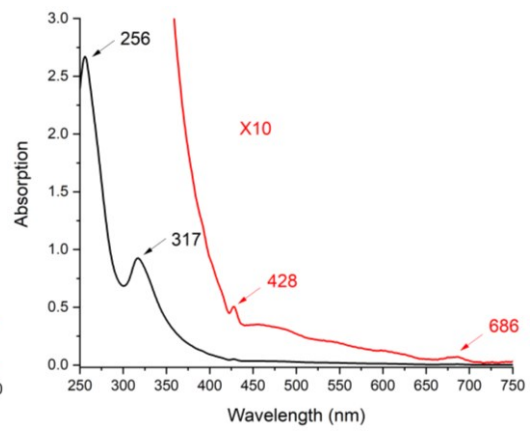


Figure S83. UV-vis absorption of compound **2l**.

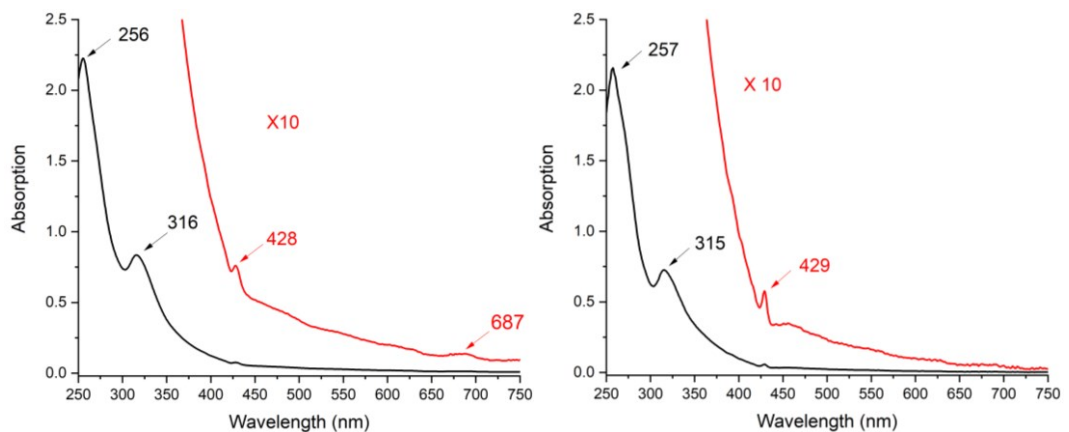


Figure S84. UV-vis absorption of compound **2m**. **Figure S85.** UV-vis absorption of compound **2n**.

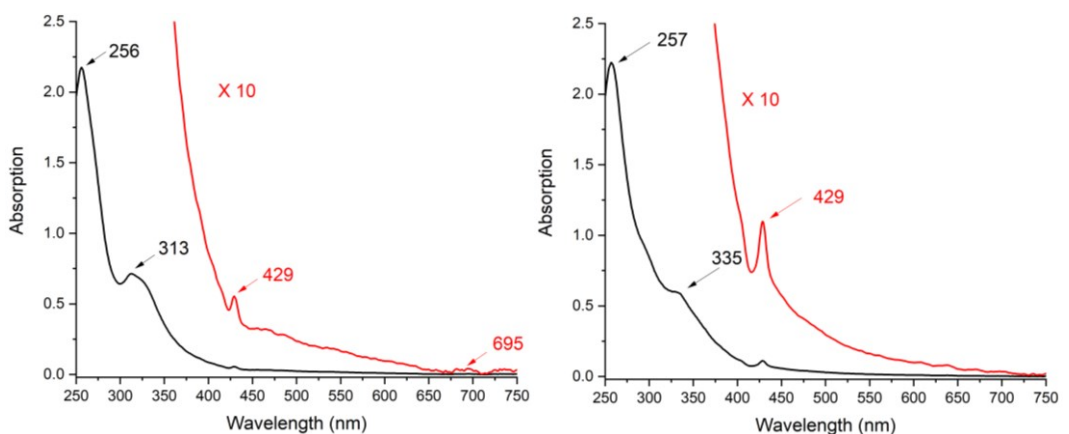


Figure S86. UV-vis absorption of compound **3a**. **Figure S87.** UV-vis absorption of compound **4a**.

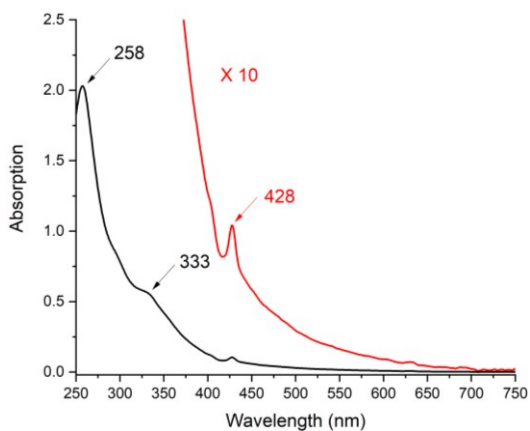


Figure S88. UV-vis absorption of compound **4a'**.

9. CV of compounds 2a–n, 3a, 4a and 4a'

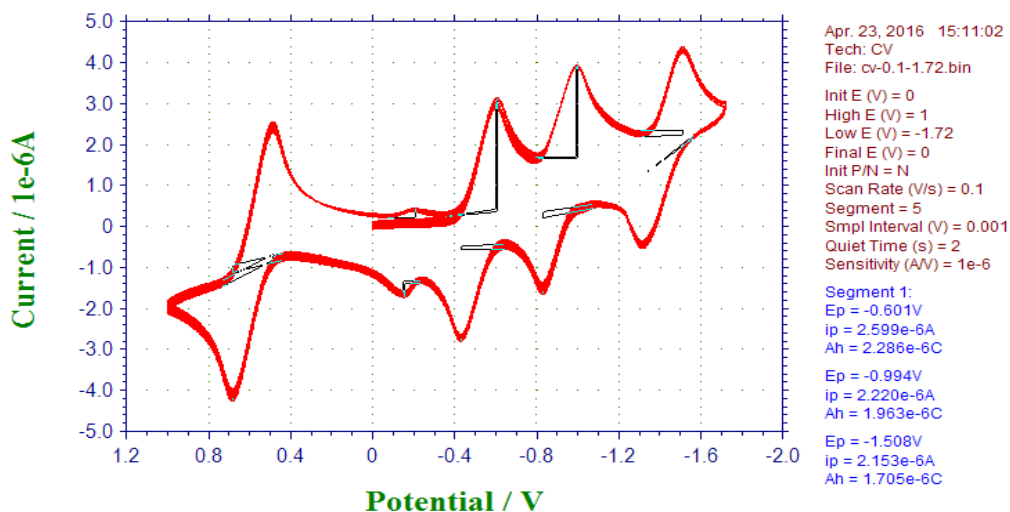


Figure S89. Cyclic voltammogram of compound **2a** (scanning rate: 100 mV s⁻¹)

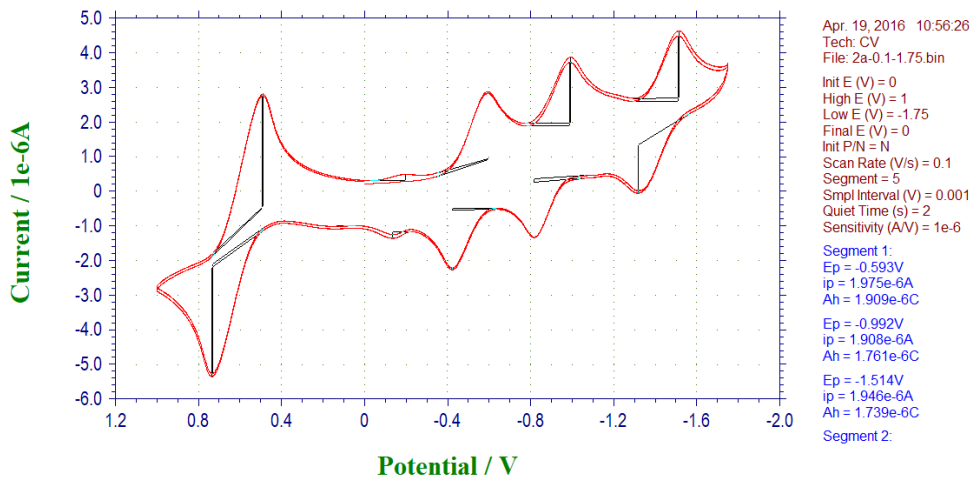


Figure S90. Cyclic voltammogram of compound **2b** (scanning rate: 100 mV s⁻¹)

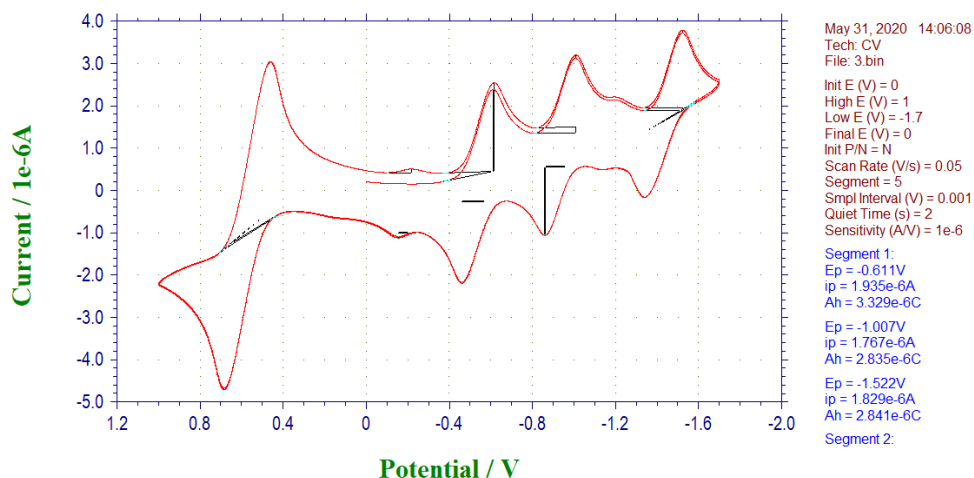


Figure S91. Cyclic voltammogram of compound **2c** (scanning rate: 50 mV s⁻¹)

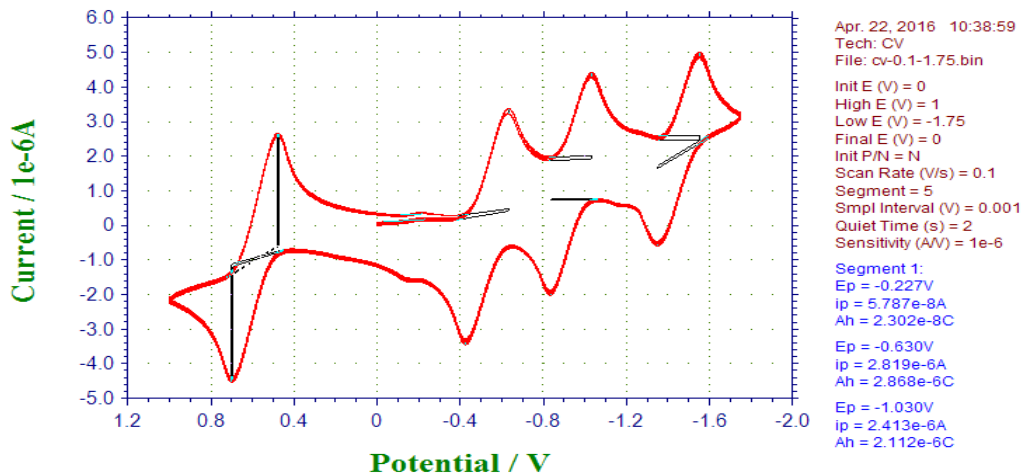


Figure S92. Cyclic voltammogram of compound **2d** (scanning rate: 100 mV s⁻¹)

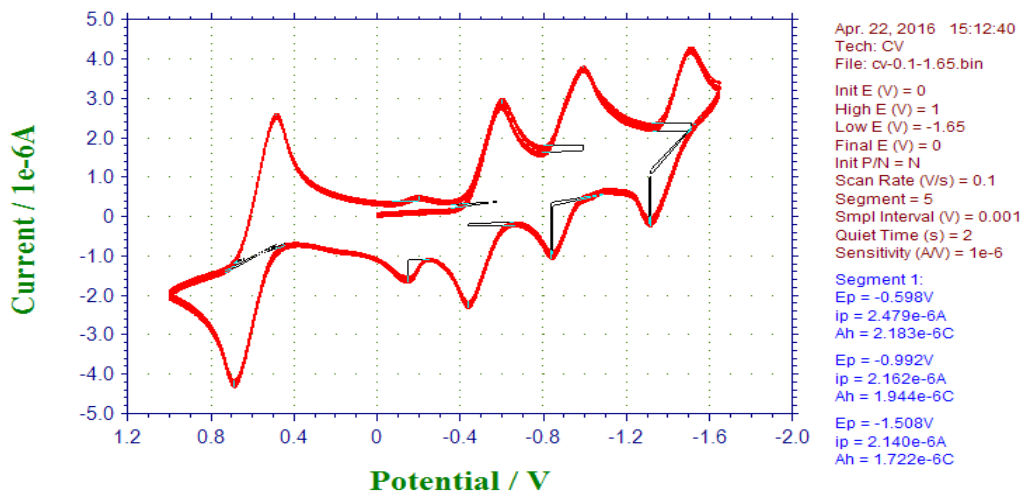


Figure S93. Cyclic voltammogram of compound **2e** (scanning rate: 100 mV s⁻¹)

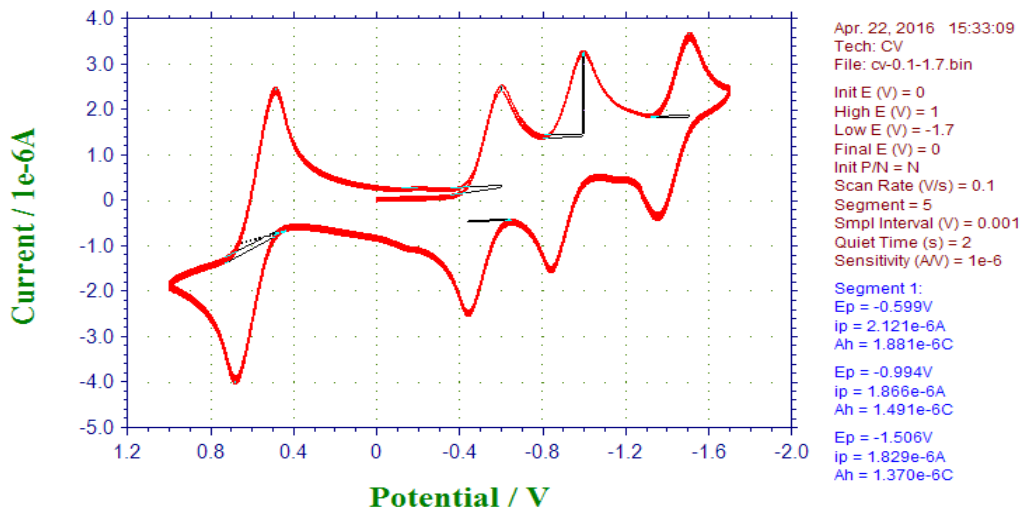


Figure S94. Cyclic voltammogram of compound **2f** (scanning rate: 100 mV s⁻¹)

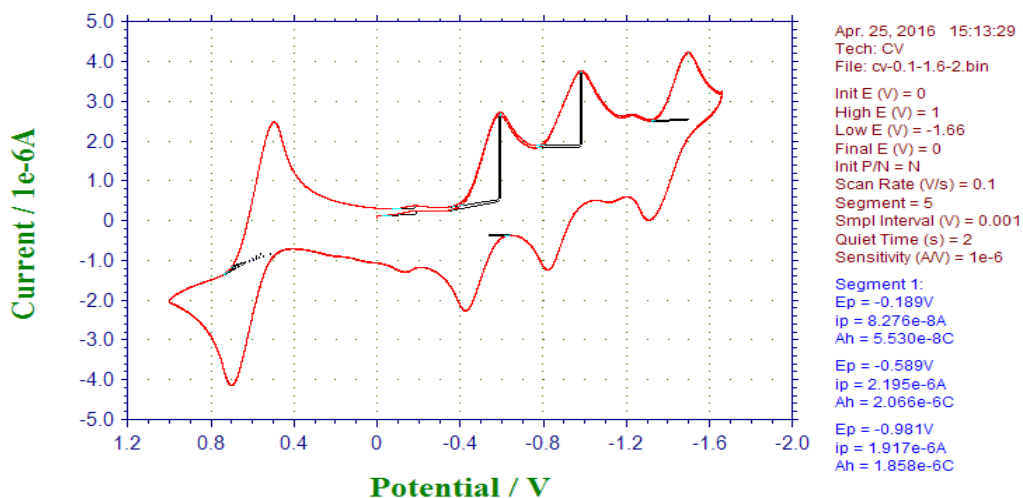


Figure S95. Cyclic voltammogram of compound **2g** (scanning rate: 100 mV s⁻¹)

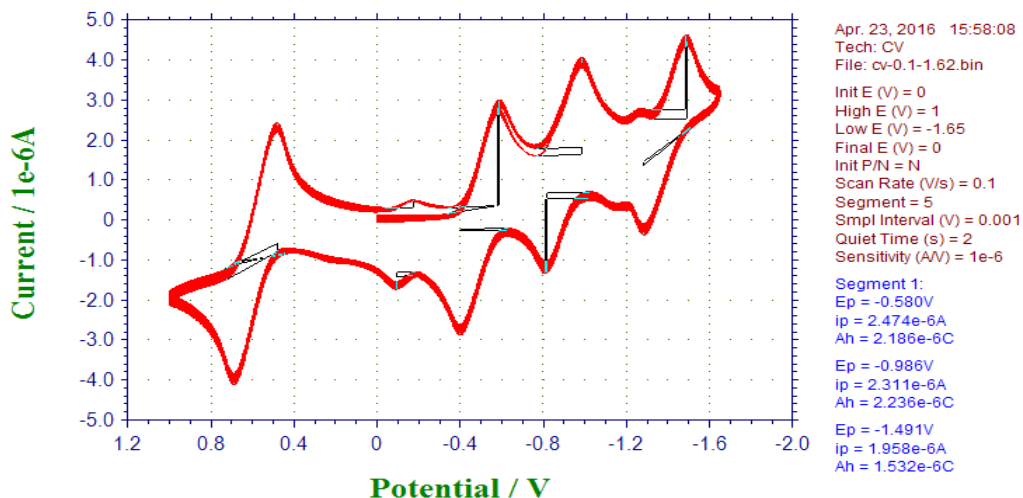


Figure S96. Cyclic voltammogram of compound **2h** (scanning rate: 100 mV s⁻¹)

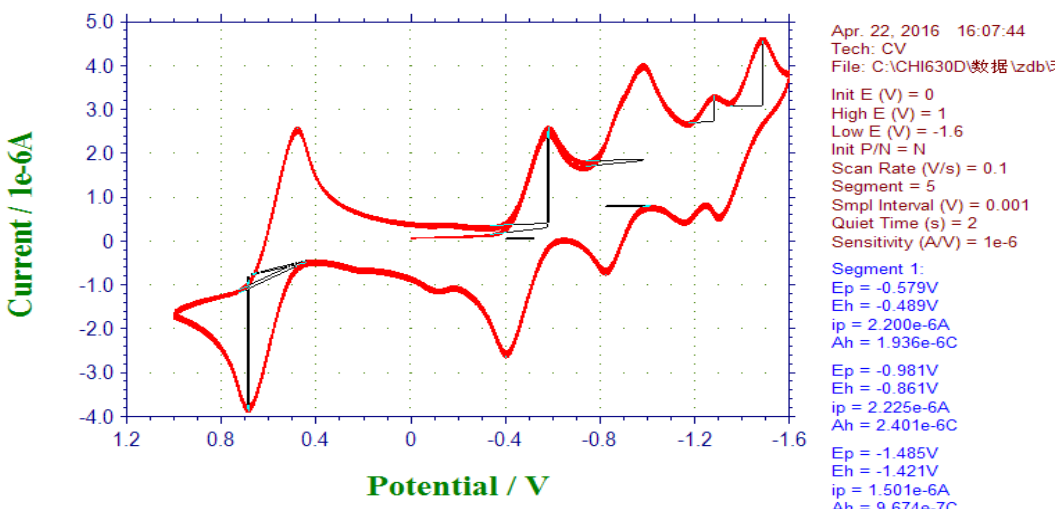


Figure S97. Cyclic voltammogram of compound **2i** (scanning rate: 100 mV s⁻¹)

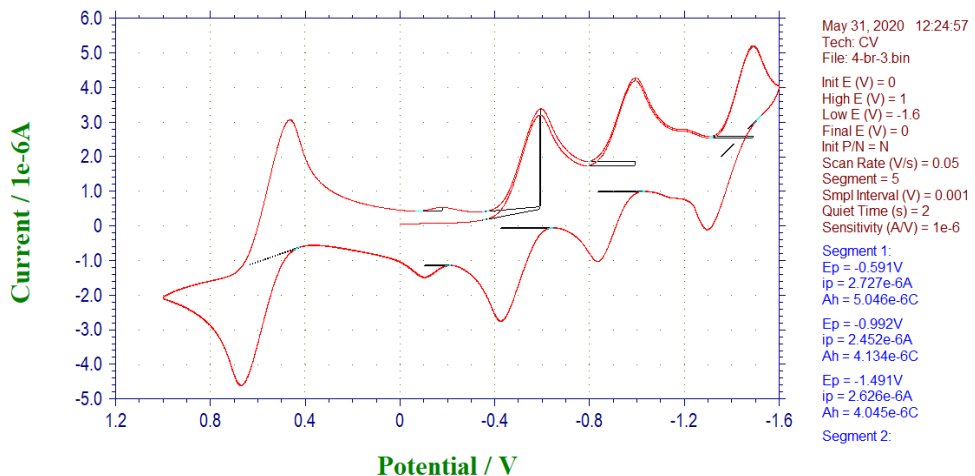


Figure S98. Cyclic voltammogram of compound **2j** (scanning rate: 50 mV s⁻¹)

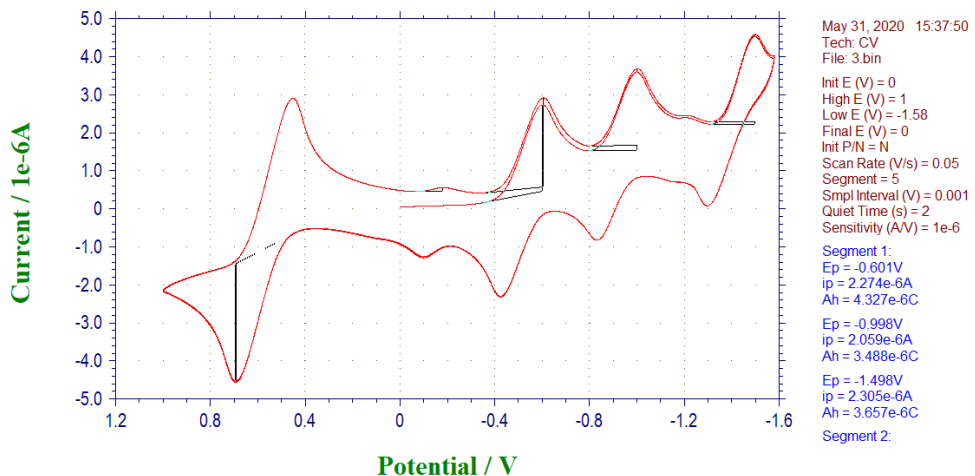


Figure S99. Cyclic voltammogram of compound **2k** (scanning rate: 50 mV s⁻¹)

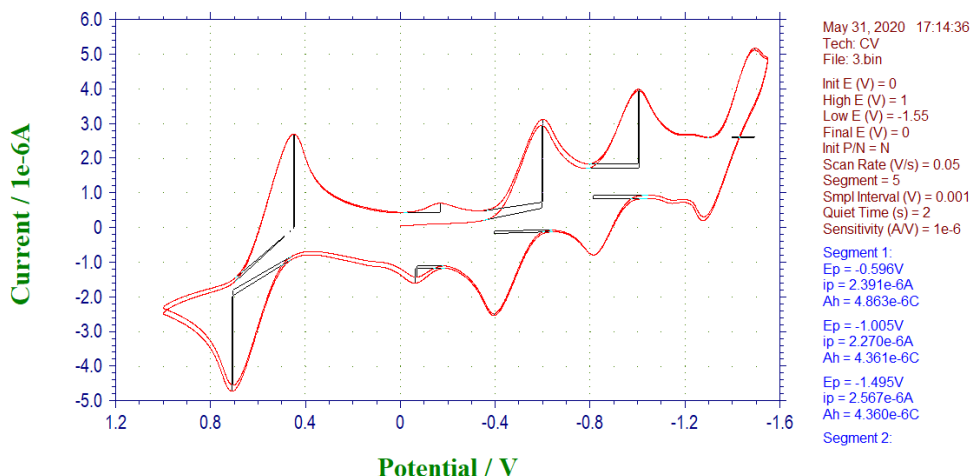


Figure S100. Cyclic voltammogram of compound **2l** (scanning rate: 50 mV s⁻¹)

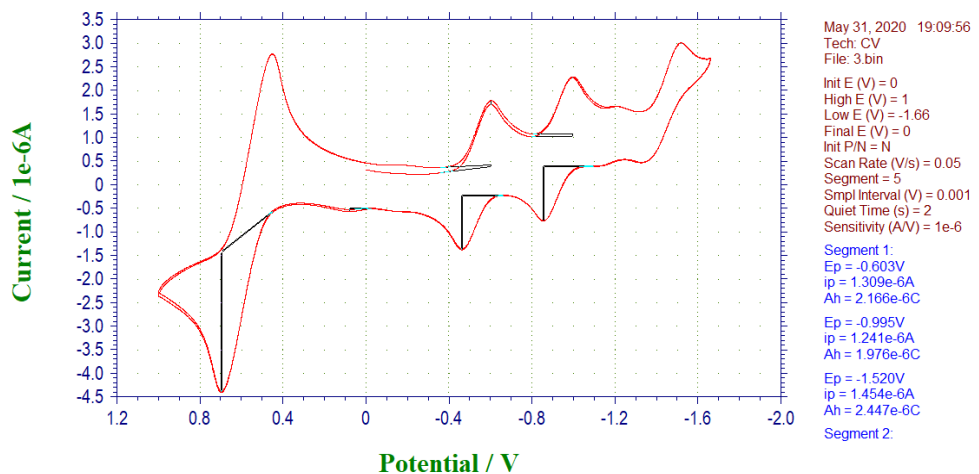


Figure S101. Cyclic voltammogram of compound **2m** (scanning rate: 50 mV s⁻¹)

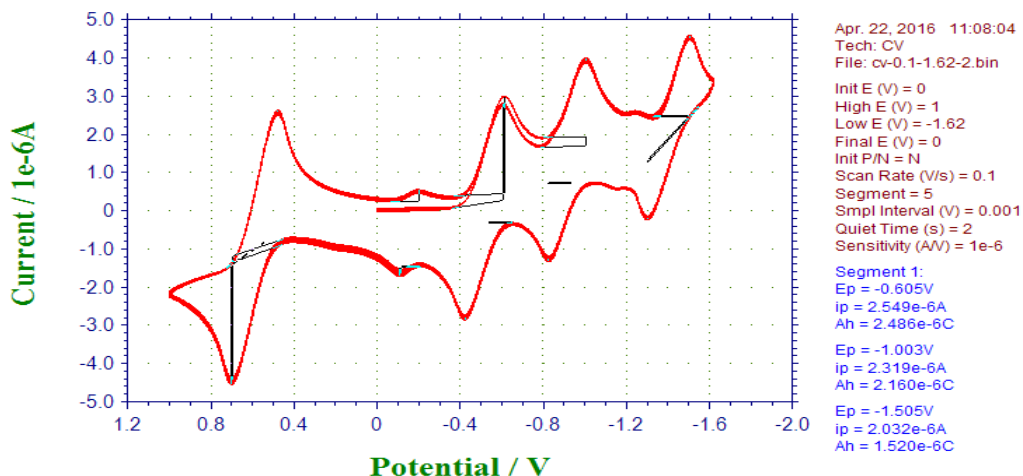


Figure S102. Cyclic voltammogram of compound **2n** (scanning rate: 100 mV s⁻¹)

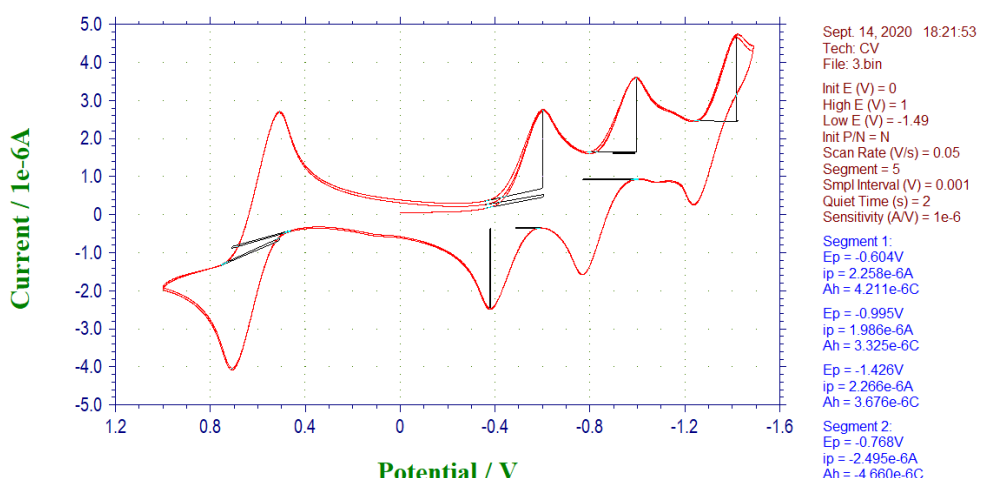


Figure S103. Cyclic voltammogram of compound **3a** (scanning rate: 50 mV s⁻¹)

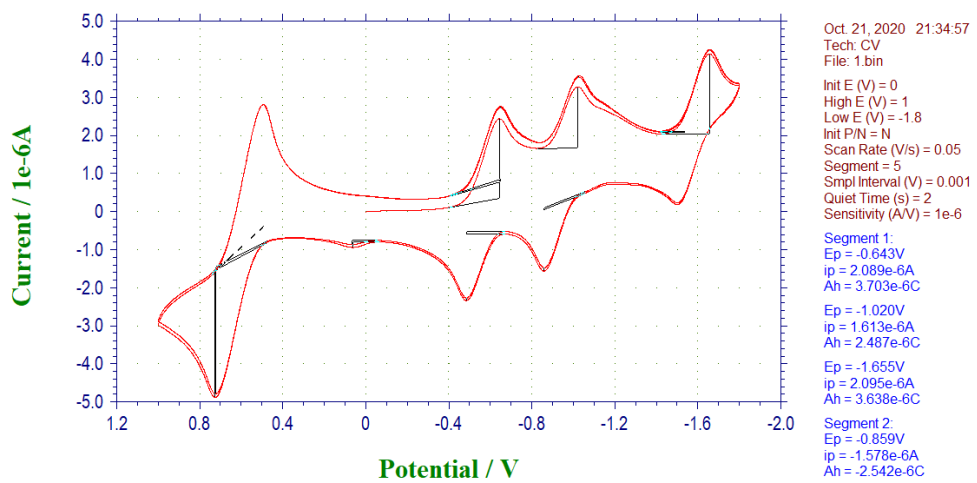


Figure S104. Cyclic voltammogram of compound **4a** (scanning rate: 50 mV s⁻¹)

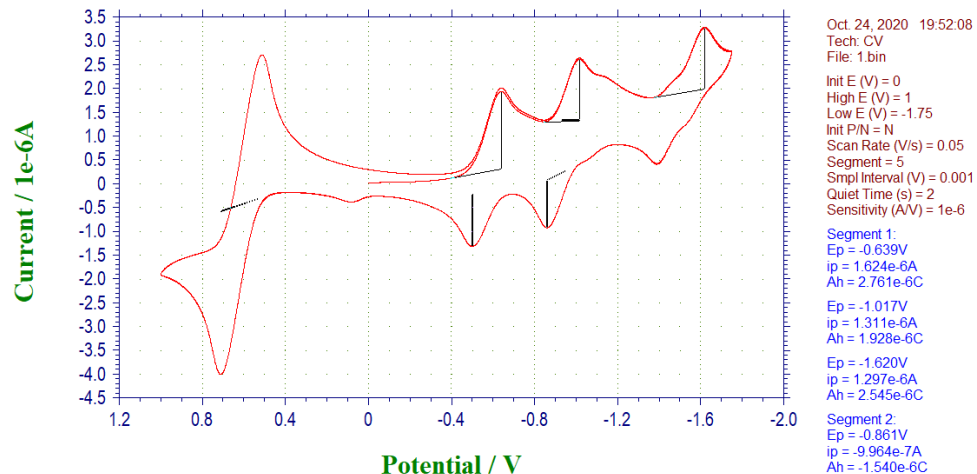


Figure S105. Cyclic voltammogram of compound **4a'** (scanning rate: 50 mV s⁻¹)

Table S3. Half-wave reduction potentials (V) of C₆₀ and C₆₀-fused lactones **2a–n**, **3a**, **4a** and **4a'**^a

Compound	E ₁	E ₂	E ₃
C ₆₀	-1.076	-1.460	-1.925
2a	-1.104	-1.498	-2.000
2b	-1.095	-1.517	-2.028
2c	-1.115	-1.506	-2.003
2d	-1.117	-1.521	-2.039
2e	-1.104	-1.502	-1.997
2f	-1.105	-1.501	-2.015
2g	-1.106	-1.500	-2.006
2h	-1.086	-1.486	-1.988
2i	-1.050	-1.461	-1.946
2j	-1.080	-1.477	-1.964
2k	-1.096	-1.493	-1.977
2l	-1.073	-1.477	-1.956
2m	-1.106	-1.498	-2.004
2n	-1.102	-1.503	-1.993
3a	-1.116	-1.508	-1.929
4a	-1.167	-1.548	-2.186
4a'	-1.180	-1.554	-2.115

^aVersus ferrocenium/ferrocene. Experimental conditions: 1 mM of compound and 0.1 M of n-Bu₄NClO₄ in anhydrous *o*-dichlorobenzene (2 mL); reference electrode: SCE; working electrode: Pt; auxiliary electrode: Pt wire; scanning rate: 100 mV s⁻¹ or 50 mV s⁻¹.

10. X-Ray data of compounds **2b** and **4a'**

Black block crystals of **2b** were obtained by slow diffusion in toluene/methanol at about 0 °C. Single-crystal X-ray diffraction data were collected on a diffractometer (Gemini S Ultra, Agilent Technologies) equipped with a CCD area detector using graphite-monochromated CuK α radiation ($\lambda = 1.54184 \text{ \AA}$) in the scan range $8.944^\circ < 2\theta < 139.682^\circ$. The structure was solved with direct methods using SHELXS and refined with full-matrix least-squares refinement using the SHELXL program within OLEX2.

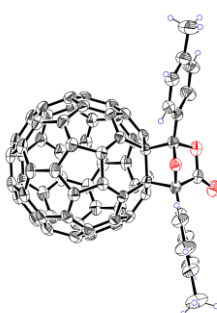


Figure S106. ORTRP drawing of compound **2b** with thermal ellipsoids at the 30% probability level. One enantiomer is shown for the ellipsoid model.

Table S4. Crystal data for **2b**.

Identification code	2065070
Empirical formula	C ₇₇ H ₁₄ O ₃
Formula weight	986.88
Temperature/K	290(2)
Crystal system	triclinic
Space group	<i>P</i> -1
<i>a</i> /Å	10.1504(4)
<i>b</i> /Å	10.2597(4)
<i>c</i> /Å	26.1604(10)
$\alpha/^\circ$	84.653(3)
$\beta/^\circ$	87.864(3)
$\gamma/^\circ$	75.323(3)
Volume/Å ³	2623.72(18)
<i>Z</i>	2
$\rho_{\text{calc}}/\text{g/cm}^3$	1.249
μ/mm^{-1}	0.598
F(000)	1000.0
Crystal size/mm ³	0.350 × 0.300 × 0.210
Radiation	Cu K α ($\lambda = 1.54184$ Å)
2 θ range for data collection/°	8.944 to 139.682
Index ranges	-7 ≤ <i>h</i> ≤ 12, -12 ≤ <i>k</i> ≤ 12, -31 ≤ <i>l</i> ≤ 31
Reflections collected	19027
Independent reflections	9625 [$R_{\text{int}} = 0.0261$, $R_{\text{sigma}} = 0.0401$]
Data/restraints/parameters	9625/0/724
Goodness-of-fit on F ²	0.997
Final <i>R</i> indexes [$I >= 2\sigma(I)$]	$R_1 = 0.0740$, $wR_2 = 0.2093$
Final <i>R</i> indexes [all data]	$R_1 = 0.0900$, $wR_2 = 0.2204$
Largest diff. peak/hole/e Å ⁻³	0.83/-0.24

Black block crystals of **4a'** were obtained by slow diffusion in carbon disulfide/hexane at about 0 °C. Single-crystal X-ray diffraction data were collected on a diffractometer (Gemini S Ultra, Agilent Technologies) equipped with a CCD area detector using graphite-monochromated CuK α radiation ($\lambda = 1.54184$ Å) in the scan range $6.74^\circ < 2\theta < 140.18^\circ$. The structure was solved with the olex2.solve structure solution program using Charge Flipping refined with full-matrix least-squares refinement using the SHELXL program within OLEX2.

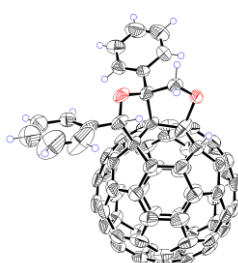


Figure S107. ORTRP drawing of compound **4a'** with thermal ellipsoids at the 30% probability level. One enantiomer is shown for the ellipsoid model.

Table S5. Crystal data for **4a'**.

Identification code	2065088
Empirical formula	C ₇₇ H ₁₃ O ₂ S ₄
Formula weight	1098.11
Temperature/K	293(2)
Crystal system	orthorhombic
Space group	<i>Pnma</i>
<i>a</i> /Å	12.49560(18)
<i>b</i> /Å	21.1248(5)
<i>c</i> /Å	16.7633(3)
$\alpha/^\circ$	90.00
$\beta/^\circ$	90.00
$\gamma/^\circ$	90.00
Volume/Å ³	4424.97(15)
<i>Z</i>	4
$\rho_{\text{calc}}/\text{g/cm}^3$	1.648
μ/mm^{-1}	2.479
F(000)	2220.0
Crystal size/mm ³	0.2 × 0.18 × 0.17
Radiation	Cu K α ($\lambda = 1.54184$)
2 θ range for data collection/°	6.74 to 140.18
Index ranges	-15 ≤ <i>h</i> ≤ 13, -24 ≤ <i>k</i> ≤ 25, -20 ≤ <i>l</i> ≤ 19
Reflections collected	10959
Independent reflections	4222 [$R_{\text{int}} = 0.0239$, $R_{\text{sigma}} = 0.0214$]
Data/restraints/parameters	4222/0/395
Goodness-of-fit on F ²	1.086
Final <i>R</i> indexes [$I >= 2\sigma(I)$]	$R_1 = 0.0659$, $wR_2 = 0.1622$
Final <i>R</i> indexes [all data]	$R_1 = 0.0748$, $wR_2 = 0.1692$
Largest diff. peak/hole/e Å ⁻³	0.28/-0.37

11. References

- (1) X.-Y. Zhang, W.-Z. Weng, H. Liang, H. Yang and B. Zhang, *Org. Lett.*, 2018, **20**, 4686–4690.
- (2) V. Nair, V. Varghese, R. R. Paul, A. Jose, C. R. Sinu and R. S. Menon, *Org. Lett.*, 2010, **12**, 2653–2655.
- (3) H.-X. Zou, Y. Li, H. Yang, J.-H. Li and J. Xiang, *Adv. Synth. Catal.*, 2018, **360**, 1439–1443.